THE EFFECT OF ASPALATHIN ON DOXORUBICIN-INDUCED CARDIOTOXICITY

SAMUKELISIWE CYNTHIA SHABALALA

Student number: 206000455

A dissertation submitted in fulfilment of the requirements for the degree of

MASTER OF SCIENCE IN BIOCHEMISTRY

Department of Biochemistry and Microbiology, Faculty of Science and Agriculture,
University of Zululand, KwaDlangezwa, KwaZulu Natal, South Africa

Supervisor: Dr Rabia Johnson

Co-supervisors: Dr Abidemi Kappo

Dr Christo Muller

December 2016

DECLARATION

I, **……**declare that the entirety of the work contained herein is my own and that it has not been submitted for any degree or examination in any other University and that all the sources I have used have been acknowledged by complete references.

Full Name: Samukelisiwe Cynthia Shabalala (student number: 206000455)

Signature:

Date:

ABSTRACT

Introduction: Doxorubicin is a highly effective first-line chemotherapeutic agent used in the treatment of a broad range of solid and hematological tumors. Though effective, the use of Doxorubicin in cancer therapy has been hindered by its cardio toxic side effects. As yet, no single chemical synthesized drug or compound are known to prevent the harmful action of Doxorubicin without reducing its anti-cancer efficacy. Therefore, the search for an effective and safe antagonist of Doxorubicin-induced cardiotoxicity remains a challenge. In recent years, researchers have investigated the use of plant-derived polyphenols as nutraceuticals to lower the risk of chronic diseases. Of particular interest is aspalathin, a plant polyphenol with known antioxidant properties.

Aim: This study aimed to investigate the potential use of aspalathin, a dihydrochalcone C-glycoside, in alleviating Doxorubicin-induced cardiotoxicity in an *in vitro* H9c2 cardio myoblast cell culture model.

Methods: H9c2 cardiomyocytes and Caov-3 cancer cells were cultured in Dulbecco's modified eagle's medium and treated with or without Doxorubicin for five days. Thereafter, cells exposed to 0.2 µM Doxorubicin were co-treated with either 20 µM Dexrazozane or 0.2 µM aspalathin daily, resulting in a cumulative dose of 1 µM Doxorubicin, 100 µM Dexrazozane and 1 µM aspalathin, respectively. Cell viability and apoptosis were evaluated using ATP and TUNEL assays. Various bioassays (glutathione, catalase, superoxide dismutase and lipid peroxidation) and gene and protein expression analyses (autophagy-related genes) were performed to assess the cardioprotective effect of aspalathin to prevent Doxorubicin-induced cardiotoxicity.

Results: This study showed that aspalathin co-treatment was able to mitigate Doxorubicin-induced oxidative stress, DNA damage, lipid peroxidation and subsequently myocardial apoptosis, while enhancing autophagy in H9c2 cardiomyocytes. Interestingly, aspalathin co-treatment diminished myocardial apoptosis in H9c2 cells, whereas the effect was augmented in Caov-3 ovarian cancer cells. Furthermore, this study showed that aspalathin was able to decrease apoptosis in a *p53-dependent* pathway, while

simultaneously inhibiting autophagy in an *AMPK/Fox01*-dependent and *mTOR*-independent manner.

Conclusion: Our study was the first to show that aspalathin was able to ablate Doxorubicin-induced cardiotoxicity without decreasing the anti-cancer efficacy of Doxorubicin, in an *in vitro* H9c2 cardio myocyte and Caov-3 ovarian cancer cell model.

ACKNOWLEDGEMENTS

First and foremost, to GOD: For granting me the capability to proceed successfully. This project would not have been a success without Him, indeed He deserves all the Glory

I would like to express my deepest and sincere gratitude to:

My supervisor, Dr Rabia Johnson: I have been extremely lucky to have a supervisor who cared so much about my work, and who responded to my questions and queries so promptly. Her perpetual energy and enthusiasm she has for her research was contagious and extremely motivated me in my research. Her positive outlook and confidence in my research inspired me and gave me confidence. Through her eyes I've seen myself as a capable, intelligent woman who could do anything. Dr Johnson, thank you for showing me how to dissect the challenges into as many different ways as possible and to look at them from different viewpoints, your smart ideas and your bright input have helped me in planning the experiments, in analysing data, in accelerating this dissertation preparation and your careful editing contributed enormously to the production of this dissertation. This dissertation would not have been possible without your extraordinary support.

My Co-Supervisors: My warmest thanks to Dr Christo Muller and Dr Abidemi Kappo I deeply appreciate your support and guidance throughout my project and thank you for your belief in me.

Director of BRIP: Dr Johan Louw, thank you for giving me the opportunity to study with BRIP.

BRIP Staff: I am using this opportunity to express my gratitude to Biomedical Research and Innovation Platform (BRIP) staff for supporting me throughout the course of this project. I am thankful for their guidance, invaluably productive criticism and friendly advice during the project work.

My sincere thanks and appreciation to Dr Phiwayinkosi Dludla, thank you for your excellent technical assistance in the Tissue Culture Lab and your kindly answers to my general questions and for your useful suggestions.

With regards to proofreading of this piece of written work, I wish to acknowledge the following: Samira Ghoor, Charna Chapman, Dr Kwazi Gabuza and Dr Charles Awortwe.

Dr. Sthandiwe Mazibuko, thank you for your encouragement, support and most of all your sense of humor.

Family: My beloved mother (Thembisile Hlomuka) I have no suitable word that can fully describe my mother's everlasting love to me. She has been my inspiration and motivation for continuing to improve my knowledge and move my career forward. She is my rock.

My uncle (Zenzo Hlomuka) and his wife (Jabu Hlomuka) for taking care of my kids, treating them as their own. Words are powerless to express my gratitude for what you have done to me.

My siblings (Thandeka, Sthembelo, Samkelo, Nompilo, Minenhle and Owesihle), my nephew (Anesu) and my niece (Zenande) for their unflagging love and continuous support.

My Best friend: Nozipho Kunene, I thank her for her friendship, love, care and unyielding emotional and morally support. For helping me get through the difficult times and for all entertainment and caring she always provides.

Lastly but not least: My deepest gratitude to my children**:** My son, Unathi Mbongwa and my daughter, Emihle Mbongwa, for understanding when I had to leave them home to pursue my career. I am sorry I wasn't present with you the way children yearn for a mother to be, I know that I missed your sport and prize giving days at school and I hope that one day you can read this dissertation and understand the reason why I spent so much time away from home. Therefore, I dedicate this work to you "Bo Mbuyisa bami" Mommy loves you.

Funders: I gratefully acknowledge the funding sources that made my Master's degree work possible. This research would not have been possible without the financial assistance from NRF Thuthuka Grant (TTK13060618617) and funding from the SAMRC: Research Capacity Development and BRIP baseline.

OUTPUTS

Symposiums, conference proceeding and workshop

Symposium

S.C Shabalala, CJF Muller, J Louw, AMP Kappo, E Joubert, and R Johnson. The effect of Aspalathin on Doxorubicin-induced cardiotoxicity. Biomedical Research and Innovation Platform symposium. 2 November 2015.

S.C Shabalala, CJF Muller, J Louw, AMP Kappo, E Joubert, and R Johnson. Aspalathin-induced autophagy inhibits doxorubicin-induced cardiotoxicity. Biomedical Research and Innovation Platform symposium. 26 October 2016.

Conference

S.C Shabalala, CJF Muller, J Louw, AMP Kappo, E. Joubert, and R Johnson. The effect of Aspalathin on Doxorubicin-induced cardiotoxicity. Stroke and hypertension conference, Johannesburg, South Africa. 19-21 August 2016.

Workshop

S.C Shabalala. Drug discovery workshop: How to progress small molecule hits from screening to efforts. Mauritius.18-22 July 2016

Table of Contents

LIST OF TABLES

LIST OF FIGURES

LIST OF ABBREVIATION

Akt	Protein kinase B
AMP	Adenosine monophosphate
AMPK	Adenosine monophosphate-activated protein kinase
ANOVA	Analysis of variance
Apaf-1	Apoptosis protease activator protein-1
ARC	Agricultural Research Council
ASP	Aspalathin
ATCC	American Type Culture Collection
Atgs	Autophagy-related genes
ATP	Adenosine triphosphate
Bax	Bcl-2-like protein 4
Bcl-2	B-cell lymphoma 2
BNIP3	Bcl-2 interacting protein 3
BSA	Bovine serum albumin
Ca^{2+}	Calcium
Caov-3	ovarian carcinoma cell line
CAT	Catalase
cDNA	Complementary deoxyribonucleic acid
Ct	Threshold cycle
CVDs	Cardiovascular diseases
Cyt c	Cytochrome c

DCFH-DA	Dichlorodihydrofluorescein diacetate
DdH2O	Double distilled water
Dexra	Dexrazoxane
DM	Diabetes mellitus
DMEM	Dulbecco’s Modified Eagle’s Medium
DMSO	Dimethyl sulfoxide
DNA	Deoxyribonucleic acid
Dox	Doxorubicin
DPBS	Dulbecco’s phosphate buffered saline
ECCC	European Collection of Cell Cultures
EGCG	Epigallocatechin gallate
ER	Endoplasmic reticulum
FBS	Fetal bovine serum
FDA	Food and Drug Administration
Fe^{2+}	Ferrous iron
Fox01/03	Forkhead box protein 01/03
GDP	Gross domestic product
GDP	Gross Domestic Product
GPx	Glutathione peroxidase
GSH	Glutathione
H_2O_2	Hydrogen peroxide
H9c2	Rat heart myogenic cell line
HCl	Hydrochloride

HF	Heart failure
HPLC	High performance liquid chromatography
HRP	Horseradish peroxidase
JNK	c-Jun N-terminal kinase
LC-3	Microtubule-associated protein 1 light chain 3
MAPK	Mitogen-activated protein kinase
MDA	Malondialdehyde
mRNA	Messenger ribonucleic acid
MS	Mass spectrometry
mTOR	Mammalian target of rapamycin
NAD	Nicotinamide adenine dinucleotide
NADH	Nicotinamide adenine dinucleotide hydrate
NaOH	Sodium hydroxide
NCDs	Non communicable diseases
NF-Kb	Nuclear factor kappa-B
NRF	National Research Foundation
Nrf2	Nuclear factor erythroid 2-related factor
O_2	Oxygen
$O_2^{\bullet-}$	Superoxide radical
$OH^{\bullet}$	Hydroxyl radical
OXPHOS	Oxidative phosphorylation
P38-MAPK	P38 mitogen-activated protein kinases
P62	Nucleoporin p62

PBS	Phosphate-buffered saline
PCR	Polymerase chain reaction
PE	Phosphatidylethanolamine
Pen/strep	Penicillin- streptomycin
PGC-1 co-activator	Peroxisome proliferator-activated receptor (PPAR) gamma
ERK	Extracellular signal-regulated protein kinase
PI	Propidium iodide
PI3K	Phosphatidylinositol 3-phosphate kinase
PMSF	Phenylmethylsulfonyl fluoride
PVDF	Polyvinylidene fluoride
Resv	Resveratrol
RNA	Ribonucleic acid
ROS	Reactive oxygen species
RT	Reverse transcription
RT	Room temperature
RT-Minus	Reverse transcriptase-Plus
RT-Plus	Reverse transcriptase-Plus
SAMRC	South African Medical Research Council
SDS-Page	Sodium dodecyl sulfate poly-acrylamide gel electrophoresis
Sirt1	Sirtuin 1
SOD	Superoxide dismutase
TBARS	Thiobarbituric Acid Reactive Substances

TBST	Tris-buffered saline containing Tween-20
TC	Tissue culture
Top2β	Topoisomerase Iiβ
Tris	Trizma
TSC1/2	The tuberous sclerosis complex 1/2
ULK1	Serine/threonine-protein kinase
Vps34	Phosphatidylinositol-3 –kinase
WHO	World Health Organisation
β-ME	β-Methylphenethylamine

CHAPTER 1

INTRODUCTION

1.1 Introduction to the present study

Implementation of cancer therapies has made notable improvements in the management and treatment of a variety of adult and pediatric cancers such as lung cancer, breast cancer, ovarian cancer as well as leukemia and sarcomas (Miller *et al*., 2016). In the last 4 decades the overall cancer survival rate has increased from 58% in the mid- 1970s to 83% in 2010 (Lipshultz and Adams, 2010). This increase in the cancer survival was ascribed to the introduction of anthracyclines as part of the chemotherapeutic regimens. Anthracycline is a class of chemotherapeutic agents derived from *Streptomyces peucetius* that are used in the management of a variety of solid and hematological tumors (Volkova and Russell, 2011). The major drugs in this class include daunorubicin, doxorubicin (Dox), epirubicin and idarubicin.

Doxorubicin, a hydroxyl derivative of daunorubicin, is a frequently prescribed first line chemotherapeutic agent used either as a monotherapy or in combination with other anti-cancer drugs in the treatment of various malignancies (Takemura and Fujiwara, 2007, Octavia *et al*., 2012). Though effective, the efficacy of Dox has been hindered by its dose-dependent (acute) and cumulative (chronic) cardiotoxic adverse effects (Diotte *et al*., 2009). Acute cardiotoxicity has a prevalence of 11% and can manifest as chest pain that occur within two–three days after receiving a high dose of Dox (Takemura and Fujiwara, 2007). The mechanism of acute cardiotoxicity has been ascribed to edema, a condition that can be clinically reversed and is for the most part manageable (Singal *et al*., 1987, Chatterjee *et al*., 2010). Conversely, chronic cardiotoxicity is irreversible, has a prevalence of 27%, occur 6-10 years after cessation of Dox treatment and is more dangerous as it manifests as heart failure (Kumar *et al*., 2012, Rahman *et al*., 2007).

The incidence of chronic cardiotoxicity is primary related to its cumulative dose, with a dose of 500-550 mg/m^2 having an incidence of 4%, however this risk increased to 36% when the dose exceeds 600 mg/m^2 (Swain *et al*., 2003). Apart from a cumulative dose, age can influence the risk of developing heart failure, with childhood cancer survivors and the elderly having an increased at risk of developing Dox-induced heart failure (Von Hoff *et al*., 1979, Octavia *et al*., 2012). Children receiving Dox treatment are particularly affected as 18% of these cancer survivors show cardiac abnormalities 4-5 years after

administration and this number is increased to 38% after 10 years (Chatterjee *et al.,* 2010). Furthermore, the prognosis in these young adults is poor with a mortality rate of 50% within a year after diagnosis (Chatterjee *et al*., 2010). As yet, numerous attempts have been made to find a better treatment regimen with lower toxicity. This include the development of anthracycline analogues. However, none have been successful to date (Nair *et al*., 1998, Narula *et al*., 1996, Smith *et al*., 2010).

Understanding the mechanisms whereby Dox can elicit cardiotoxicity can aid in the development of alternative chemotherapeutic drugs that can lessen its cardiotoxic side effects. It is well known that hydroxyl radical ($OH^{\bullet}$) production is the main proposed theory by which Dox induces its cardio toxic side effect and this was evident in the observed increase in reactive oxygen species (ROS) and lipid peroxidation in biopsies from heart failure patients on Dox treatment (Doroshow, 1983, Minotti *et al.,* 2004, Swain *et al*., 2003, Takemura and Fujiwara, 2007). Thus, needless to say, current focus is on the use of antioxidant therapy to lessen the venomous action of Dox on cardiac cells (Thorn *et al*., 2011).

Plant-derived polyphenols have recently drawn the attention of researchers due to their health promoting and antioxidants properties (Lecour and Lamont, 2011, Pandey and Rizvi, 2009, Zern and Fernandez, 2005). Moreover, plant-derived polyphenols are known to have no (or less) adverse side effects and recently strong evidence came to the forefront implicating polyphenols to be effective against the development of various diseases including diabetes mellitus, cancers and cardiovascular diseases (CVDs) (Pandey and Rizvi, 2009, Scalbert *et al.,* 2005).

In the present study, of particular interest was Aspalathin (ASP), a dihydrochalcone *C*-glucoside that is unique to *Aspalathus linearis* (commonly known as rooibos). Aspalathin is known to have strong antioxidant properties (Snijman *et al*., 2009, Chen *et al*., 2013) and was able to protect cardiomyocytes against high glucose-induced oxidative stress and cell apoptosis (Johnson *et al*., 2016). In a study done by Dludla *et al.* It was shown that this compound was able to decrease cardiac dysfunction by suppressing oxidative stress, inflammation and cell apoptosis in both an *in vitro* and *ex vivo* cell culture model

(Dludla *et al*., 2014). Furthermore, preliminary data from our group showed that H9c2 cells exposed to 33 mM glucose and post treated with ASP resulted in a 2-fold increase in various anti-oxidant genes (*DJ1, Nrf2, PARK, Nqo1, Gpx, UCP2, Txnrd, SOD1, Prdx1 and GSH*) inferring that ASP exerts its cardioprotective effect through the inhibition of glucose-induced oxidative stress. However, the effect of ASP to protect the myocardium against Dox-induced cardiotoxicity has not yet been established.

Thus, in this present study, we hypothesized that ASP can decrease cardiotoxicity and myocardial apoptosis.

1.2 Aims of the study

In this study, we aim to investigate the potential use of ASP, a dihydrochalcone C-glycoside, in alleviating Dox-induced cardiotoxicity in an H9c2 cell culture model.

Specific Aims:

1. To investigate if ASP treatment can alleviate oxidative stress, lipid peroxidation and cell apoptosis in H9c2 cells exposed to Dox.
2. To determine if ASP co-treatment can decrease cardiotoxicity without reducing the anti-cancer efficacy of Dox.
3. To compare the effect of ASP co-treatment with the current FDA approved drug, Dexrazoxane.
4. To determine the mechanism by which ASP may alleviate Dox-induced cardiotoxicity.

CHAPTER 2

LITERATURE REVIEW

2.1 Non-communicable diseases

Non-communicable diseases (NCDs) are a major contributor to the global burden of disease and can be defined as a chronic condition that is non-transmissible and non-infectious (Kim and Oh, 2013). NCDs are responsible for almost 70% of all deaths globally and is expected to increase by a further 17% over the next 10 years (WHO, 2008). This increase in morbidity and mortality of NCDs does not only result in a reduced quality of life and loss of human life expectancy, but imposes a heavy financial cost on a country's health system and national budget. It has been projected that NCDs will globally cost more than US$ 7 trillion, representing 48% of global gross domestic product (GDP) in the next 20 years (Bloom *et al.*, 2011). Globally, CVDs are the leading cause of NCDs deaths accounting for 17.5 million, followed by cancers (7.6 million), chronic respiratory diseases (4.2 million) and diabetes (1.3 million) (World Heart Federation, 2014). In total, these NCDs account for about 80% of all deaths (WHO, 2016). In South Africa (S.A), NCDs accounts for 43% of all deaths, with CVDs being the major cause of mortality in Sub-Saharan Africa (Figure 2.1) (World Heart Federation, 2016).

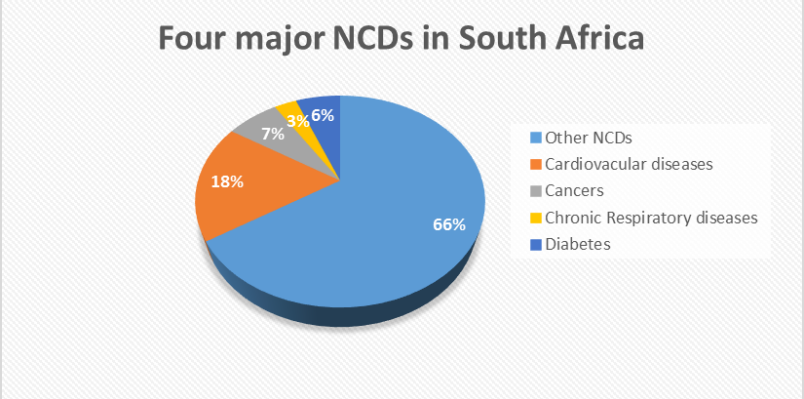

Figure 2.1: Non-communicable diseases (NCDs) in South Africa: Cardiovascular diseases are the major cause of mortality globally as well as in South Africa, accounts for 43% of all deaths (WHO, 2014). Adapted from (South African Heart Association, 2014)

2.2 Cardiotoxicity of chemotherapeutic agents

Cardiovascular diseases are classified as the major cause of morbidity and mortality globally, affecting over 26 million individuals (WHO, 2016). About 17.5 million people died of CVDs in 2012, representing 31% of the global deaths (WHO, 2016).

2.2.1 The effect of cancer treatment on CVD

In cancer survivors, CVDs are the most frequent cause of morbidity and mortality in long-term cancer survivors. This increase in mortality is a result of increased cardiotoxicity associated with cancer treatment (Aleman *et al*., 2014). Improvement in remedial therapies for cancer have contributed to an enhanced cancer survival rate, however, cardiotoxicity still remains a problem especially among young adult cancer survivors (Hudson *et al*., 2012). The incidence of heart disease is remarkably increased in young cancer survivors compared to their unaffected siblings (Lipshultz and Adams, 2010). This increase in the heart failure incidence is associated with a number of chemotherapeutic agents which includes anthracyclines, trastuzumab, capecitabine, arsenic trioxide and tyrosine kinase inhibitors (Table 2.1).

Table 2.1: Effect of chemotherapeutic agents on cardiac structure and function

Chemotherapeutic agents	Effect on the heart	Time of onset	Severity
Anthracyclines	Myocytes toxicity	Weeks (acute) to decades (chronic)	Dose-dependent Chronic irreversible and acute reversible
Trastuzumab	Contractile dysfunction	Weeks	Reversible
Arsenic trioxide	Prolong QT intervals	Immediate	Rarely result in death
Tyrosine kinase inhibitors	Vasculature, Myofibril dysfunction, Edema or Prolong QT interval	Days to months	Temporarily
Capecitabine	Coronary vessels	Immediate	Reversible

Adapted from: Ewer and Ewer, (2015)

As mentioned, the listed chemotherapeutic agents are known to mitigate cancer, but increase the incidence of heart failure. Various observational studies confirmed that chemotherapeutic agents are known to cause long-term cardiovascular side effects,

decreasing the quality of life of cancer survivors (Shakir and Rasul, 2009, Octavia *et al*., 2012). Cardiovascular side-effects induced by these anti-cancer drugs can be either reversible or irreversible. Reversible cardiotoxicity induces temporary cardiac dysfunction, while irreversible cardiotoxicity is associated with myocardial death leading to left ventricular dysfunction that can progress to heart failure (Chatterjee *et al*., 2010). Anthracyclines, a class of one of the most effective chemotherapeutic agents, are known to induce irreversible cardiovascular side effects.

2.3. Anthracyclines

Anthracyclines are highly effective chemotherapeutic agents that are valuable in the treatment of a wide variety of adult and pediatric cancers (Octavia *et al*., 2012). The family of anthracyclines was identified in the early 1950s with the discovery of daunorubicin from the soil bacterium *Streptomyces peucetius* (Di Marco *et al*., 1981, Volkova and Russel 2011). However, daunorubicin was only found to be effective against the treatment of specific leukemia's and lymphomas (Tan *et al*., 1967). In the 1960's, a derivative of daunorubicin, later renamed as doxorubicin (Dox), was identified and was shown to be a more effective chemotherapeutic agent (Volkova and Russel, 2011). Since the introduction of anthracyclines, the 5-year cancer survival rate has increased from 50% in the mid-1970s to approximately 80% in 2010 and this was observed in both pediatric and adolescent cancer survivors (Figure 2.2) (Lipshultz and Adams, 2010). However, the effective use of anthracycline chemotherapy is hampered due to its cardio toxic side effect (Smith *et al*., 2010), especially in the case of Dox that induces cardiotoxicity in a dose-dependent manner. The current knowledge of anthracycline-induced cardiotoxicity is derived from a retrospective study where patients with cancer developed heart failure during and after chemotherapy (Groarke and Nohria 2015).

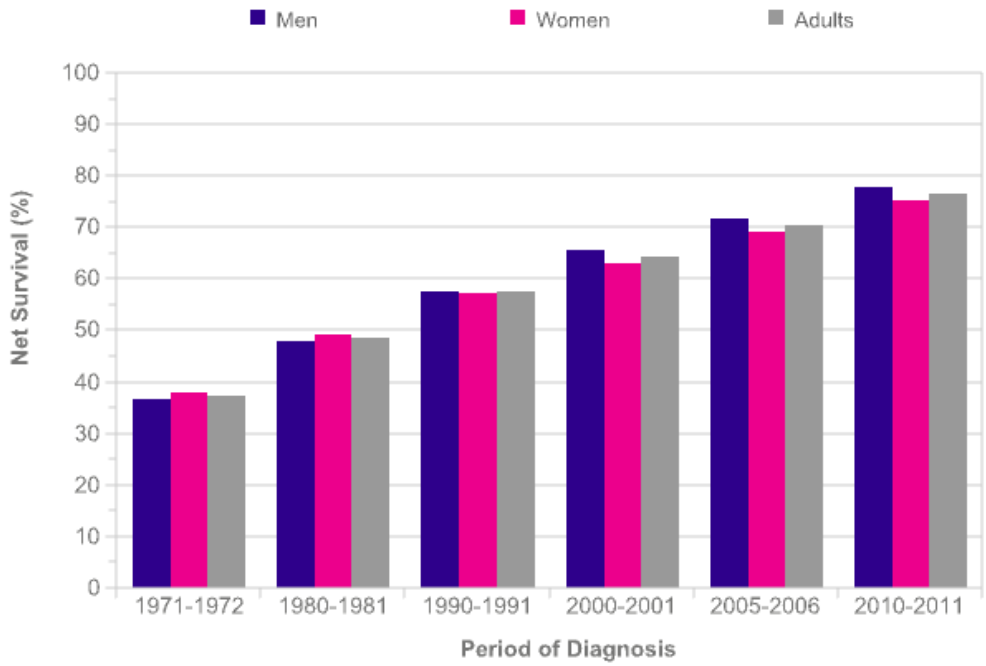

Figure 2.2: The 5-year cancer survival rates: The survival rate has increased from less than 50% in 1971 to approximately 80% in 2011. Taken from (Cancer Research UK, 2013)

2.3.1 Doxorubicin efficacy and cardiotoxicity

Doxorubicin (Dox), sold under the trade name of Adriamycin, has been employed in the treatment of a wide variety of hematological malignancies, carcinomas and solid sarcomas (Dimitrakis *et al*., 2012). Though Dox has become one of the most effective chemotherapeutic agents, its efficacy has been hindered by its dose-dependent (acute) and cumulative (chronic) cardio toxic side effects (Von Hoff *et al*., 1979). Dox-induced cardiotoxicity usually occurs within 2-3 days after receiving a high dose of Dox, also referred to as an acute onset (Hydock *et al*., 2009, Takemura and Fujiwara, 2007). This type of cardiotoxicity is characterized by a prolonged Q-waves and T-waves interval and is prominently identified in adults older than 65 years and children younger than 5 years (Takemura and Fujiwara, 2007). The acute cardiotoxicity can be reversed and clinically managed (Chatterjee *et al*., 2010). However, this is not the case with chronic Dox-induced cardiotoxicity that is known to develop 10-15 years after the cessation of Dox chemotherapy (Kumar *et al*., 2012). Chronic Dox-induced cardiotoxicity is characterized by left ventricular dysfunction, a distinctive heart failure (HF) pathology that cannot be

clinically managed or reversed (Rahman *et al*., 2007). The manifestation of this lethal form of cardiotoxicity is directly related to the cumulative dose of Dox. In a study by Swain and colleagues (2003), it was shown that patients who received a cumulative dose of 400 mg/m^2 of Dox were associated with a 5% increased risk of HF. This risk increased by 26% and 48% with the use of 550 mg/m^2 and 700 mg/m^2 of Dox, respectively (Table 2.2) (Swain *et al*., 2003). Furthermore, in the respective analyses which included more than 4000 patients receiving Dox treatment, 2.2% of these patients developed congestive heart failure (Von Hoff *et al*., 1979). This study went on to demonstrate that a cumulative dose of more than 550mg/m^2 resulted in a severe increase of heart failure. Interestingly, Billingham and colleagues (1978) showed that patients receiving a little as 240 mg/m^2 of Dox, developed histopathological changes as could be seen in myocardial biopsies (Billingham *et al*., 1978). Thus needless to say, chronic Dox-induced cardiotoxicity remains a severe problem, especially in pediatric oncology (Lipshultz *et al*., 2013) as there is no safe dose of Dox for children younger than five years. Years after the cessation of Dox treatment, these young cancer survivors who would be in the prime of their life, supposed to be part of the work force but due to the delayed onset of cardiotoxicity. They will instead be a financial burden on individuals (poor households), the country's health system and the national budget. Despite these pitfalls, the use of traditional cytotoxic drugs continues to be the mainstay treatment for several types of cancer (Ojha *et al*., 2016).

Table 2.2: Dose related incidence of Dox-induced heart failure

Dox dosage (mg/m^2)	Incidence (%)
400	3-5
450	5-8
500	6-26
700	48

2.4 Mechanism by which Dox induces apoptosis of cancer cells

Understanding the mechanism by which Dox induces apoptosis in cancer cells will allow for the development of improved strategies to attenuate cardiac damage. It has been proposed that the pathogenesis of Dox-induced cardiotoxicity is multifactorial and can be directly linked to the metabolism and chemotherapeutic activity of the anti-cancer agent (Octavia *et al*., 2012). In cancer cells, the chemotherapeutic efficacy of Dox is known to be associated with the enhanced production of ROS, which leads to the aggravation of oxidative stress and subsequent lipid peroxidation (Barrera, 2012). Dox-induced apoptosis in cancer cells has been linked to the ability of the chemotherapeutic agent to inhibit the deoxyribonucleic acid (DNA) topoisomerase-II β (Top2β) enzyme which leads to activation of p53 and subsequent death of cancer cells (Cummings *et al*., 1991, Gewirtz, 1999, Gamen *et al*., 2000, Ravizza *et al*., 2004). It has been proposed that the clinical concentration of Dox does not always induce apoptosis in cancer cells by triggering p53 (Laurent and Jaffrezou, 2001). However, it was shown that Dox-induced apoptosis by releasing cytochrome c (Cyt c) from the mitochondria (Green and Leeuwenburgh, 2002), inferring that Dox can induce apoptosis in a p53-dependent and independent manner.

2.5 Mechanisms of Dox-induced cardiac injury

More than four decades after Dox was introduced for the first time, the exact mechanism by which Dox-induced cardiotoxicity occur is still unclear. However, several mechanisms have been proposed that may contribute to the pathogenesis of Dox-induced cardiotoxicity (Figure 2.3). This includes i) increased oxidative stress and lipid peroxidation (Wallace, 2003, Singal *et al*., 1987), ii) DNA damage and apoptosis (Kotamraju *et al*., 2000, L'Ecuyer *et al*., 2006) and more recently iii) autophagy.

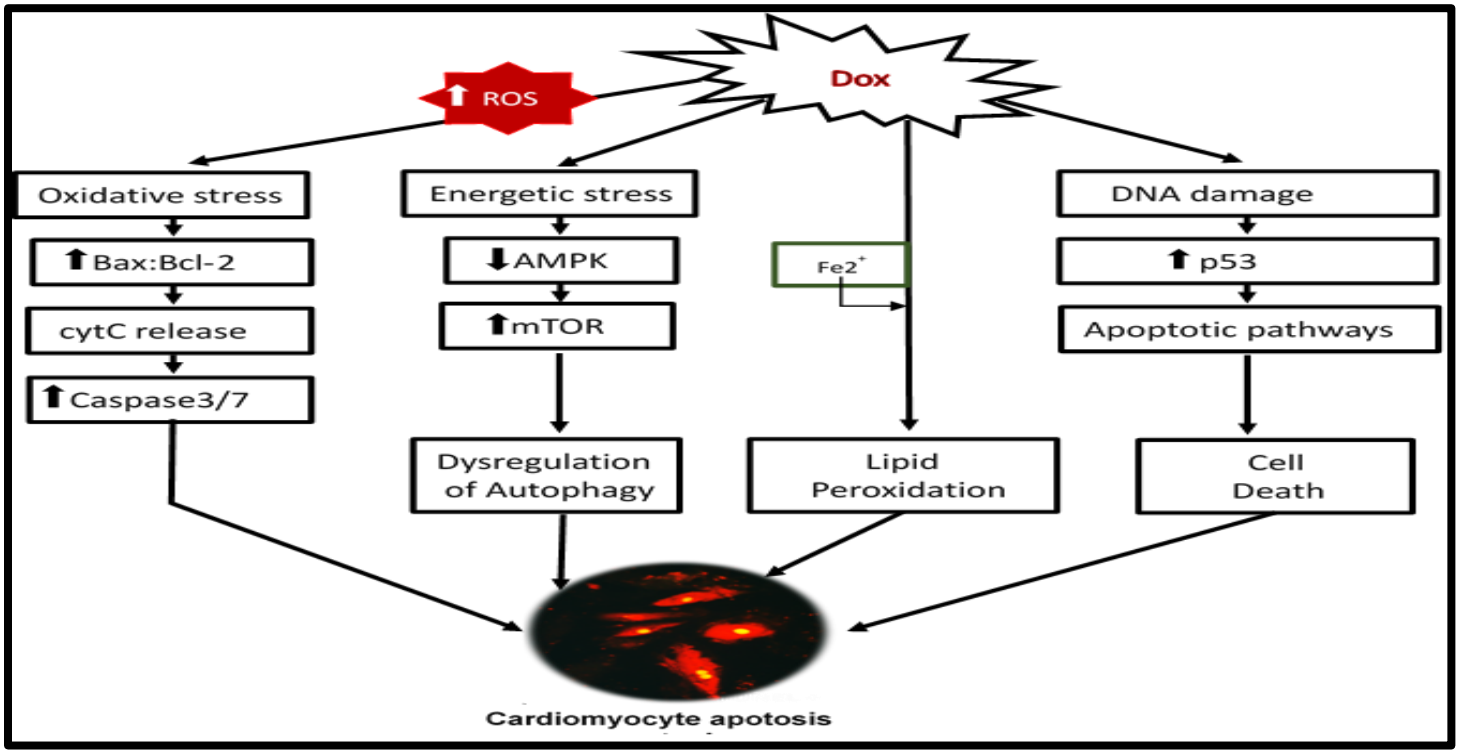

Figure 2.3: Proposed mechanisms of Dox-induced cardiotoxicity: Several mechanisms have been proposed to aggravate Dox-induced cardiotoxicity. Formation of reactive oxygen species (ROS) accounts for the primary mechanism through which Dox leads to the formation of reactive oxygen species and subsequent cell death. Dox directly intercalates with DNA topoisomerase -II β as well as forming a Dox-iron complex, leading to increased lipid peroxidation and cardiac death. Dox has also been shown to dysregulate autophagy through an mTOR/AMPK dependent pathway. AMPK: 5' AMP-activated protein kinase, Bax: Bcl-2-like protein 4, Bcl-2: B-cell lymphoma-2, Cyt c: Cytochrome C, Fe^{2+}: Ferrous iron, mTOR: Mammalian target of rapamycin, ROS: reactive oxygen species.

2.5.1 Oxidative stress

Oxidative stress can be defined as a condition in which an imbalance exist between the bodies pro- and antioxidant system (Bhattacharyya *et al*., 2014). Increased oxidative is a consequence of aberrant ROS production, a process associated with impaired endogenous antioxidant levels (Nita and Grzybowski, 2016). Increased oxidative stress is well-known process known to play a major role in oxidative DNA damage and subsequent lipid peroxidation as observed during Dox-induced cardiotoxicity. Lipid peroxidation is the oxidative degradation of lipids, which results in the formation of reactive aldehydes, such as malondialdehyde (MDA) and 4-hydroxynonenal (HNE).

2.5.1.1 Dox-induced cardiotoxicity and increased oxidative stress

Oxidative stress is one of the primary mechanisms of Dox-induced cardiotoxicity, prompted by excessive generation of ROS (Wallace, 2003, Octavia *et al*., 2012). This statement has been supported by the cytoprotective effect of various antioxidants tested against Dox-induced cardiotoxicity (Kumar *et al*., 2002). Furthermore, various studies have proved that Dox induces its cardio toxic effect by directly altering mitochondria through increased ROS production.

Mitochondria as a target for Dox-induced cardiotoxicity oxidative stress.

Studies have shown that Dox accumulates in mitochondria and disrupts the mitochondria electron chain resulting in an enhanced production of ROS (Sarvazyan, 1996). Moreover, mitochondria's NADH-dependent enzymes reduce Dox to a corresponding semiquinone radical that can undergo redox cycling to form superoxide radicals ($O_2^{\bullet-}$) and H_2O_2 (Minotti *et al*., 2004) (Figure 2.4). The resultant $O_2^{\bullet-}$, in the presence of ferrous iron (Fe^{2+}), is further converted to a highly reactive hydroxyl radical ($OH^{\bullet}$). Furthermore, Dox has been suggested to interact with Fe^{3+} forming a Dox-Fe^{2+} complex that undergoes redox cycling, increasing the generation of $OH^{\bullet}$ (Ichikawa *et al*., 2014). These highly reactive radicals can react with proteins, lipids and DNA molecules, causing DNA damage and lipid peroxidation (Sharma *et al*., 2012, Valko *et al*., 2004). This enhanced production of reactive radicals can be neutralized by the body's endogenous antioxidant defense system. These antioxidants include enzymatic antioxidants such as SOD, CAT and

glutathione peroxidase (GPx), as well as a non-enzymatic antioxidant, GSH (Bhattacharyya *et al.*, 2014).The primary role of these endogenous antioxidants is to detoxify highly reactive radicals. SOD is known to catalyze the reduction of $O_2^{\bullet-}$ into O_2 and H_2O_2 (Fukai and Ushio-Fukai, 2011). In the presence of metal Fe^{2+}, H_2O_2 is further reduced to $OH^{\bullet}$. To prevent this increase in the production of $OH^{\bullet}$, CAT detoxifies H_2O_2 to form O_2 and water (Bhattacharyya *et al*., 2014). In the presence of low levels of CAT, GPx together with GSH forms a glutathione complex which convert H_2O_2 to O_2 and water. However, increased oxidative stress within the heart can be detrimental as it lacks a strong antioxidant defense mechanism (Aryal *et al*., 2014). Thus, chronic exposure of Dox is the primary cause of oxidative damage in vulnerable cardiac cells. This in turn induces cell membrane permeability leading to myocardial dysfunction and subsequently the development of cardiac dysfunction.

2.5.2 Apoptosis

Mitochondrial depolarization and subsequent apoptosis is a hallmark of additional Dox-induced cardiotoxicity. Both *in vivo* and *in vitro* studies have shown that Dox treatment induces oxidative stress which is associated with the activation of cardiomyocyte apoptosis (Kotamraju *et al*., 2000, Tsang *et al*., 2003). Apoptosis can be defined as a highly regulated form of programmed cell death. This process is suggested to depend on the activation of caspases (Elmore, 2007) and is regulated by two evolutional conserved pathways, the extrinsic and intrinsic pathways (Elmore, 2007). The extrinsic pathway, also known as death receptor pathway is characterized by the activation pro- apoptotic ligands and receptors on the cell surface (Kalimuthu and Se-Kwon, 2013). This activation of pro-apoptotic receptors leads to formation of the death-inducing signalling complex. The intrinsic pathway is characterized by the release of Cytochrome c (Cyt c) from the mitochondria into the cytosol where it activates caspases (Crompton, 2000). The release of Cyt c is regulated by the members of B-cell lymphoma 2 (Bcl-2) family of proteins which includes both pro-apoptotic Bcl-2-like protein 4 (Bax) and anti-apoptotic (Bcl-2) proteins (Tsujimoto, 1998). Bax is located in the cytosol, and upon activation, Bax translocates to the outer mitochondrial membrane. This translocation of Bax to the membrane

depolarizes the mitochondrial membrane and stimulates the release of Cyt c into the cytosol, whereas Bcl-2 inhibits the release of Cyt c from mitochondria (Saelens *et al*., 2000). Once released, Cyt c in the cytosol forms an apoptosome complex with an adaptor protein, apoptosis protease activator protein-1 (Apaf-1) and caspase 9 resulting in the activation of caspase 3 (Parrish *et al*., 2013). Studies have shown that Dox decreases the ratio of Bcl-2/Bax, triggering cardiomyocyte apoptosis (Tsang *et al*., 2003, Spallarossa *et al*., 2004). Furthermore, increasing evidence has shown that Dox-induced apoptosis in cardiac cells is associated with the activation of a tumor suppressor protein, p53 (Liu *et al*., 2004, L'Ecuyer *et al*., 2006). Various studies have shown that p53 induces apoptosis through the increased expression of Bax while suppressing Bcl-2 levels (Yee and Vousden, 2005).

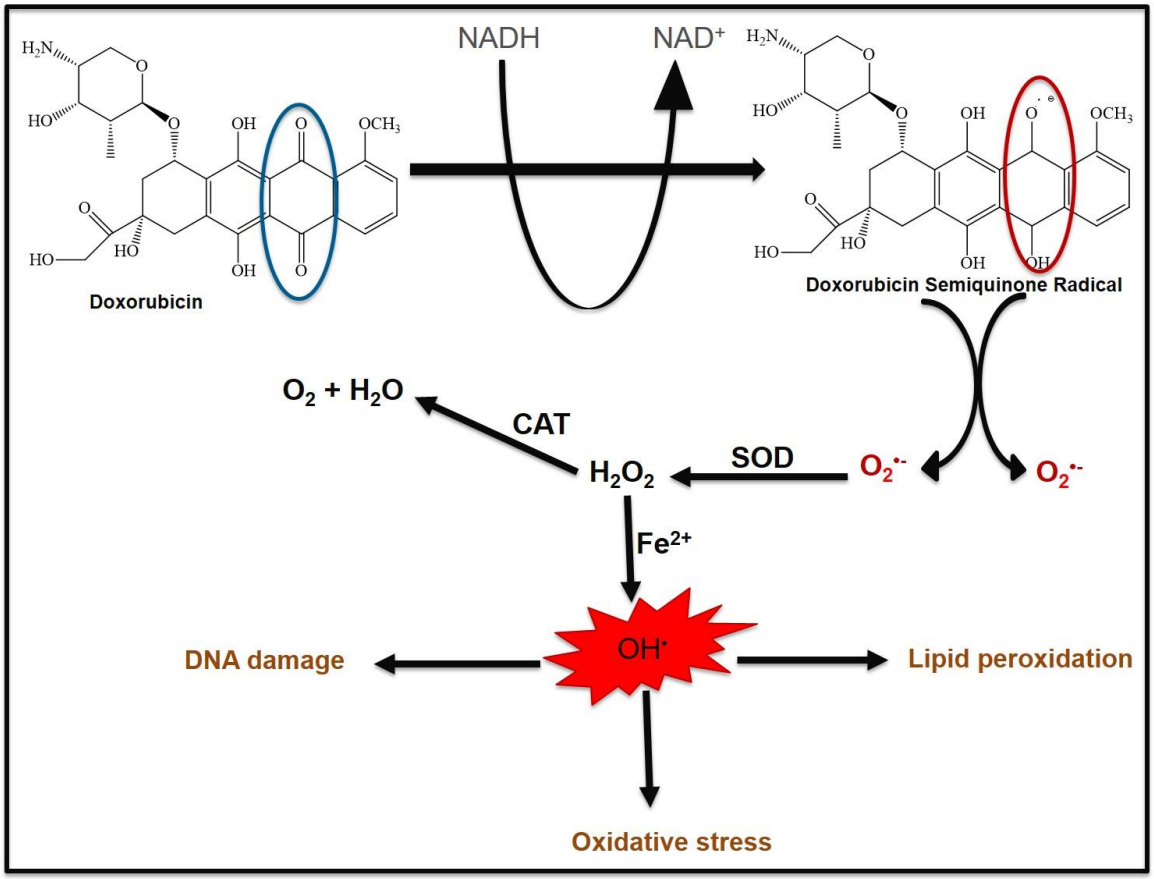

Figure 2.4: Dox mediated redox cycling: Dox is reduced by mitochondrial nicotinamide adenine dinucleotide hydrate (NADH)-dependent enzymes into a semiquinone. This semiquinone undergoes redox cycling to generate superoxide anion, which is detoxified by superoxide dismutase (SOD) to yield hydrogen peroxide (H_2O_2) and water. Hydrogen peroxide, in the presence of iron (Fe^{2+}) is converted to a highly reactive hydroxyl radical $OH^{\bullet}$ that reacts with DNA, proteins and lipids leading to DNA damage and subsequent lipid peroxidation. **CAT**: Catalase, **Fe^{2+}**: Iron, **H_2O_2**: Hydrogen peroxide, **H_2O:** Water, **$OH^{\bullet}$**: Hydroxyl radical, **$O_2^{\bullet}$**: Superoxide anion, **O_2**: Oxygen, **SOD**: superoxide. Adapted from: (Riddick et al., 2005)**.**

2.5.3 Autophagy

Autophagy can be defined as a highly conserved process that eliminates long-lived proteins and damaged organelles from the cell (Hale *et al*., 2013). This dynamic process is essential for normal cellular maintenance and homeostasis. However, autophagy is known to be involved in the pathogenesis of various diseases such as cardiomyopathy, myocardial hypertrophy and ischemic/reperfusion injury (Xie *et al*., 2011). Various forms of autophagy have been described including (i) macro autophagy (ii) micro autophagy and (iii) chaperone-mediated autophagy (Mizushima, 2007). Macro autophagy (referred to as autophagy), is the most studied form of autophagy and is highly preserved within eukaryotic cells. This form of autophagy is characterized by the formation of an autophagosome, a specialized double membrane vesicle, that engulfs aggregated proteins and damaged organelles (Yang and Klionsky, 2009). Once formed, the autophagosome is sequestrated and ultimately fuses with the lysosome where it is degraded (Nakatogawa *et al*., 2009).

2.5.3.1 Stimulation of autophagy

Stimulation of autophagy results in the stimulation of a signalling cascade that will either induce or inhibit autophagy (Figure 2.5). This signalling cascade can be activated by nutrient deprivation or energy depletion. Conversely, autophagy can be inhibited by insulin and growth factor signalling (Inguscio *et al*., 2012).

I. The response to energy depletion: It has been reported that the induction of autophagy is inversely proportional to the synthesis of proteins within a cell (Lilienbaum, 2013). During starvation or energy depletion, the energy consumption process such as protein synthesis is supressed as adenosine triphosphate (ATP) levels decrease. The decrease in the ratio of ATP to adenosine monophosphate (AMP) leads to phosphorylation of adenosine monophosphate-activated protein kinase (AMPK), a well-known energy sensor (He and Klionsky, 2009). The activation of AMPK results in the increased expression of tuberous sclerosis complex 1/2 (TSC1/2), which inhibits the mammalian target of rapamycin (mTOR),

a known suppressor of autophagy (Inoki *et al*., 2003). This suppression of mTOR enhances autophagy turnover and subsequently increases ATP production through recycling of nutrients (He and Klionsky, 2009).

II. The response to nutrient deprivation: Nutrient deprivation can also induce autophagy via an mTOR independent pathway. In this pathway NAD activates Sirtuin 1 (Sirt1) to deacetylate Forkhead box protein 03 (Fox03) which then directly activates autophagy-related genes (Atgs) (Ou *et al*., 2014). Once activated, these Atgs form a complex that will regulate the different steps in the autophagy process.

III. The response to insulin and stimulation of growth factors: Autophagy can be negatively regulated to maintain normal cellular function. The regulation of autophagy during insulin signalling and hormonal growth is different compared to nutrient regulation.(Sengupta *et al*., 2010) However, both stimuli converge on mTOR (He and Klionsky, 2009). During insulin or hormonal signalling, the phosphatidylinositol-4, 5-bisphosphate 3-kinase (PI3K)/serine-threonine protein kinase (Akt) pathway is activated. Activation of Akt leads to the inhibition of the TSC1/2 complex. Inhibition of this complex results in the activation of mTOR and suppression of autophagy (Laplante and Sabatini, 2009).

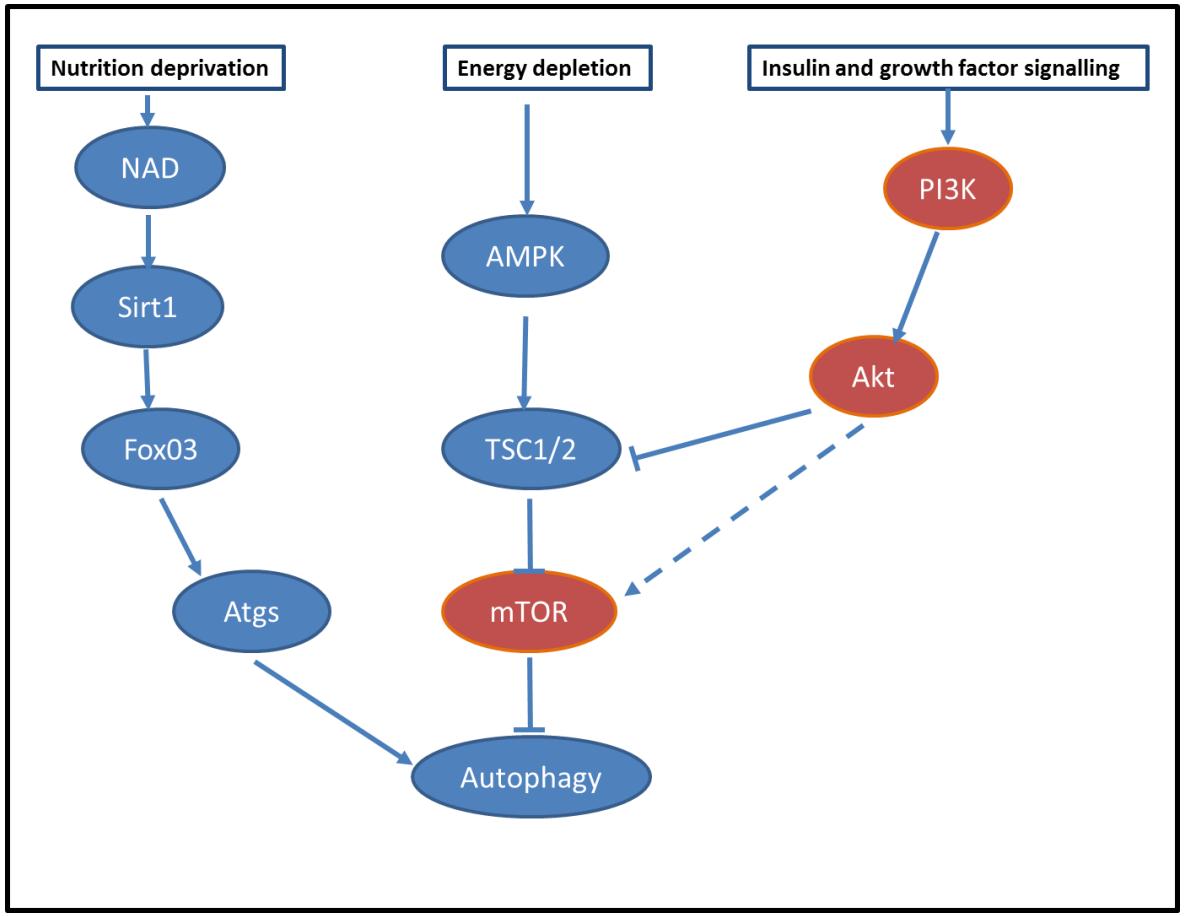

Figure 2. 5: Stimulation of autophagy via various stress-induced mechanisms: During stress stimuli such as nutrient deprivation, energy depletion, oxidative stress and insulin resistance nicotinamide adenine dinucleotide (NAD) and adenosine monophosphate (AMP) are stimulated resulting in the activation of adenosine monophosphate kinase (AMPK) and subsequently activation of mTOR. Sirt1 stimulation regulates autophagy via deacetylation of Forkhead box 03 (Fox03) and autophagy-related genes.

2.5.3.2 Autophagosome formation and maturation into autolysosomes

The formation of the autophagosome is under the control of Atgs that are required to form a core complex (He and Klionsky, 2009). This complex is regulated by five core steps during the autophagy process and includes initiation, nucleation, elongation, maturation and degradation (Eskelinen and Saftig, 2009) (Figure 2.6).

As previously described, mTOR is one of the main negative regulators of autophagy. During stress stimuli, the inhibition of mTOR results in the activation of Atg1, activated Atg1 then forms a complex with Atg13 to initiate the autophagy process (He and Klionsky, 2009). Activated Atg1 triggers the formation of a Beclin1/phosphatidylinositol-3-kinase (Vps34) complex through phosphorylating Beclin1, an essential protein in the nucleation of the autophagosomal vesicle. (Kihara *et al*., 2001). However, the formation of this complex can be inhibited by the interaction of Bcl-2 with BH3 domain of Beclin 1 (Kang *et al*., 2011). Nevertheless, Pattingre *et al* (2005) showed that the Beclin 1 complex is inhibited by the endoplasmic reticulum (ER)-localized Bcl-2 and not the mitochondrial-localized Bcl-2 (Pattingre *et al*., 2005). After the process of nucleation, autophagosomal elongation and maturation occurs. This process involves the activation of microtubule-associated protein 1 light chain 3 (LC3), a protein that plays a major role in the formation and maturation of the autophagosomes (He and Klionsky, 2009). During this process LC3-I conjugates with phosphatidylethanolamine (PE) forming an insoluble form, LC3-II (Kabeya *et al*., 2000). This conjugation of LC3-I to PE is regulated by the Atg12/5/Atg16 complex and Atg7 (He and Klionsky, 2009).The non-soluble LC3-II is then inserted into the autophagosomal membrane where it promotes elongation and maturation of the autophagosomal membrane together with Atg12-Atg5 complex (Yang *et al*., 2015). In the final stage the cargo of the autolysosome is degraded and the resultant amino acids are recycled into the cytoplasm.

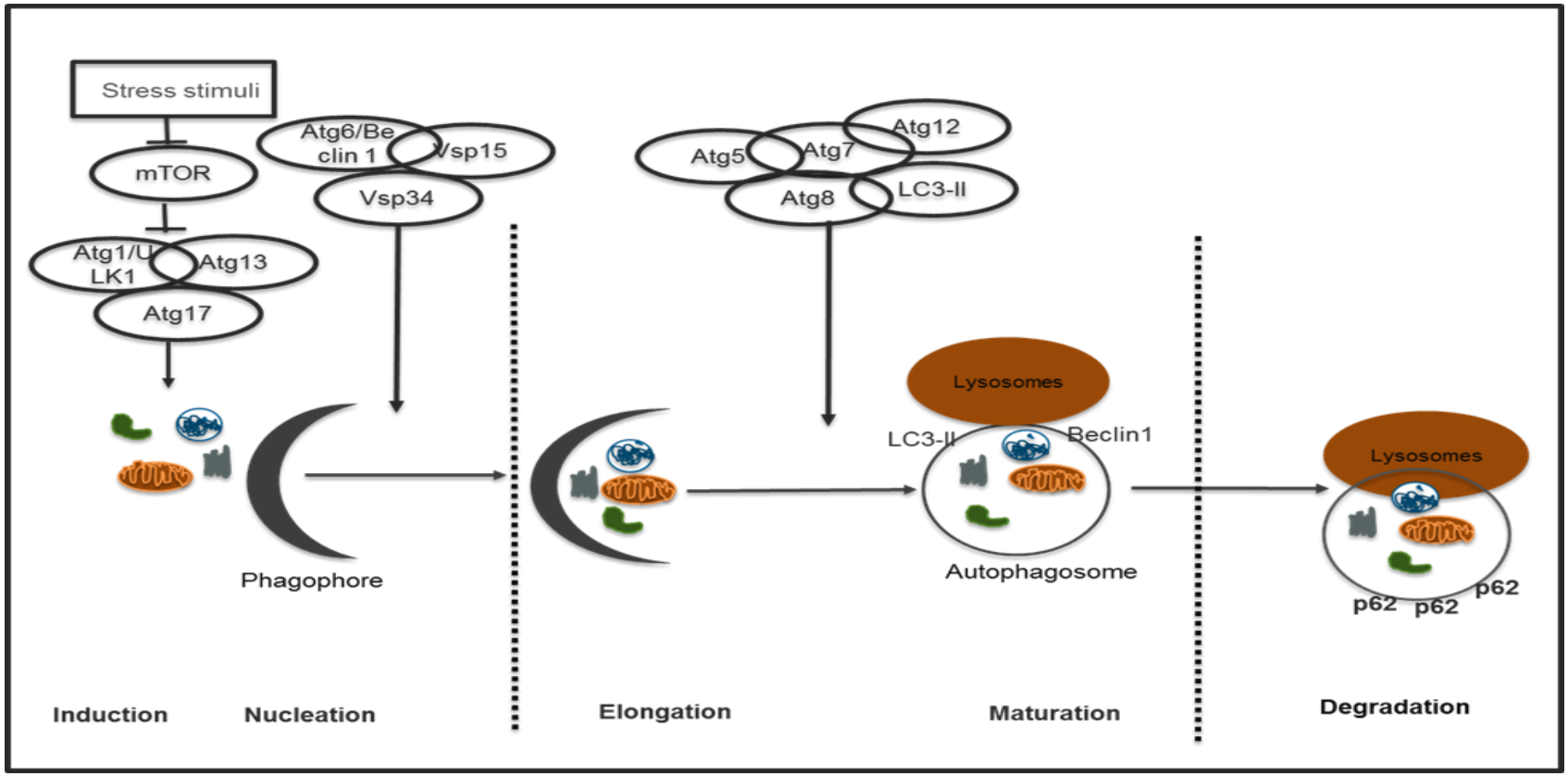

Figure 2.6: A schematic diagram of the autophagosome formation and maturation: During autophagy a double membrane-bound vesicle called the autophagosome is sequestrated to lysosomes where proteolytic degradation occurs. Adapted from (Eskelinen and Saftig, 2009).

2.5.3.3 The role of autophagy in Dox-induced cardiotoxicity

Autophagy plays a dual role in the management and progression of cardiac dysfunction. Under physiological conditions, autophagy is constitutively expressed in order to enhance normal cellular function and survival. This process is carefully regulated as excessive dysregulation of autophagy can be detrimental to normal cardiac function. In a condition such as ischemic preconditioning, autophagy is enhanced through sustained expression of LC3-II and Beclin-1 (Park *et al*., 2009, Fan *et al*., 2014), whereas during hypertrophy excessive induction of autophagy is harmful and can lead to autophagic cell death (Dirks-Naylor *et al*., 2013). Several studies have concluded that downregulation of autophagy under physiological conditions is an adaptive response used by the biological system to protect the myocardium from cell death (Mei *et a*l., 2015, Nishida *et al*., 2008).

In recent years the beneficial effect of autophagy in Dox-induced cardiotoxicity has been extensively explored using various *in vitro* and *in vivo* models (Lu *et al*., 2009, Liu *et al*., 2016, Kawaguchi *et al*., 2012, Sishi *et al*., 2013, Kobayashi *et al*., 2010, Dimitrakis *et al*., 2012). However, conflicting reports has been obtained regarding the role Dox plays in the regulation of autophagy in cardiac cells. Numerous studies suggested that Dox up-regulates cardiac autophagy and contributes to the pathogenesis of Dox-induced cardiotoxicity (Wang *et al*., 2014, Dimitrakis *et al*., 2012, Lu *et al*., 2009, Kobayashi *et al*., 2010), while others support the notion that Dox induces cardiotoxicity through the suppression of autophagy (Sishi *et al*., 2013, Kawaguchi *et al*., 2012)Supporting this theory, the study done by Xu *et al*. (2012) revealed that Dox activated Beclin1, enhancing autophagy (Xu *et al*., 2012), while another study done by Liu *et al.* (2015) showed that Dox treatment decreased the expression of Bcl-2 with an associated decrease in autophagy (Liu *et al*. 2015). In addition, Wang *et al*. (2014) demonstrated that Dox enhances autophagy as observed through an increased AMPK phosphorylation and inhibition of mTOR (Wang *et al*. 2014). In contrast, Kawaguchi *et al*. (2012) (showed that Dox suppress autophagy as observed by a decrease in AMPK phosphorylation and dephosphorylation of ULK1 (also called Atg1) (Kawaguchi *et al*., 2012). Supporting these findings, Sishi *et al*. (2013) demonstrated that Dox suppresses the expression of LC-3 which was associated with a significant increase in Nucleoporin p62 (p62) in H9c2 rat

cardio myoblasts (Sishi *et al*., 2013). These conflicting findings can largely be attributed to the type of animal model employed as well as the experimental conditions used. This was evident in a systematic review done by Dirks-Naylor (2013), where the author reported that Dox treatment supresses autophagy in a mouse model, while in a rat model this process was found to be activated (Dirks-Naylor *et al*., 2013).

2.6 Potential strategies to prevent Dox-induced cardiotoxicity

Evidence based scientific reports have indicated that chronic exposure of Dox can induce irreversible myocardial damage. Therefore, the implementation of preventative measures that is more effective to protect cancer survivors is of great importance. Numerous attempts have been made in the prevention of Dox-induced cardiotoxicity, which include (i) limiting the dosage of Dox, (ii) development of analogous Dox compound and (iii) the use of cardioprotective agents that can be administered in combination with Dox.

2.6.1 Limiting the dose of Dox

To date, most clinicians limit the cumulative dose of Dox to >450 mg/m^2 as each increment of Dox above the recommended cut off range increase the probability of developing cardiotoxicity (Rahman *et al*., 2007). However, by doing this, clinicians exposed cancer patients to suboptimal oncologic treatment which could result in a reduced efficacy of Dox with an associated increase in cancer mortality.

2.6.2 Dox analogies

The use of Dox structural analogy has been established as a second approach to reduce the cardiotoxicity while maintaining the anti-cancer efficacy of Dox. Epirubicin is the most extensively investigated chemotherapeutic agent, and also the most promising analogy of Dox. Epirubicin has been favored over Dox as it produces less side effects (Smith *et al*., 2010). However, various randomized control studies have found Epirubicin to be as severe as Dox in inducing cardiotoxicity (Nair *et al*., 1998)

2.6.3 Cardioprotective agents

Combination therapy is a common treatment regimen used by clinicians to boost the efficacy of a drug while simultaneously preventing the development of cardio toxic side effects. Similarly, during cancer therapy Dox is given in combination with several drugs to boost its chemotherapeutic efficacy with the purpose of suppressing cardiotoxicity. Alpha-tocopherol (Vitamin E) was the first antioxidant reported to reduce Dox-induced oxidative stress. However, the use of Vitamin E was limited as it was unable to prevent mitochondrial dysfunction caused by long term administration of Dox (Berthiaume *et al*., 2005). Other combination therapies included the used of Vitamin C, mercaptopropionyl glycine (MPG), probucol and amlodipine in the prevention of Dox-induced cardiotoxicity (el-Missiry *et al*., 2001, Yamanaka *et al*., 2003). However, to date, very little evidence has come to the forefront to support the cardioprotective effect of these natural compounds and synthetic drugs against the prevention of Dox-induced cardiotoxicity

As previously mentioned, the interaction of Dox with Fe^{2+} plays a major role in the formation of highly reactive radicals. Therefore, much attention has been drawn to iron chelators for their potent ability to remove excess Fe^{2+} from the cell system. However, except for Dexrazoxane (Dexra), most of the iron chelators tested were unable to protect against Dox-induced cardiotoxicity.

2.6.3.1 Dexrazoxane as a cardioprotective agent

Dexra was discovered in 1972 by Kurt Hellman and is currently the only FDA approved drug used in combination with Dox to reduce cardiotoxicity (Arts and Hollman, 2005). The exact mechanism by which Dexra prevents cardiotoxicity is unknown, but it has been postulated that Dexra forms a complex with free Fe^{2+} to prevent the formation of superoxide radicals. Moreover, Dexra has been shown to degrade DNA Top2β which lessens Dox-induced DNA damage. However, treatment with Dexra has been reported to result in secondary malignancies in cancer survivors and also decreases the efficacy of Dox (Tebbi *et al*., 2007).Thus, the need to find new and improved chemotherapeutic drugs, that can be used in combination with Dox to decrease cardiotoxicity without reducing the efficacy of the chemotherapeutic agent is important.

2.7 Polyphenols

It is well known that Dox-induced cardiotoxicity occurs concomitantly with an increase in cardiac oxidative stress. This is evident by ROS-induced damage such as lipid peroxidation, along with reduced levels of endogenous antioxidants as can be observed in the myocardium of cancer survivor (Tocchetti *et al*., 2014). In recent years, there has been much interest in the possible health benefits of plant polyphenols as a rich source of antioxidants that are known to decrease lipid peroxidation induced by increased ROS. These beneficial effects of polyphenols have been attributed to their structural diversity which consists of aromatic connected rings with three carbons C6-C3-C6 (Habauzit and Morand, 2012). Moreover, the use of plant polyphenols is currently being investigated as possible adjunctive therapy in combination with Dox to protect the myocardium from Dox-induced oxidative stress (Chlopcikova *et al*., 2004, Patil and Balaraman, 2011). Accumulating experimental evidence has shown that polyphenols, specifically flavonoids can prevent Dox-induced cardiotoxicity largely due to their anti-cancer, chemotherapeutic and cardioprotective properties (Huang, 2013, Chung *et al*., 2010). Among others, polyphenols such as resveratrol (Resv), quercetin, catechin and curcumin have been extensively investigated in Dox-induced cardiotoxicity.

2.7.1 Resveratrol (Resv)

Resveratrol is a natural phytoalexin found in the skin of grapes, berries and red wine in significant amounts. Resv is known to possess a complex of health benefits including antioxidant and anti-apoptotic properties. In addition, Resv is known to scavenge free radicals (Mukherjee *et al*., 2010). The antioxidant properties of Resv have been linked to its lipophilic nature as shown in Figure 2.7A. This prompted researchers, to investigate the ability of Resv to reverse Dox-induced cardiotoxicity. Laboratory evidence suggests that Resv alleviates enhanced oxidative stress and apoptosis while also modulating autophagy induced by Dox treatment. Tatlidede *et al*. (2009) showed that Resv attenuates Dox-induced oxidative stress and prevents lipid peroxidation as observed by increased SOD and decreased malondialdehyde (MDA) activity (Tatlidede *et al*., 2009). Furthermore, more recently Resv has been shown to prevent Dox-induced apoptosis in cardiac cells observed by decreaseing in p53 and Bax expression (Sin *et al*., 2015). In

addition, various studies have shown that Resv can protect cardiac cells against Dox-induced dysregulation of autophagy (Xu *et al*., 2012, Dutta *et al*., 2014). In a meta-analysis done by Gu *et al*. (2015), the authors report on the use of Resv as an adjunctive therapy to protect the myocardium from Dox-induced cardiotoxicity without reducing the efficacy of Dox. In the latter analysis the authors found that Resv potentiates the chemotherapeutic efficacy of Dox and concluded that combined use of Dox with Resv may be a plausible chemotherapeutic modality that can decrease cancer survival while limiting cardiac damage (Gu *et al*., 2015).

2.7.2 Quercetin

Quercetin (3,30,40,5,7-pentahydroxyflavone) is a potent plant-derived flavonoid found in fruit and vegetables (Bravo, 1998). Quercetin is known to have antioxidant, anti-inflammatory, anti-cancer and cardioprotective activities. Matouk *et al*. (2013) reported that quercetin, as a monotherapy or in combination with Dox, was able to decrease lipid peroxidation and this effect was enhanced upon co-administration with losartan (Matouk *et al*., 2013). Though an effective anti-oxidant, long-term treatment with quercetin is known to increase apoptosis and decrease phase II antioxidant enzymes (Ferraresi *et al*., 2005). However, to date no research has been done on the role of Quercetin on autophagy.

2.7.3 Epigallocatechin gallate (EGCG)

Epigallocatechin gallate is a type of catechin with phytochemical properties found in high concentrations in a variety of plant-based foods and beverages such as green tea. The consumption of EGCG has been associated with a variety of beneficial effects which includes iron chelating and antioxidant properties. In addition, EGCG may impact the autophagic proteins to have autophagy properties through phosphorylation of PI3K/Akt and mTOR (Chen *et al*., 2016). The role of these compounds on Dox-induced cardiotoxicity has been evaluated both *in vitro* and *in vivo* settings (Kozluca *et al*., 1996, Hrelia *et al*., 2002). EGCG has been shown to exert cardioprotective effect against Dox-induced cardiotoxicity through inhibition of ROS production and apoptosis in cultured

cardiomyocytes (Hrelia *et al*., 2002). An *in vivo* study done by Kozluca *et al*., (1996) showed that co- administration of catechin with Dox in rats prevented Dox-induced cardiotoxicity as observed by improved QT intervals (Kozluca *et al*., 1996).

2.7.4 Curcumin

Curcumin is a yellowish chemical produced by some plants and has been identified as the major secondary metabolite of *Curcumina longa* (commonly known as turmeric). Recently, curcumin has received substantial attention due to it cardioprotective effects, free radical scavenging activity and antioxidants properties which can be ascribed to the structural diversity of curcumin. This includes the phenolic and non-phenolic rings found at the two ends of curcumin heptadiene chain (Figure 2.7D) (Sökmen and Akram Khan, 2016). Moreover, the cardioprotective effect of curcumin against Dox-induced cardiotoxicity have been extensively reported (Mohamad *et al*., 2009, Carlson *et al*., 2014, Imbaby *et al*., 2014). In a study done by Imbaby and colleagues (2014), it was shown that curcumin improves cardiac enzymes, oxidative stress and apoptosis induced by Dox treatment in rats (Imbaby *et al*., 2014). Katamaru *et al*. (2014) have reported that the cardioprotective effects of curcumin is facilitated by autophagy as observed through regulation of JNK phosphorylation (Katamaru *et al*., 2014). However, curcumin is not currently used as an anti-cancer or a cardioprotective agent because of its poor absorption, biodistribution, metabolism, and bioavailability.

2.7.5 Aspalathin

Aspalathin is a dihydrochalcone C-glucoside that is unique to Aspalathus linearis. Aspalathus linearis (commonly known as rooibos) is a plant endemic to South Africa that grows in the Cederberg mountain region of the Western Cape, South Africa (Figure 2.8) (Dahlgren, 1968, Jourbet *et al*., 2008). Rooibos is a popular health beverage with potent therapeutic properties. This herbal tea can be enjoyed in both fermented and unfermented forms (green rooibos), with the unfermented version being richer in anti-oxidants compared to fermented rooibos tea (van der Merwe *et al*., 2006). Aspalathin (ASP) is a unique flavonoid present in relatively high quantities in unfermented rooibos tea

compared to fermented rooibos tea (Dludla *et al*., 2014, Stalmach *et al*., 2009). Literature has reported on the anti-oxidant, anti-diabetic and anti-mutagenic effects of ASP (Mazibuko *et al*., 2015, Muller *et al.,* 2012, Snijman *et al*., 2007). Moreover, Snijman and colleagues compared the scavenging effect of ASP with catechin and quercetin and ASP the most potent radical scavenger. The presence of C-2 and C-6 hydroxyl groups as well as alpha methylene groups in the structure of ASP have been suggested to be the major contributors to the compound antioxidant effect (Figure 2.7E) (Snijman *et al*., 2009). More recently, Johnson and colleagues (2016) have shown that ASP was able to protect the diabetic myocardium against high glucose-induced oxidative stress and cell apoptosis (Johnson *et al*., 2016). However, the effect of ASP to reduce Dox-induced cardiotoxicity has not been investigated. Therefore, it would be of great interest to investigate whether ASP co-administration with Dox can protect the myocardium against Dox-induced cardiotoxicity without reducing the anti-cancer efficacy of Dox.

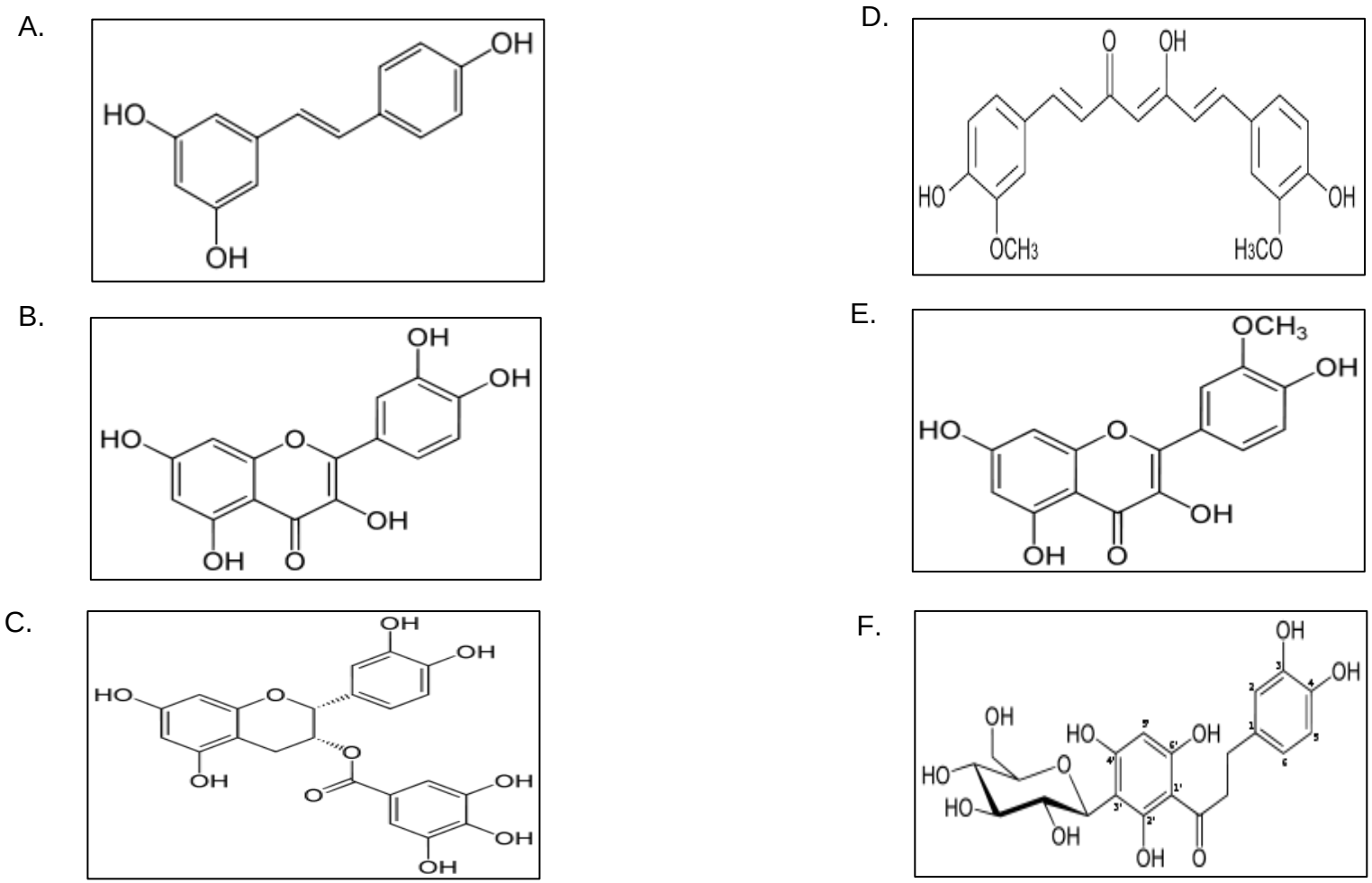

Figure 2.7: Chemical structure of polyphenols currently known to possess anti-oxidant and anti-apoptotic activity :A) Resveratrol, B) Quercetin, C) Epigallocatechin gallate, (EGCG), D) Curcumin, E) Isorhmnetin and F) Aspalathin. Taken from (Sin et al., 2015, Sökmen and Akram Khan, 2016, Bravo, 1998, Chen et al., 2016)

A.

B.

C.

D.

Figure 2 8: *Aspalathus linearis* (commonly known as rooibos teas). (A) *Aspalathus linearis* a species of fynbos (B) endemic to the Clanwilliam and only grows in the Cedarberg region of the Western Cape. The plant is enjoyed as an herbal tea, either as a (A) fermented (red) or (D) unfermented (green) tea (Herbal Teas Online, 2015).

CHAPTER 3

MATERIALS AND METHODS

This chapter gives a comprehensive description of materials and methods used in this study. Appendix A includes a list of chemicals, reagents, kits, consumables and equipment used with the relevant companies' details. Additional information pertaining to the methods used will be listed in Appendix B.

3.1 ATCC culture strains

H9c2 rat derived cardio myoblasts were purchased from the European Collection of Cell Cultures (ECACC No. 8809294) while Caov-3 ovarian carcinoma cells (American Type Culture Collection (ATCC)® HTB75™) were a kind gift from Dr Mervin Meyer from the University of the Western Cape. All cell culture stocks were stored in vapour phase in a liquid nitrogen tank (Appendix B).

3.2 Cell culture

3.2.1 Thawing of cryopreserved cells for culture

H9c2 cardio myoblasts and Caov-3 ovarian carcinoma cells were thawed in a 37°C circulating water bath until a small ice pellet remained. Cells were then transferred to a 15 mL tube containing 10 mL of pre-warmed Dulbecco's modified eagle's medium (DMEM) (supplemented with 10% fetal bovine serum (FBS) and 1% of 100 U/mL of penicillin-100 µg/mL streptomycin (pen/strep)), and centrifuged at 800 x g for 5 min to remove any residue of dimethyl sulfoxide (DMSO). Thereafter, the supernatant was discarded and the cell pellet was gently re-suspended in 18 mL of DMEM (supplemented with 10% FBS and 1% pen/strep) and transferred to a 75 cm^2 flask. The flask containing cells was then incubated at 37°C under standard tissue culture (TC) conditions (5% CO_2 and 95% humidified air) for three days or until it reached 70-80% confluency.

3.2.2 Trypsinization of cells

H9c2 and Caov-3 cultured cells were removed from the CO_2 incubator and the media was removed from the flask by aspiration. Cells were then washed with pre-warmed Dulbecco's phosphate-buffered saline (DPBS) followed by the addition of 4 mL (for cells in a 75 cm^2 flask) of trypsin and the flask incubated under standard TC conditions for 4 min to dislodge cells. Cells were then viewed under a Nikon Eclipse Ti inverted microscope to confirm dislodgement, after which 8 mL of DMEM (supplemented with

10% FBS and 1% pen/strep) was added to the T75 flask to stop the trypsinization process. Cells were then gently mixed to obtain a single cell suspension, transferred to a 50 mL centrifuge tube and spun at 212 x g for 5 min. Subsequently, the media was aspirated and the cell pellet was re-suspended in 10 mL pre-warmed DMEM (supplemented with 10% FBS and 1% pen/strep). Cell density and viability were determined (section 3.2.4) before cells were seeded in the appropriate tissue culture (TC) plates for assay purposes (section 3.2.5).

3.2.3 Sub-culturing and maintenance of cells

Upon 70-80% confluency, cells were trypsinized as previously described (section 3.2.2.). After trypsinization, cells were sub-cultured in T75 cm^2 flasks to obtain a media to a cell ratio of 1:9. Both cell types (H9c2 and Caov-3) were sub-cultured in pre-warmed DMEM (supplemented with 10% FBS and 1% pen/strep) and incubated under standard TC conditions until they reached 70-80% confluency. Media was refreshed every second day and sub-culturing of cells was kept below 20 passages to prevent modulation of the cell phenotype and to avoid contact inhibition.

3.2.4 Determination of cell viability

After trypsinization (section 3.2.2.), total cell count was determined by mixing 10 µL of the cell suspension with 10 µL of a 0.4% (w/v) trypan blue solution. Thereafter, 10 µL of the cell suspension/trypan blue mix was transferred to an automatic cell counting chamber to determine the number of viable cells using a Countess™ Automated Cell Counter.

3.2.5 Seeding of cells in multi-well plates

After cell count, cells were seeded at the required seeding density (Table 3.1.) in multi-well TC plates and incubated under standard TC conditions for 2 days in DMEM (supplemented with 10% FBS and 1% pen/strep). Treatment was initiated on day 3 and cells were cultured in DMEM (without phenol red and glutamate, supplemented with 2% FBS).

Table 3.1: Seeding of H9c2 and Caov-3 cells in multi-well plates

Cell type	Multi-well plate (well)	Growth area (cm^2)	Seeding density (cells/well)	Volume (µL)
H9c2 and Caov-3	6	10	2×10^5	3 000
	24	2.0	5×10^4	1 000
	96	0.3	2×10^4	200

3.3 Dose study

3.3.1 Determination of time and dose response of Aspalathin (ASP)

A working stock solution of 1 mM Aspalathin (ASP) was prepared in DMEM (without phenol red and glutamate, supplemented with 2% FBS) and filter sterilized using a 0.22 µm filter. A log dilution of the compound was prepared from the working stock (100 µg/ml, 10 µg/mL, 1 µg/mL, 0.1 µg/mL and 0.01 µg/mL) in DMEM (without phenol red and glutamate, supplemented with 2% FBS).

3.3.2 Determination of time and dose response of Doxorubicin (Dox)

Doxorubicin was used at a cumulative dose of 1 µM (0.2 µM / day) for a total of 5 days, as previously described by Goldswain *et al* (2014).

3.3.3 Determination of time and dose response of Dexrazoxane (Dexra)

Dexrazoxane is the only FDA approved cardioprotective agent and was used at a dose of 100 µM for 5 days as previously described by of Deng *et al* (2014).

3.4 Treatment conditions

H9c2 cardio myoblasts exposed to 0.2 µM Dox were either pre- or co-treated with ASP to assess the most effective preventative treatment before initiation of the experimental design as described in section 3.4.1 and 3.4.2. H9c2 cells treated with either media or Dox were used as a positive and negative control, respectively.

3.4.1 ASP pre-treatment

H9c2 cardio myoblasts were pre-treated with 1 µM ASP for 6 hrs, subsequently cells were exposed to a 0.2 µM Dox daily for 5 days resulting in a cumulative dose of 1 µM. Cells treated with DMEM (without phenol red and glutamate, supplemented with 2% FBS) at a final concentration of 0.001% DMSO were used as vehicle control.

3.4.2 ASP co-treatment

H9c2 cardio myoblasts exposed to 0.2 µM Dox were co-treated with either 20 µM Dexra or 0.2 µM ASP daily for 5 days, resulting in a cumulative dose of 1 µM Dox, 100 µM Dexra and 1 µM ASP, respectively. To investigate whether or not ASP co-treatment reduces the anti-cancer efficacy of Dox, Caov-3 ovarian carcinoma cells were exposed to either Dox or ASP or the combination of Dox and ASP at a dose of 0.2 µM daily for 5 days.

3.5 Biochemical analysis

3.5.1 Assessment of metabolic activity using ATP assay

ATP assay is a tool that is used measure the metabolic activity and cytotoxicity of compounds. Following completion of the pre-determined experimental conditions, ATP assays were performed using the ViaLight™ plus kit according to manufacturer's instructions. Briefly, cells seeded in a white 96-well plate were removed from the incubator and media was aspirated until ~50 µL of the culture media remained. Fifty microliters of ATP cell lysis buffer was added to each well and incubated at room temperature (RT) for 10 min. Thereafter, 100 µL of the AMP plus reaction mixture was added to each well and incubated for an additional 2 min at RT. Luminescence was read in a Biotek® FLX 800 plate reader using Gen 5® software.

3.5.2 Assessment of apoptosis

3.5.2.1 TUNEL assay

TUNEL assay is an established method to detect apoptotic cells that undergo extensive DNA fragmentation during the last stage of apoptosis. In this study, DNA nicks were detected by DeadEnd™ Fluorometric TUNEL assay according to

manufacturer's instructions. Briefly, following pre-determined experimental conditions, the supernatant of cells grown in a 24-well plates was aspirated and cells were washed in DPBS before they were fixed in 4% paraformaldehyde for 15 min. Thereafter, cells were washed twice in DPBS before 0.2% (v/v) Triton X-100 was added for 5 min to permeabilize the cell membrane. Cells were then washed in DPBS for 5 min and equilibrated in 100 µL of equilibration buffer. After 5 min, the equilibration buffer was removed and replaced with 50 µL of terminal deoxynucleotidyl transferase (TdT) reaction mix, and the plate containing the cells was incubated at 37°C (in humidified air in a 5% CO_2 incubator) for 60 min. After incubation, cells were rinsed twice in a 2x SSC buffer for 15 min. TUNEL-positive cells were detected by direct visualization of green fluorescent stain. The apoptotic rate was calculated as the average number of condensed TUNEL-positive cells in non-overlapping fields of 1 mm^2 under 10x magnification field (average of at least 5 fields per well) using a Nikon Eclipse Ti inverted fluorescent microscope and NIS Elements imaging software.

3.5.2.2 Caspase 3/7 activity

Caspase 3/7 activity is a luminescent assay used to measure pro-apoptotic activity in an *in vitro* cell base system. Apoptosis was assessed using a Caspase-Glo® 3/7 activity kit according to the manufacturer's instructions. Briefly, following the pre-determined experimental conditions, both H9c2 and Caov-3 cells were lysed in 350 µL ice cold lysis buffer and proteins extracted as described in section 3.6.2.1 and 3.6.2.2. Twenty microliters of the cell lysates was then transferred to a 96-well plate. Thereafter, an equal amount of Caspase-Glo® reagent (~20 µL) was added to each well and the plate was incubated in the dark. After 30 min luminescence was measured in a BioTek® FLX 800 plate reader using Gen 5® software. Results were normalized to pre-determined protein content using RC DC™ protein assay.

3.5.3 Measurement of antioxidant activity for oxidative stress

3.5.3.1 Assessment of superoxide dismutase activity (SOD)

Superoxide dismutase (SOD) is one of the most important antioxidative enzymes that catalyzes the dismutation of the superoxide anion into hydrogen peroxide and molecular oxygen. Superoxide Dismutase activity was quantified using a Biovision

assay kit according to manufacturer's instruction. Briefly, following the pre-determined treatment conditions, cells cultured in a 24-well plate were lysed with 100 µL of ice cold 0.1 M trizma/hydrochloride (Tris/HCl), pH 7.4 (containing 0.5% Triton X-100, 5 mM β-Methylphenethylamine (β-ME) and 0.1 mg/mL Phenylmethylsulfonyl fluoride (PMSF)). Crude lysates were then centrifuged at 14 000 x g for 5 min at 4°C. Thereafter, 20 µL of the cell lysates was transferred to a clean 96-well plate and samples and controls were prepared as per Table 3.2. Thereafter, the plate was incubated at 37°C for 20 min before SOD activity was measured at 450 nm using a Biotek® ELX 800 plate reader using Gen 5® software. SOD activity was calculated using a formula in Figure 3.1.

Table 3.2: Preparation of sample for SOD activity

Reagents	**Sample (µL)**	**Blank 1 (µL)**	**Blank 2 (µL)**	**Blank 3 (µL)**
Sample solution	20	-	20	-
Distilled water	-	20	-	20
Wst working solution	200	200	200	200
Enzyme working solution	20	20	-	-
Dilution buffer	-	-	20	20

$$\text{SOD Activity} = \frac{(A_{\text{blank 1}} - A_{\text{blank 3}}) - (A_{\text{sample 1}} - A_{\text{blank 2}})}{(A_{\text{blank 1}} - A_{\text{blank 3}})} \times 100$$

Figure 3.1: Equation used to calculate the SOD activity.

3.5.3.2 Assessment of catalase activity

Catalase is an antioxidant enzyme that inhibit increased oxidative stress by catalysing H_2O_2 into a molecule of H_2O water and O_2. Catalase activity was measured using a Catalase assay kit according to the manufacturer's instructions. Briefly, cells were harvested in DPBS using a rubber policeman. Cells in 2 mL microfuge tubes were then centrifuged at 2 000 x g for 10 min at 4°C. Thereafter, the supernatant was removed and the cell pellet was homogenized in 1 mL ice cold 50 mM potassium phosphate

buffer (pH 7.0 containing 1 mM Ethylenediaminetetraacetic acid) and centrifuged at 10 000 x g for 15 min at 4°C. The supernatant was removed and stored at -80°C until required. Samples were assayed by transferring 20 µL of the formaldehyde standard, bovine liver positive control (supplied in the kit) and sample supernatant to a 96-well plate in duplicate. To this, 100 µL dilution buffer and 30 µL of methanol were added and the reaction was initiated by the addition of 20 µL of hydrogen peroxide. The plate was incubated at RT for 20 min and the reaction was terminated by the addition of 30 µL of potassium hydroxide and catalase purpald, respectively. Thereafter, the plate was incubated at RT for 10 min on a plate shaker after which 10 µL of catalase potassium periodate was added to each well and incubated for an additional 5 min at RT on a shaker. Absorbance was read at 540nm with a Biotek® ELX 800 plate reader using Gen 5® software.

3.5.3.3 Assessment of glutathione (GSH) activity

GSH activity assay is a luminescent-based assay, which detects and quantifies the antioxidant GSH in various biological samples. GSH content was determined using a GSH/GSSH-Glo™ assay kit according to the manufacturer's instructions. Briefly, following the pre-determined experimental conditions, media from cells grown in a white 96-well plate, was discarded and either replaced with 50 µL total glutathione lysis reagent or oxidized glutathione lysis reagent. Thereafter, cells were placed on an orbital shaker for 5 min at RT before 50 µL of a luciferin generation reagent was added to each well and the plate was incubated for an additional 30 min at RT. Following the 30 min incubation period, 100 µL of luciferin detection reagent was added and the plate was incubated at RT on a shaker for 15 min. Thereafter, luminescence was measured in a Biotek® FLX 800 plate reader using Gen 5® software.

3.5.4 Assessment of lipid peroxidation using thiobarbituric acid reactive substances (TBARS)

The TBARS assay is an established method that quantifies lipid peroxides based on the production of MDA, biomarker that measure oxidative stress. Lipid peroxidation was assessed using the OxiSelect™ TBARS assay Kit according to the manufacturer's instructions. Briefly, following pre-determined experimental conditions, media was discarded and cells were re-suspended in 1 mL of DPBS to which 10 µL of

100 x Butylated hydroxytoluene solution was added. Cells were transferred to a 2 mL microfuge tube and homogenized for 1 min at 250 Hz using a Qiagen TissueLyser. The homogenate was placed on ice while the MDA standards were prepared at concentrations of 125, 62.5, 31.5, 15.25, 7.81, 3.91, 1.95 and 0.98 µM respectively. One hundred microliters of sample and MDA standards were transferred to 1.5 mL microfuge tubes to which 100 µL of the sodium dodecyl sulfate lysis solution was added. Samples were mixed by vortexing before incubation at RT for 5 min. Thiobarbituric acid reagent (250 µL) was added to each tube, mixed thoroughly and incubated at 95°C for 45-60 min. Thereafter, the tubes were cooled at RT in an ice bath for 5 min and centrifuged at 864 x g for 15 min. The resultant supernatant of the MDA standards and samples were transferred to a clear 96-well plate and the absorbance was read at 532 nm in a BioTek® ELX800 plate reader using Gen 5® software.

3.6 Assessment of gene and protein expression analysis

3.6.1 Gene expression analysis

3.6.1.1 RNA extraction

Ribonucleic acid was extracted using TRIzol® reagent according to the manufacturer's instructions. Briefly, treatment media was removed from cells growing on a 6-well TC plate and washed 3 times with DPBS. After the third wash, the DPBS was replaced with 1 mL of TRIzol® and cells were harvested using a rubber policeman. The lysates were then transferred to 2 mL tubes containing a stainless steel beads and homogenized using a Qiagen TissueLyser at 25 Hz for 2 min x 2. The tubes containing the lysed cells were then centrifuged at 13 000 x g for 10 min at 4°C and the supernatant was transferred to a new 1.5 mL tube. Subsequently, 0.2 mL of chloroform was added to each tube, mixed intermittently for 3 min and centrifuged at 13 000 x g for 15 min at 4°C. Thereafter, the upper aqueous phase was transferred to a new 1.5 mL Eppendorf tube without disturbing the white organic phase. RNA was precipitated by the addition of 0.5 mL isopropanol, inverted several times before the samples were incubated overnight at -20°C. The following day, the RNA was pelleted by centrifuging at 13 000 x g for 30 min at 4°C. The supernatants were discarded, the pellet was washed twice with 1 mL of 70% ethanol and centrifuged at 13 000 x g for 15 min at 4°C. This wash step was repeated twice. After the final wash, the supernatant was discarded and the pellet was allowed to air dry for 30 min in a PCR hood. To dissolve

the pellet, the RNA sample was re-suspended in 50 µL RNase free water and incubated at 55°C for 10 min.

3.6.1.2 RNA Purification

Ribonucleic acid was purified using a Qiagen RNeasy Mini kit according to manufacturer's instructions. Briefly, a volume of 350 µL of RLT lysis buffer followed by 250 µL of 96% ethanol was added to the RNA solution. The samples were transferred to an RNeasy spin column and centrifuged at 13 000 x g for 15 sec and the flow-through was discarded. Thereafter, 500 µL of RPE buffer was added to the RNeasy spin column, before the spin column was centrifuged for 15 secs at 13 000 x g and the flow-through was discarded. This step was repeated twice. Subsequently, the RNeasy spin column containing the RNA was placed in a new 2 mL collection tube and centrifuged at 13 000 x g for 1 min to completely dry the membrane. The RNA was eluted by placing the RNeasy spin column into a new 1.5 mL Eppendorf tube to which 50 µL of RNase free water was added directly to the spin column membrane and allowed to stand for 1 min. RNA was eluted by centrifugation at 13 000 x g for 1 min. The RNA eluent containing the RNA was then stored at -80°C until required.

3.6.1.3 RNA quantification

Ribonucleic acid was quantified using a NanoDrop® 1000 spectrophotometer. Two microliters of distilled water was pipetted onto the pedestal of the NanoDrop® to initialize the spectrophotometer and to blank the machine. Thereafter, the absorbance of each sample was determined by adding 2 µL of each sample onto the pedestal and the samples were read in duplicate. The ratio of 260 nm to 280 nm was used to evaluate the purity of the RNA samples while the ratio of 260 to 230 was used to assess the RNA for any DNA contamination.

3.6.1.4 RNA integrity

Ribonucleic acid integrity was determined using the Agilent 2100 Bioanalyzer, according to manufacturer's instructions. Briefly, the bioanalyzer was decontaminated by placing 350 µL of RNaseZAP for 1 min followed by 350 µL of RNase-free water for

10 secs on the electrodes. Once decontaminated, the lid of the bioanalyzer was left open for 10 secs for the electrodes to dry. Ribonucleic acid samples were prepared by transferring 20 µL of samples and RNA ladder to 0.5 µL microfuge tubes, which were placed in a heating block at 70ºC for 2 min. The denatured samples and ladder were then loaded onto the RNA chip with the conditioning solution and primed. The RNA 6000 Nano chip was inserted on the chip priming station (Figure 3.2) and 9 µl of gel-dye mix was added into the well-marked G (dark). The plunger was positioned at the 1 mL mark of the chip priming station, and it was pressed until it was held by the clip. After exactly 30 secs, the plunger was released. Thereafter, 9 µl of gel-dye mix was added into 2 wells marked G (light); 5 µl of RNA 6000 Nano marker was added in all 12 sample wells and in the ladder well; this was followed by the addition of 1 µL of RNA ladder into the ladder well; 1 µL of RNA sample into each of the 12 sample wells; and 1 µL of sample ladder into each unused well. The chip was vortexed at 542 x g for 30 sec; and placed in the chamber of the Agilent bioanalyzer and run within 5 min. When the run was complete the chip was removed, and electrodes were washed by placing a chip filled with 350 µl of RNase-free water into the chamber for 10 sec. Integrity of RNA samples was determined using 2100 Expert Software.

.

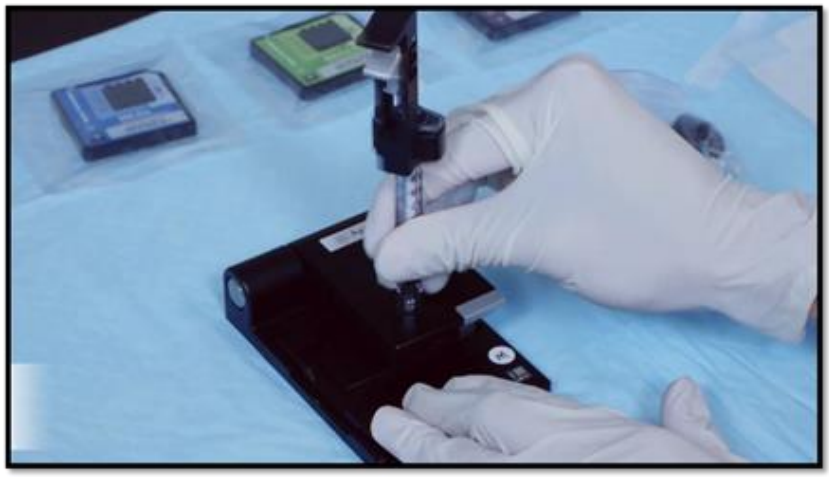

Figure 3.2: A representative image demonstrating the chip priming station.

3.6.1.5 DNase treatment of RNA

To remove any DNA contaminants, RNA samples were treated with DNase using a Turbo DNase-free ™ kit following manufacturer's instructions. Briefly, 5 µL of 10x

DNase buffer and 1.5 µL of DNase were added to a 20 µg of RNA to make a total reaction volume of 50 µL in RNase-free water. Samples were mixed and incubated at 37°C for 30 min after which an additional 1.5 µL of DNase was added before samples were incubated at 37°C for an additional 30 min. The reaction was stopped by adding 10 µL of DNase inactivation reagent, and mixed by placing the tubes on an orbital shaker for 2 min. Thereafter, the samples were centrifuged at 10 000 x g for 1.5 min and the supernatant was transferred to a new 1.5 microfuge tube. RNA concentration was determined using a Nanodrop® 1000 spectrophotometer (section 3.6.1.3).

3.6.1.6 Complimentary DNA (cDNA) synthesis of RNA

The Applied Biosystems, High-Capacity cDNA kit was used according to manufacturer's instructions to transcribe total RNA into cDNA. An amount of 1 µg DNase treated RNA was transferred to a 0.2 mL tube to obtain a final volume of 10 µL made up in RNase-free water. A master mix containing (Table 3.3) high quality deoxynucleotide triphosphates (dNTPs), reaction buffer, random primers, RNase inhibitor, RNase-free water and reverse transcriptase master mix was prepared into 2 separate tubes labelled reverse transcriptase-Plus (RT-Plus) and reverse transcriptase-Minus (RT-Minus). The RT-Minus master mix tube, which served as a negative control contained the same constituents as the RT-Plus tube; however, the reverse transcriptase enzyme was replaced with RNase-free water. The cDNA synthesis reaction was prepared in a final volume of 20 µL in RNase-free water by adding 10 µL of RT-Plus or RT-Minus master mix into a 0.2 mL tube containing 1 µg of RNA. The tubes were then briefly mixed by vortexing, spun down and placed in an Applied Biosystem Instrument (ABI) 2720 thermal cycler. The thermal cycler machine was set to incubate at 25°C for 10 min, 37°C for 120 min, and 85°C for 5 secs to deactivate the reverse transcriptase enzyme. Once the reaction was completed, cDNA samples were stored at -80 ºC until further use.

Table 3.3: Reaction mixture used to reverse transcribe the DNase treated RNA

Reaction mixture	R-Plus Volume/Reaction (µL)	R-Minus Volume/Reaction (µL)

*1µg DNase treated RNA	10	10
10× RT buffer	2	2
25× dNTP mix	0.8	0.8
10× Random primers	2	2
RNase inhibitor	1	1
Reverse transcriptase	1	-
Nuclease-free water	3.2	4.2
Total volume	20	20

Legend to table: *1µg RNA made up to a final volume of 10 µL in RNase-free water

3.6.1.7 Testing cDNA for genomic DNA contamination

To test for genomic DNA contamination, cDNA generated from the RT-Plus and RT-Minus reverse transcriptase reactions were amplified using *Actin-β* (*ActB*) exon spanning primers (Table 3.4). A master mix was prepared by the addition of 1 µL of each primer pair (*ActB*, 10 µM), 12.5 µL SYBR® Green PCR master mix and RNase-free water to a final volume of 24 µL (Table 3.4). Twenty-four microliters of SYBR® green master mix was then added to 1 µL of either RT-Plus or RT-Minus cDNA in a MicroAmp® Optical 96-well Reaction Plate. The plate was sealed, mixed on a plate shaker for 10 min and then briefly centrifuged at 3 000 x g for 2 min before the plate was placed in the ABI 7500 Sequence Detection System for quantitative PCR analysis. The cDNA was amplified using the cycling conditions described in Table 3.5. The quantity of cDNA for each reaction was determined from the default threshold cycle (Ct) and baseline obtained during the exponential phase. After the run, Ct values were exported to Microsoft Excel and the Ct values of the RT-Minus samples were subtracted from the corresponding RT-Plus samples. If the difference in Ct values were equal to or greater than 10 between the corresponding RT-Minus and RT-Plus strand, the presence of contamination was seen as negligible.

Table 3.4: A master mix used in the direction of contaminated genomic DNA

Components	Volume/ Reaction (µL)	Final Concentration
SYBR Green PCR Mix	12.5	1x
ActB Forward primer (10 µM) 5'GGGCCCGGACTCATCGTACT-3'	1	400 nM

ActB Reverse primer (10 µM) 5'-GCCTCACTGTCCACCTTCCA-3'	1	400 nM
RNase-free water	9.5	
cDNA	1	-
Total	**25**	

Table 3.5: Universal cycling conditions used for testing of cDNA

Step	Temperature °C	Time	Cycles
Activation and Denaturation	50 95	2 min 10 min	1
Fluorescence data collection	95 60	15 sec 1 min	40
Dissociation Curve	95 60 95	15 sec 1 min 15 sec	1

3.6.1.8 Quantitative Real-time PCR analysis (QRT-PCR)

Quantitative Real-time PCR was performed to simultaneously detect and quantify target DNA molecules, using Taqman gene expression probe assays from Applied Biosystems (Table 3.6). A standard curve was prepared from a 10-fold serial dilution (100-0.001), while the synthesized cDNA was diluted using a ratio of 1:5 in RNase-free water. A PCR mixture was prepared containing 0.5 µL of Taqman® gene expression assay (Table 3.6), 5 µL Taqman® universal PCR master mix, and RNase water to a final volume of 9 µL (Table 3.7). Nine microliters of the PCR mixture was then added to 1 µL of the serial diluted standards, target and control cDNA separately in a 96-well PCR plate and all samples were run in duplicate. The plate was sealed, placed on a plate shaker for 10 min and then briefly centrifuged at 3 000 x g for 2 min. Thereafter, the plate was placed in an ABI 7500 Sequence Detection System Instrument (Applied Biosystems) to conduct the QRT-PCR reactions (SDS V1.4) using the PCR cycling conditions as described in Table 3.5. The quantity, mean and standard deviation values were calculated by the ABI Standard Quantification (AQ)

software (SDS V1.4) using a threshold (Ct) of 0.1, the baseline was set between 3 and 15 cycles. Data was subsequently exported to Microsoft Excel to calculate the relative expression values. Beta actin (*ActB*) and phosphoribosyltransferase1 (*Hprt1*) were used as endogenous housekeeping genes. The mean quantity of target values was divided by the mean quantity of the house keeping genes *ActB and* (*Hprt*). The fold-difference was then calculated between the normalized control and treated samples by dividing the normalized treated samples by the control.

Table 3.6: List of Taqman probe assays used in QRT-PCR analysis

Probe symbol	Probe name	Probe assay
House Keeping Gene		
ActB	Beta actin	Rn00667869_m1
Hprt1	Hypoxanthine Phosphoribosyltransferase 1	Rn01527840_m1
Autophagy Markers		
Atg5	Autophagy-Related 5	Rn01767063_m1
Atg7	Autophagy- Related 7	Rn01492725_m1
Becln1	Beclin 1, Autophagy-related 6	Rn00586976_m1
BNIP3	Bcl-2/Adenovirus E1B 19kDa Interacting Protein 3	Rn00821446_g1
mTOR	Mechanistic Target of Rapamycin (Serine/Threonine Kinase)	Rn00693900_m1
Prkaa2	Protein Kinase, AMP- Activated, Alpha 2 Catalytic Subunit	Rn00576935_m1
Fox01	Forkhead box O1	Rn01494868_m1

Table 3.7: PCR-reaction mix use to conduct the QRT-PCR reaction

PCR Reaction	Per Reaction (µL)
Taq polymerase master mix	5
Probe assay	0.5
Nuclease-free water	3.5
cDNA	1
Total	**9**

3.6.2 Protein expression

3.6.2.1 Total protein isolation

Following the pre-determined experimental conditions, Caov-3 cells grown on a clear 6-well TC plate were washed twice with warm DPBS. DPBS was removed and replaced with 350 µL of ice cold cell lysis buffer (per 75 cm^2). Cells were then scraped using a cell scraper and transferred to 2 mL tubes containing stainless steel beads. The microfuge tubes containing the lysates were then placed in a pre-cooled TissueLyser block and homogenized 5 times using a Qiagen TissueLyser at 25 Hz for 60 sec, alternating with 1 min in the TissueLyser and 1 min on ice. Lysates containing the proteins were then centrifuged for 15 min at 15 890 x g at 4°C. The resultant supernatant containing the protein lysates were removed and transferred to a new 1.5 mL tube and stored at -20°C until required.

3.6.2.2 Protein concentration determination

Protein concentration was determined using the Reducing agent and detergent compatible (RC DC) protein assay kit according to manufacturer's instructions. Briefly, 5 µL of each (commercially available) Bovine serum albumin (BSA) standard (0.125, 0.25, 0.5, 1, 1.5 and 2 mg/ml) and samples were transferred to a clear 96-well plate. Thereafter, 25 µL of reagent A (consisting of 20 µL RC Reagent C and 1 mL of RC reagent A) and 200 µL of reagent B was added to each well of a 96-well plate containing standards and samples. The plate was mixed for 10 secs and incubated at RT for an additional 10 min before absorbance was read at 695 nm using a BioTek® ELX800 plate reader and Gen 5® software.

3.6.2.3 Gel electrophoresis

Thirty micrograms of protein lysates were mixed with equal volumes of a 2x sodium borate (SB) buffer. Thereafter, protein lysates containing SB buffer were denatured at 95ºC for 5 min. Twelve microliters of Western C marker and 30 µg of denatured protein samples were loaded onto either 10 or 12% Mini-Protean® TGX™ Gel placed in a Biorad Mini Protein® Tetra Cell tank filled with 1 x Tris/Glycine/SDS running buffer. Thereafter, gel electrophoresis was initiated at 150 V for 60 min.

3.6.3 Western blot analysis

3.6.3.1 Transfer of gel to PVDF membrane

Western blot analysis is a technique used to detect and quantify the expression of a specific protein using an antibody, within a complex mixture of proteins. Following gel electrophoresis, separated proteins were transferred using a polyvinylidene fluoride (PVDF) membrane as the membrane is highly hydrophobic and offers better retention of the adsorbed proteins. The PVDF membrane was cut to size (8 x 6 cm) and pre-wetted with 100% methanol for 1 min before the membrane was washed for 5 min in distilled water. Thereafter, the PVDF membrane, Whatman paper, gel and the fiber pads were equilibrated on an orbital shaker in a transfer buffer for 20 min. Subsequently, the cassette was placed with the black negative side facing downwards and the 'transfer sandwich' was prepared by placing the fiber pad on the positive side followed by Whatman filter paper, gel, PVDF membrane, Whatman filter paper and the fiber pad as shown in (Figure 3.3). The transfer cassette was closed and placed in a Mini Trans-Blot® tank. The tank was filled with enough transfer buffer to cover the cassette. Thereafter, the proteins were transferred at 160 V for 75 min in a 4°C cold room.

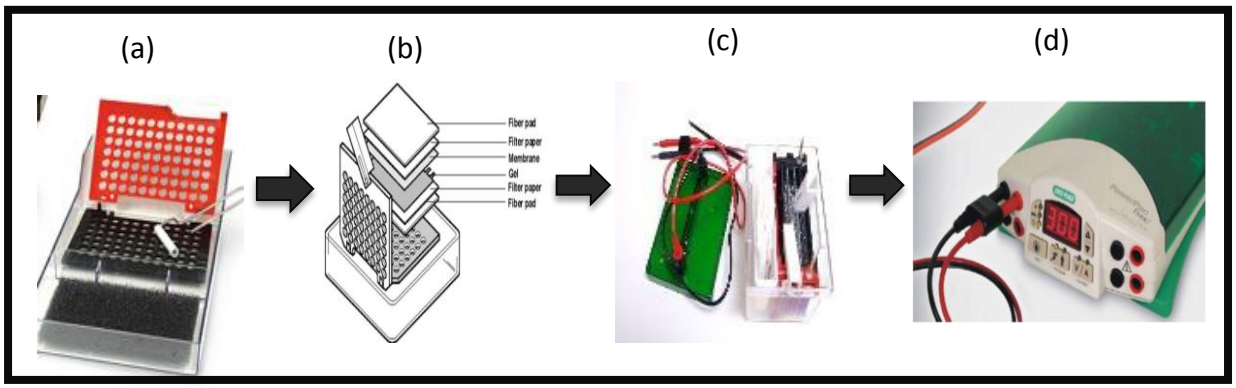

Figure 3.3: Schematic representation of the transfer Sandwich used to transfer proteins for Western blot analysis. The transfer sandwich was prepared in the following order: Fiber pad, Whatman paper, gel, Polyvinylidene fluoride (PVDF) membrane, Whatman paper and fiber pads were loaded into a transfer cassette.

3.6.3.2 Ponceau S stain

To ensure complete transfer, the PVDF membrane was removed from the cassette and submerged in 50 mL of Ponceau S Staining Solution before it was placed on an orbital shaker for 5 min. The stain was reversed by washing the membrane in a 1x Tris-buffered saline containing Tween-20 (TBST-20) for 1 min.

3.6.3.3 Labelling of membrane with Antibody

The PVDF membrane containing the proteins of interest was blocked in 5% (w/v) non-fat milk in 1x TBST-20 at RT for 2 hrs on an orbital shaker. Subsequently, the membrane was labelled with the relevant primary antibody (Table 3.8) in 1x TBST-20 overnight at 4ºC on an orbital shaker. The following day, the membrane was washed 3x for 10 min in 1x TBST-20 at RT. Subsequently, the membrane was labelled with the relevant horseradish peroxidase (HRP) conjugated secondary antibody in 2.5% (w/v) non-fat milk in 1x TBST-20 at RT for 90 min. After 90 min, the membrane was washed 3x for an additional 10 min in 1x TBST-20 before detection and quantification of proteins using a Chemidoc-XRS imager and Quantity One software. All proteins were normalized to β-actin antibody that was used as a loading control.

3.6.3.4 Stripping of Blot

Membranes were immersed in a Western blot stripping buffer and incubated for 13 min at RT. Thereafter, the stripping solution was removed and the membrane was washed 3x in 1x TBST-20 for 10 min.

Table 3.8: List of antibodies and the dilution used for Western blot analysis

Antibody	Dilution	% Gel	Cat #	Company
Primary				
Bax	1: 250	12	Sc-493	Santa Cruz
Bcl-2	1: 1 000	12	2870S	Cell Signalling
LC3-A/B	1: 1 000	12	4108S	Cell Signalling
p53	1: 500	12	9282S	Cell Signalling
p62	1: 1 000	12	5114S	Cell Signalling
t-mTOR	1: 1 000	10	2983S	Cell Signalling

p-mTOR	1: 1 000	10	2974S	Cell Signalling
pAMPK	1: 800	12	3535S	Cell Signalling
β-Actin	1: 1 000	12	Sc-47778	Santa Cruz
Secondary				
Donkey anti-mouse IgG-HRP	1: 4 000	-	Sc-23181	Santa Cruz
Donkey anti-rabbit IgG-HRP	1: 4 000	-	Sc-2012	Santa Cruz

Legend to Figure: **Cat #:** catalogue number

3.7 Proteome profiler array

A protein profiler was used to determine the effect of ASP on Caov-3 ovarian carcinoma cells using Human Apoptosis Proteome Profiler™ arrays kit following the manufacturer's instructions. Briefly, following pre-determined experimental conditions, cells were lysed and proteins quantified as previously described method in section 3.6.2.2. Thereafter, the arrays containing the antibodies of interest were blocked in Array Buffer 1 for 1 hr at RT in a 4 well-multi dish. Expression of profiler proteins were evaluated according to the manufacturer's instructions. After 1 hr incubation, the buffer was replaced with 250 µg of proteins from each experimental condition and incubated on an orbital shaker overnight at 4°C. The following day, arrays were washed with 1x wash buffer 3 times for 10 mins. Following the last wash, the wash buffer was replaced with 1.5 mL of detection antibody per well and the multi well containing the arrays were incubated for 1 hr at RT on an orbital shaker before the arrays were washing 3x for an additional 10 mins. Subsequently, the arrays were incubated with Streptavidin-HRP. Thereafter, the arrays were washed 3x for 10 mins before detection and quantification of proteins using a Chemidoc-XRS imager and Quantity One software.

3.8 Statistical analysis

Data were expressed as the mean ± standard error of mean (SEM) of 3 independent biological experiments, containing at least 3 technical replicates. GraphPad Prism was used for calculation of one-way multivariate ANOVA, followed by a Turkey post hoc test or student t-test where appropriate. A p-value of ≤ 0.05 was deemed as statistically significant.

CHAPTER 4

RESULTS

4.1 Determination of optimal dose of ASP

ATP as a measurement of metabolic activity was used to determine the most effective time and dose for ASP treatment. Results in Figure 4.1A showed that ASP induced a concentration-dependent response, with both 0.1 µM (123.7 ± 4.9; $p < 0.05$ compared to 100) and 1 µM (122.3 ± 3.8; $p < 0.05$ compared to 100) ASP being the most effective concentration compared to the control. Half maximal effective concentration (EC_{50}) analysis (Figure 4.1B) showed that ASP was not toxic at any of the concentrations or exposure times tested (including the highest dose), with 48 hrs exposure at a dose of 1000 µM having a best-fit value of 76.8%. Therefore, EC_{50} values were not employed and the highest effective dose of 1 µM was used for all subsequent experiments.

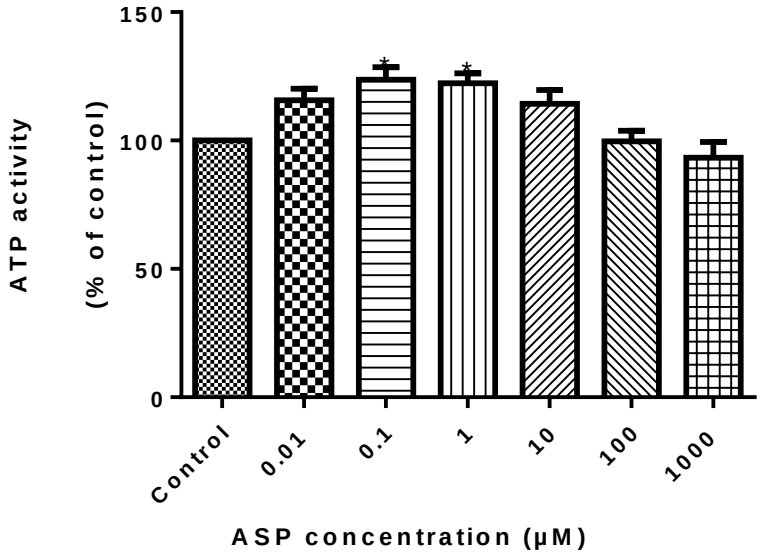

Figure 4.1 A: Determination of time and dose response of H9c2 cells exposed to aspalathin (ASP*).* ATP as a measurement of metabolic activity of H9c2 cardio myoblasts was tested at varying concentrations and doses of ASP. ASP at 1 µM was selected as the most effective dose and used in all subsequent experiments. Data is represented as three independent biological experiments, each with three technical replicates (n=9). Results are expressed as the mean ± SEM. *$p < 0.05$ compared to control.

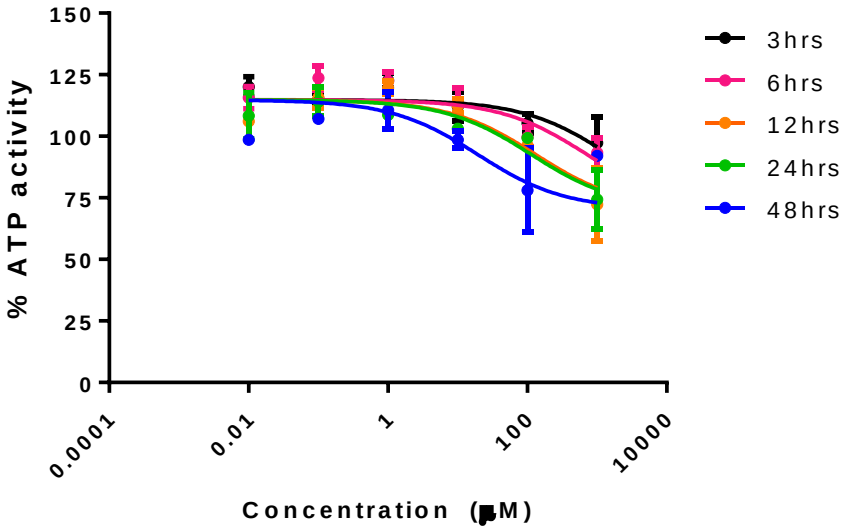

Figure 4.1B: Half maximal effective concentration (EC50) determination of aspalathin (ASP) on H9c2 cells. EC_{50} analysis did not induce a toxic effect even after testing at the highest concentration at the specified exposure times. The highest ASP dose (1000 µM) for 48 hrs had a best-fit value of 76.8. Data is represented as three independent biological experiments, each with three technical replicates (n=9). Results are expressed as the mean ± SEM.

4.2 Determination if ASP pre- or co-treatment was more effective

To examine the most effective prophylactic treatment of ASP on Dox-induced cardiotoxicity, H9c2 cells were either pre- or co-treated with 1 µM ASP. Analysis of results showed that treatment at a dose of 0.2 µM Dox daily for 5 days resulted in a significant decrease in ATP activity (40.85 ± 6.3%, $p < 0.001$) when compared to the normal control (100%) (Figure 4.2). Co-treatment with ASP significantly ablated this effect when compared to the Dox control group (91.16 ± 12.45% compared to 40.85 ± 6.3%, $p < 0.001$). Co-treatment with Dox and Dexra (73.8 ± 11.96%), as well as pre-treatment with ASP and Dox (59.61 ± 9.9%), increased metabolic activity when compared to the Dox only control group, although not significantly. Thus, co-treatment of Dox with ASP was employed for all consecutive experiments.

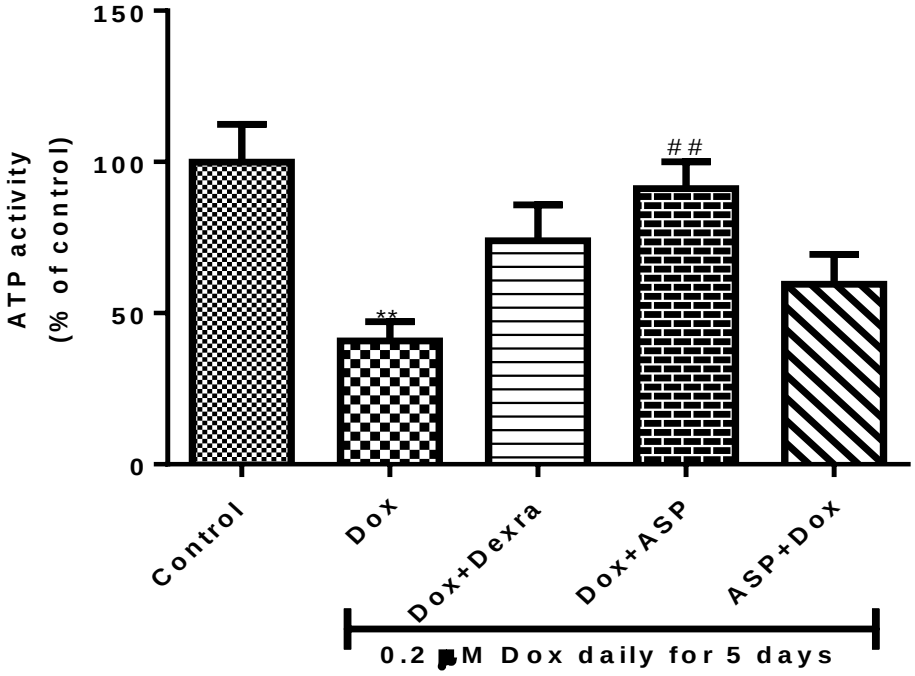

Figure 4.2: The effect of aspalathin (ASP) pre- and co-treatment on metabolic activity of H9c2 cells exposed to Dox. H9c2 cells were either treated with 0.2 µM Dox or co-treated with either 20 µM dexrazoxane (Dexra) or 0.2 µM aspalathin (ASP) daily for 5 days. H9c2 cells were also pre-treated with 1µM ASP for 6 hrs before treating with 0.2 µM Dox for 5 days. Data is represented as three independent biological experiments, each with three technical replicates (n=9). Results are expressed as the mean ± SEM. **$p < 0.01$ versus control and $^{\#\#}p < 0.01$ versus Dox.

4.3 ASP attenuates Dox-induced oxidative stress in H9c2 cardio myoblasts

The most accepted theory has suggested that Dox-induced cardiotoxicity is due to increased oxidative stress (Wallace, 2003). In this study, SOD, GSH and CAT activities were investigated to determine if ASP can increase the cells endogenous antioxidant capacity.

4.3.1 SOD activity

Dox treatment of H9c2 cells showed a significant decrease in SOD activity (71.2 ± 2.3%, $p < 0.001$) when compared to the normal control (88.30 ± 1.97%). ASP co-treatment significantly increased SOD activity by 8.2% (79.4 ± 2.8%, $p < 0.05$) (Figure 4.3) when compared to Dox control group while the combination of Dox and Dexra was able to increase SOD activity, although not significantly (76 ± 2.6%).

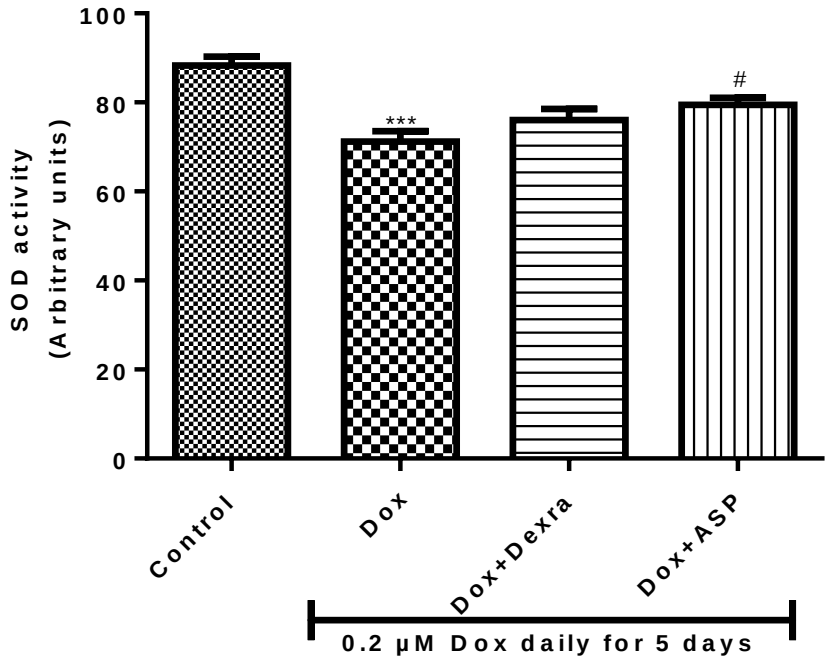

Figure 4.3: The effect of doxorubicin (Dox) and aspalathin (ASP) co-treatment on superoxide dismutase (SOD) activity in H9c2 cells. H9c2 cells were either treated with 0.2 µM Dox or co-treated with either 20 µM dexrazoxane (Dexra) or 0.2 µM aspalathin (ASP) daily for 5 days. Data is represented as three independent biological experiments, each with three technical replicates (n=9). Results are expressed as the mean ± SEM. ***$p < 0.001$ versus control and $^{\#}p < 0.05$ versus Dox.

4.3.2 CAT activity

In this study we observed that chronic exposure of H9c2 cells to Dox significantly decreased CAT activity when compared to the normal control (from 16.93 ± 1.8 mol/min/ml to 9.4 ± 1.02 mol/min/ml, $p < 0.01$) (Figure 4.4). Co-treatment with ASP was able to improve endogenous CAT activity (16.23 ± 1.98 nmol/min/ml, $p < 0.05$) when compared to the Dox control group. This result suggests that ASP may contribute to the cellular defense of CAT against Dox-induced cardiotoxicity. Interestingly, co-treatment with the FDA approved drug, Dexra, did not show a similar effect (Figure 4.4).

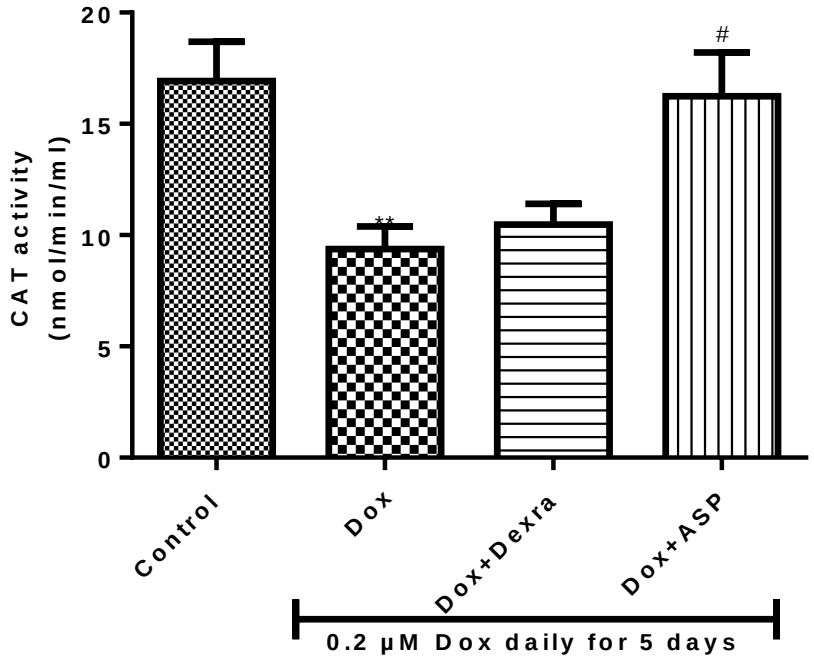

Figure 4.4: The effect of doxorubicin (Dox) and aspalathin (ASP) co-treatment on catalase (CAT) activity in H9c2 cells. H9c2 cells were either treated with 0.2 µM Dox or co-treated with either 20 µM dexrazoxane (Dexra) or 0.2 µM aspalathin (ASP) daily for 5 days. Data is represented as three independent biological experiments, each with three technical replicates (n=9). Results are expressed as the mean ± SEM. **$p < 0.01$ versus control and $^{\#}p < 0.05$ versus Dox.

4.3.3 GSH activity

The myocardium is particularly susceptible to decreased GSH activity that occur as a result of increased ROS stresses which contributes to the progression of heart failure. As anticipated, we observed that GSH level were significantly decreased after Dox treatment when compared to the normal control (31 ± 2.6%, $p < 0.001$ compared to 100%) (Figure 4.5). However, co-treatment with ASP increased the activity of GSH (48 ± 1.2%) although not significantly. Conversely, a significant increase in GSH activity was observed after H9c2 cells were co-treated with Dox and Dexra (51 ± 5.1%, $p < 0.01$).

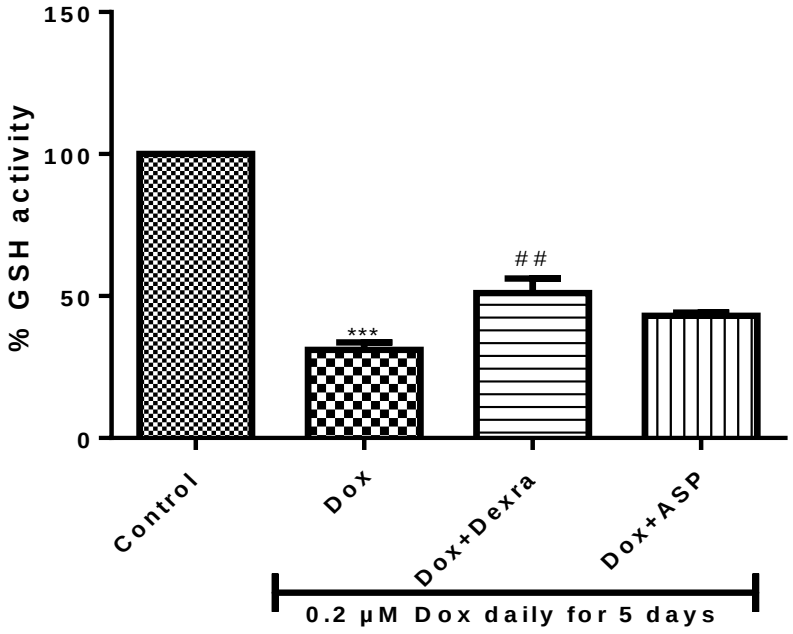

Figure 4.5: The effect of doxorubicin (Dox) and aspalathin (ASP) co-treatment on glutathione (GSH) activity in H9c2 cells. H9c2 cells were either treated with 0.2 µM Dox or co-treated with either 20 µM dexrazoxane (Dexra) or 0.2 µM aspalathin (ASP) daily for 5 days. Data is represented as three independent biological experiments, each with three technical replicates (n=9). Results are expressed as the mean ± SEM. ***$p < 0.001$ versus control and $^{\#\#}p < 0.01$ versus Dox.

4.4 The effect of ASP on lipid peroxidation

Results obtained showed that chronic exposure of H9c2 cardio myoblasts to Dox resulted in a significant increase in MDA activity (27.75 ± 2.1, $p < 0.001$) when compared the normal control group (11.50 ± 1.4). Treatment with Dox and ASP significantly decreased lipid peroxidation (17.75 ± 2.1, $p < 0.01$) when compared to the Dox control group. Similarly, a significant reduction was observed when the H9c2 cardio myoblasts were co-treated with Dox and Dexra (17.75 ± 0.7, $p < 0.01$) (Figure 4.6).

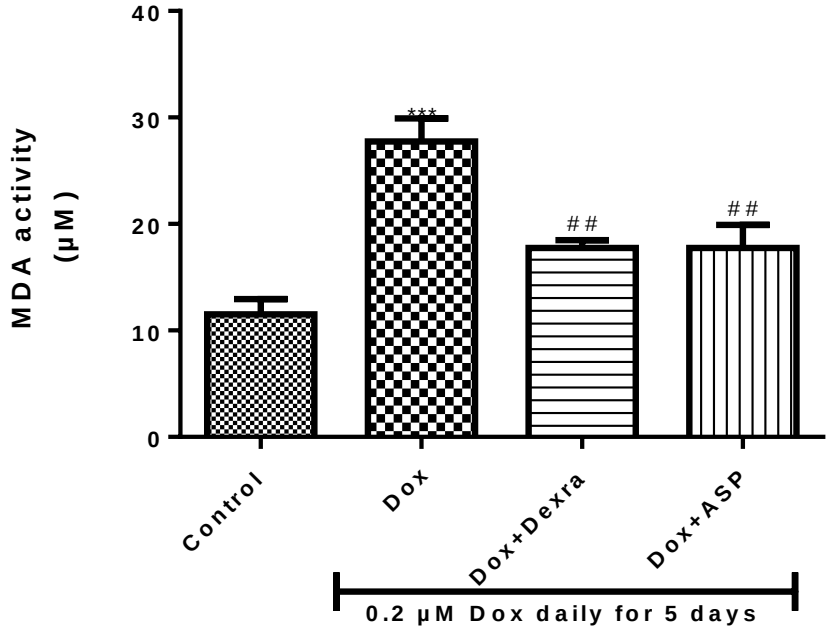

Figure 4.6: The effect of ASP on lipid peroxidation on H9c2 cells treated with 0.2 µM Dox for 5 days. MDA activity was measured in order to evaluate lipid peroxidation. H9c2 cells were either treated with 0.2 µM Dox or co-treated with either 20 µM dexrazoxane (Dexra) or 0.2 µM aspalathin (ASP) daily for 5 days. Data is represented as three independent biological experiments, each with three technical replicates (n=9). Results are expressed as the mean ± SEM. ***$p < 0.001$ versus control and $^{\#\#}p < 0.01$ versus Dox.

4.5 ASP attenuated the Dox-induced myocardial apoptosis

4.5.1 Effect of ASP on the expression of p53

Alterations in p53 protein expression induced by Dox treatment were analyzed using western blot analysis. The results obtained demonstrated that Dox treatment alone significantly increased the expression of p53 (138.1 ± 9.7%, $p < 0.01$), an indicative of DNA damage when compared to untreated cells. Co-treatment with ASP resulted in a significant decrease in the expression of p53 (108.2 ± 6.5%, $p < 0.05$) when compared to Dox treated cells. A combination of Dox and Dexra decreases p53 expression, but not significantly (129.6 ± 7.9%) (Figure 4.7)/

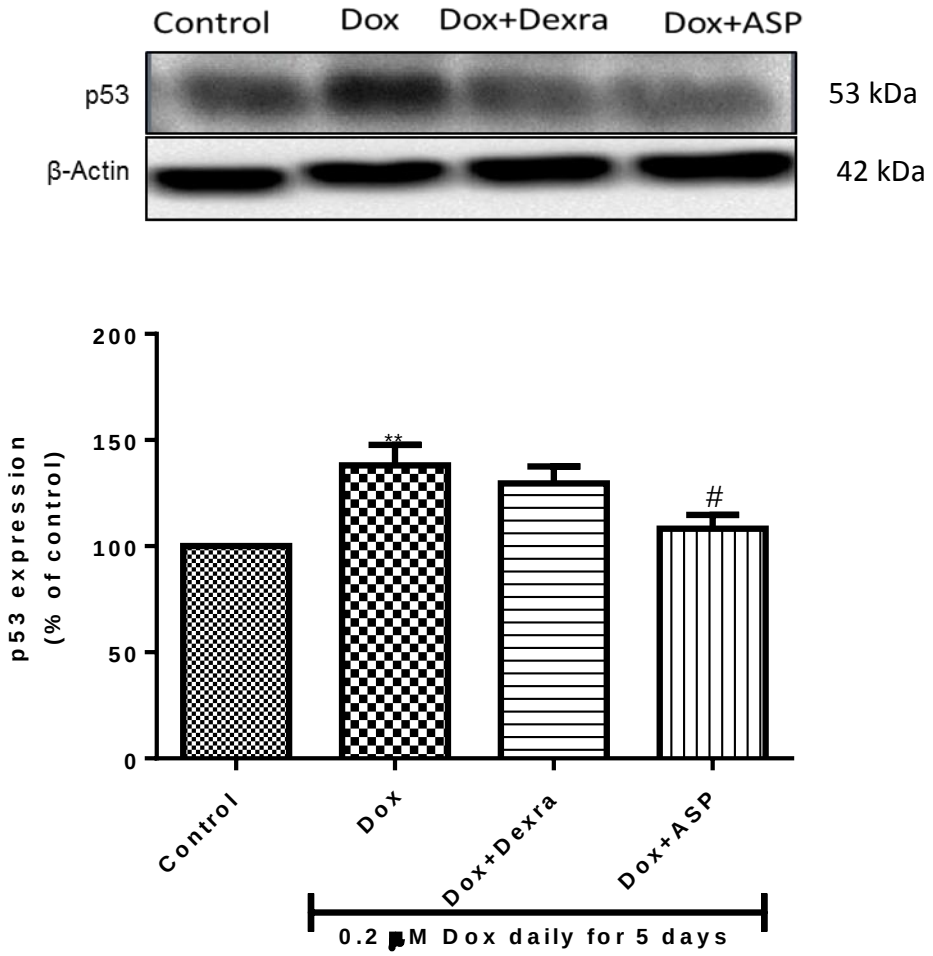

Figure 4.7: The effect of ASP on p53 expression on Hc2 cells treated with 0.2 μM Dox for 5 days. H9c2 cells were either treated with 0.2 μM Dox or co-treated with either 20 μM dexrazoxane (Dexra) or 0.2 μM aspalathin (ASP) daily for 5 days. Data is represented as three independent biological experiments, each with three technical replicates (n=9). Results are expressed as the mean ± SEM. **$p < 0.01$ versus control and $^{\#}p < 0.05$ versus Dox.

4.5.2 Bcl-2 / Bax ratio

The effect of Dox and ASP on the expression levels of Bcl-2 family proteins was evaluated in H9c2 cardio myoblasts using western blotting analysis. A decrease in Bcl-2/Bax ratio up-regulates caspase 3 and increases apoptosis. In this study a decrease in Bcl-2 protein expression was observed after Dox treatment (Figure 4.8). Upon determining the Bcl-2/Bax ratio, a significant decrease in the Bcl-2/Bax ratio was observed when cells were exposed to Dox (0.38 ± 0.05, $p < 0.01$ compared to 0.9 ± 0.14) when compared to the normal control. Interestingly, co-treatment with ASP or Dexra significantly increased the Bcl-2/Bax ratio (0.65 ± 0.06, $p < 0.01$ or 0.61 ± 0.08, $p < 0.01$) when compared to Dox treatment alone (Figure 4.8).

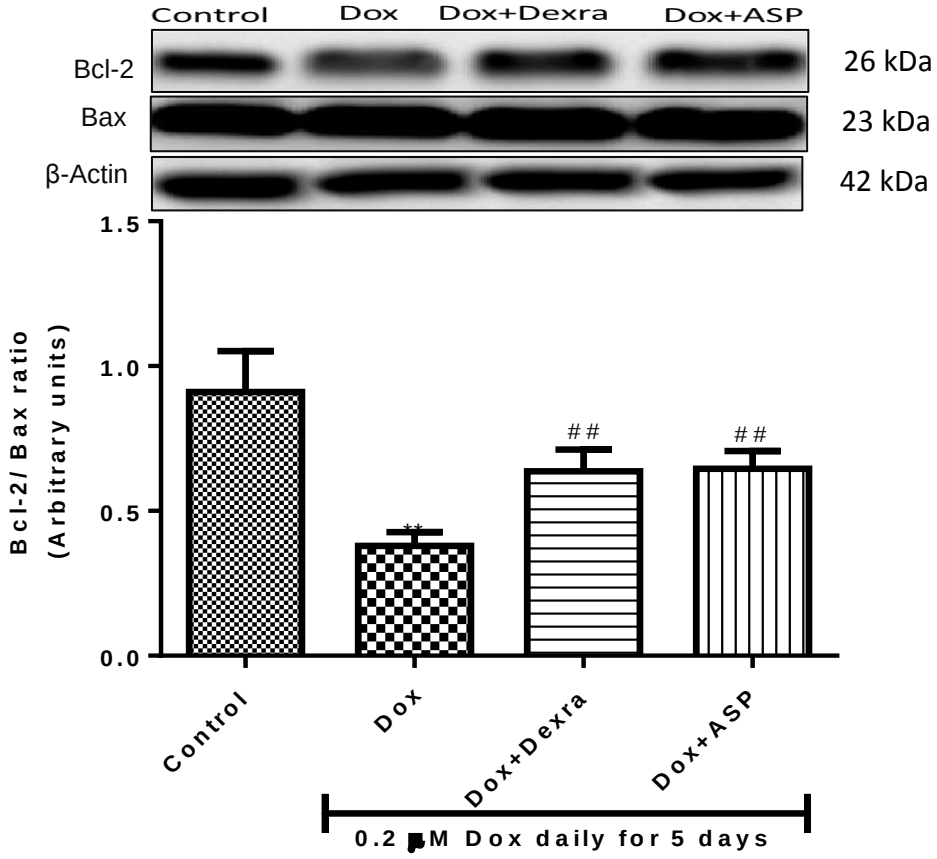

Figure 4.8: The effect of ASP on Bcl-2/Bax ratio on H9c2 cells treated with 0.2 μM Dox for 5 days. H9c2 cells were either treated with 0.2 μM Dox or co-treated with either 20 μM dexrazoxane (Dexra) or 0.2 μM aspalathin (ASP) daily for 5 days. Data is represented as three independent biological experiments, each with three technical replicates (n=9). Results are expressed as the mean ± SEM. **$p < 0.01$ versus control and $^{\#\#}p < 0.01$ versus Dox.

4.5.3 Caspase 3/7 activity

The Caspase-Glo® 3/7 activity assay was used as a measurement of Dox-induced apoptotic cell death of H9c2 cardio myoblasts. H9c2 cardio myoblasts exposed to Dox displayed increased caspase 3/7 activity (205.9 ± 24.16%, $p < 0.01$) when compared to the normal control (100 ± 5.5%, $p < 0.01$) (Figure 4.9). Co-treatment with Dox and Dexra (76.85 ± 10.92%, $p < 0.01$) as well as Dox and ASP (103.9 ± 19.87%, $p < 0.05$) significantly decreased Dox-induced apoptosis when compared to Dox control group.

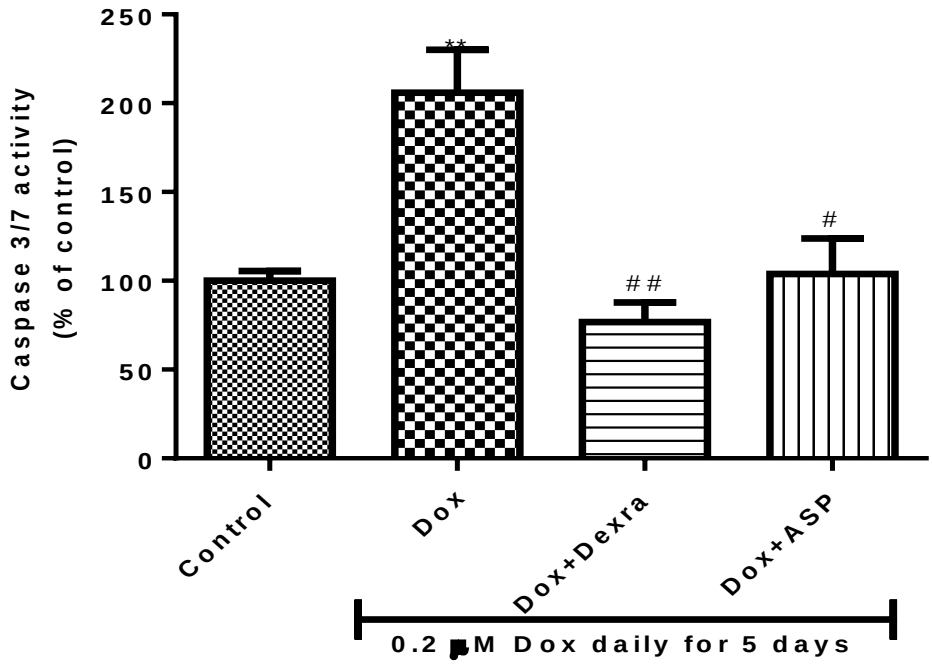

Figure 4.9: The effect of ASP on Caspase 3/7 activity on H9c2 cells treated with 0.2 µM Dox for 5 days. Except for the vehicle control group, H9c2 cells were either treated with 0.2 µM Dox or co-treated with either 20 µM dexrazoxane (Dexra) or 0.2 µM aspalathin (ASP) daily for 5 days. Data is represented as three independent biological experiments, each with three technical replicates (n=9). Results are expressed as the mean ± SEM. **$p < 0.01$ versus control and $^{\#}p < 0.05$ and $^{\#\#}p < 0.01$ versus Dox.

4.5.4 ASP decreases DNA fragmentation

TUNEL staining is one of the most widely used methods to detect DNA fragmentation, a hallmark of apoptosis. Results obtained showed that chronic exposure of H9c2 cardio myoblasts to Dox resulted in an internucleosomal fragmentation of DNA as shown by a significant increase in TUNEL positive cells (2.5 ± 0.39 to 8.47 ± 0.89, $p < 0.0001$) when compared to normal control (Figure 4.10A and B). By contrast, co-treatment with ASP effectively ameliorated Dox-induced DNA fragmentation by significantly decreasing the number of TUNEL positive cells (3.3 ± 0.48, $p < 0.0001$). Correspondingly, a significant decrease in the number of TUNEL positive cells were observed when H9c2 cardio myoblasts were co-treated with Dox and Dexra (3.9 ± 0.84 $p < 0.0001$).

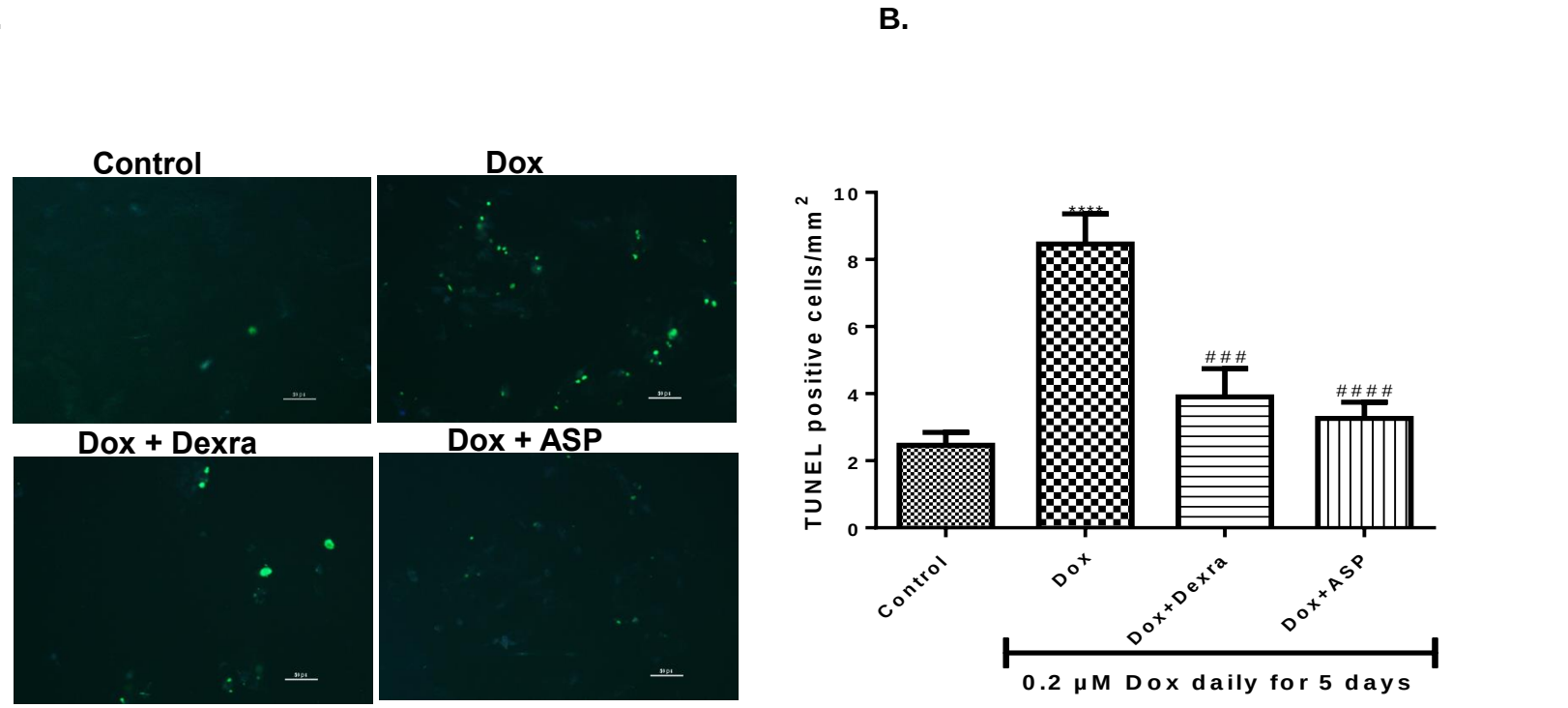

Figure 4.10: The effect of Aspalathin on Dox-induced DNA fragmentation. A) Photomicrograph of TUNEL staining. B) Bar graph representing a quantitative analysis of TUNEL-positive cells. The apoptotic rate was calculated as the average number of condensed TUNEL-positive cells of non-overlapping fields of 1 mm^2 under a 10x magnification field (average of at least 5 fields per well). This was done blinded and evaluated by 2 independent researchers. Except for the vehicle control group, H9c2 cells were either treated with 0.2 µM Dox or co-treated with either 20 µM dexrazoxane (Dexra) or 0.2 µM aspalathin (ASP) daily for 5 days. Data is represented as three independent biological experiments, each with three technical replicates (n=9). Results are expressed as the mean ± SEM. ****$p < 0.0001$ versus control and $^{###}p < 0.001$ and $^{####}p < 0.0001$ versus Dox.

4.6 ASP prevents Dox-induced apoptosis and activates autophagy

4.6.1 The effect of ASP on the expression of LC3-II

The expression of LC3-II is widely used as a marker to monitor autophagy as it correlates with the number of autophagic vacuoles. In addition, LC3-II is a known biomarker for autophagy as it initiates the formation of the autophagosome. In this study, the expression of LC3-II was evaluated using Western blot analysis. Results obtained showed that Dox treatment decreased expression of LC3-II *(*38.71 ± 2.1%, $p < 0.01$*)*, suggesting the inhibition of autophagy upon Dox treatment when compared to the untreated control group (100%) (Figure 4.11). Interestingly, Dox in combination with ASP moderately increased the expression of LC3-II (54.33 ± 3.9%, $p < 0.05$) when compared to Dox control group while co-treatment with Dox and Dexra did not have an effect on LC3-II expression versus Dox alone (43.86 ± 6.07%).

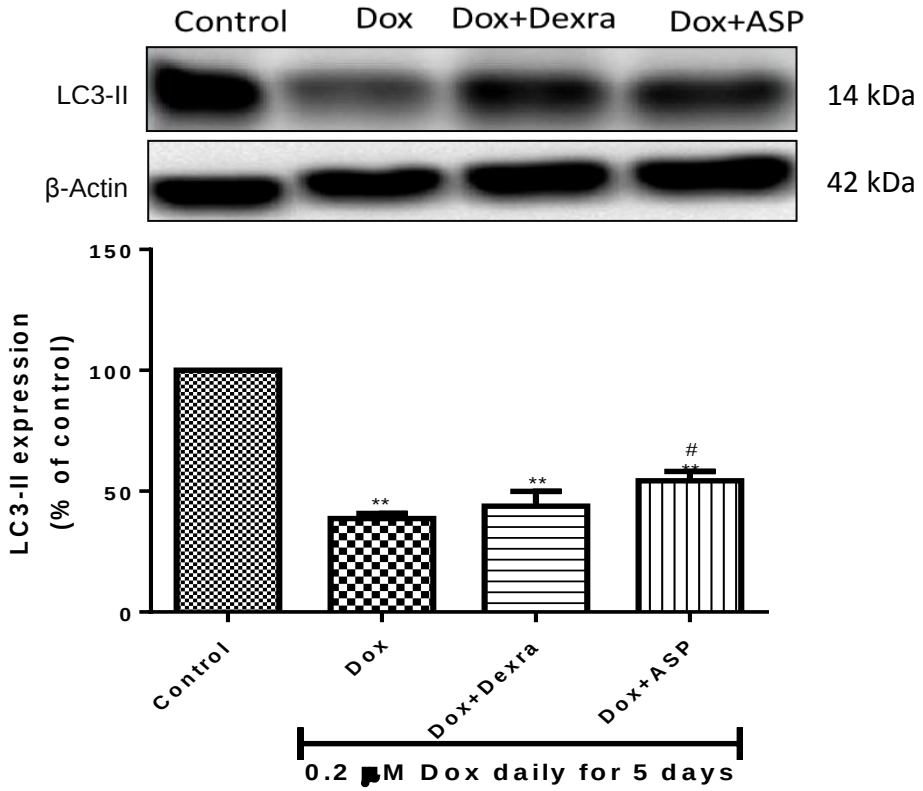

Figure 4.11: The expression of LC3-II in Dox-induced cardiotoxicity. Except for the vehicle control group, H9c2 cells were either treated with 0.2 µM Dox or co-treated with either 20 µM dexrazoxane (Dexra) or 0.2 µM aspalathin (ASP) daily for 5 days. All blots were normalized to beta actin as loading control. Data is represented as three independent biological experiments, each with three technical replicates (n=9). Results are expressed as the mean ± SEM. **$p < 0.01$ versus control and $^{\#}p < 0.05$ versus Dox.

4.6.2 The effect of ASP on p-AMPK expression

Dox-induced AMPK inhibition is known to result in increased p53 accumulation within the cell. Subsequently, in this study the effect of ASP on p-AMPK activation was investigated. A decrease in p-AMPK expression was observed after H9c2 cardio myoblasts were treated with a cumulative dose of 1 µM Dox for 5 days (from 100% to 54.56 ± 8.8%, $p < 0.01$), indicating that Dox treatment inhibited p-AMPK expression. However, co-treatment with Dox and ASP was able to significantly increase p-AMPK expression by approximately 41% (95.41 ± 11.2%, $p < 0.01$) when compared to the Dox treated control. Similarly, an increased p-AMPK activity was observed when H9c2 cells were co-treated with Dox and Dexra (71.82 ± 3.5%), though not significant (Figure 4.12).

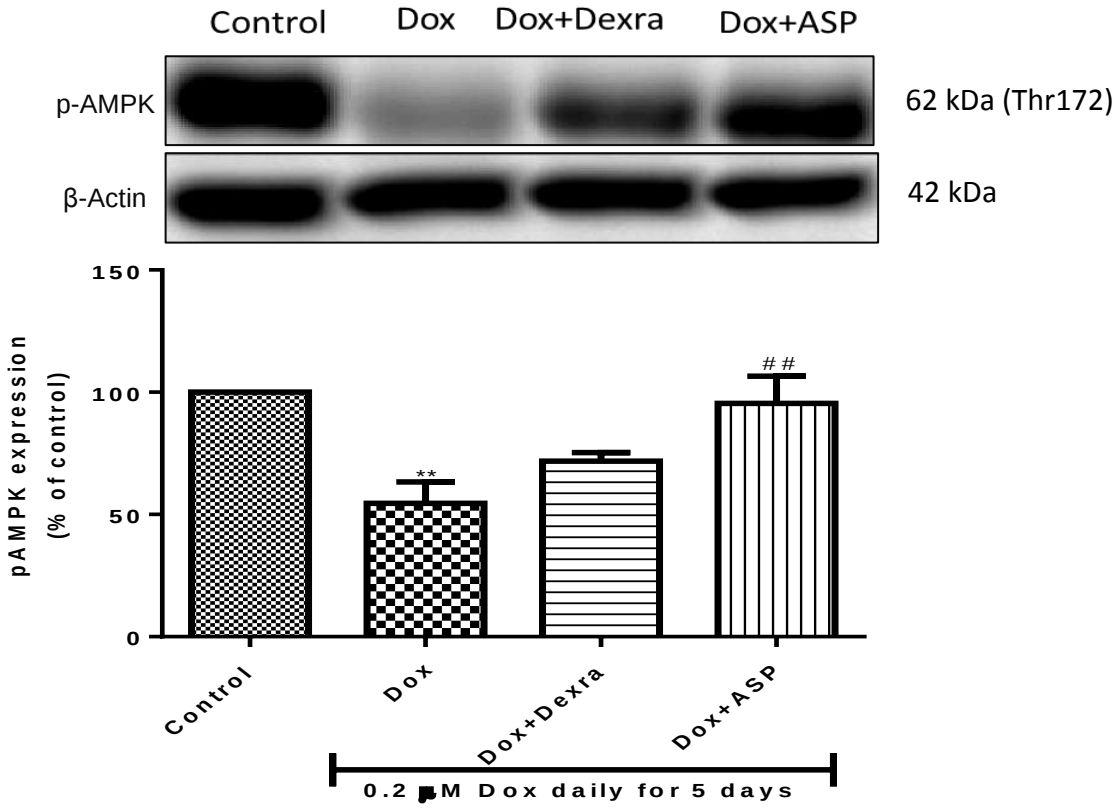

Figure 4.12: The expression of p-AMPK in Dox-induced cardiotoxicity. H9c2 cells were either treated with 0.2 µM Dox or either co-treatment with 20 µM dexrazoxane (Dexra) or 0.2 µM ASP daily for 5 days. All blots were normalized to beta actin as the loading control. Data is represented as three independent biological experiments, each with three technical replicates (n=9). Results are expressed as the mean ± SEM. **$p < 0.01$ versus control and $^{\#\#}p < 0.01$ versus Dox**.**

4.6.3 The effect of ASP on the expression of mTOR

MTOR is a protein kinase and key inhibitor of autophagy, a process that contributes to cell survival. To establish the role of mTOR signaling in DOX-induced cardiotoxicity, the ratio of p-mTOR\t-mTOR was evaluated using Western blot analysis. A slight increase in the p-mTOR\t-mTOR ratio (0.161 ± 0.0.019) was observed upon Dox treatment when compared to the normal control group (0.12 ± 0.025*)*. However, co-treatment of Dox with either ASP or Dexra was unable to ablate this response (0.17 ± 0.01 or 0.16 ± 0.02*,* respectively) (Figure 4.13).

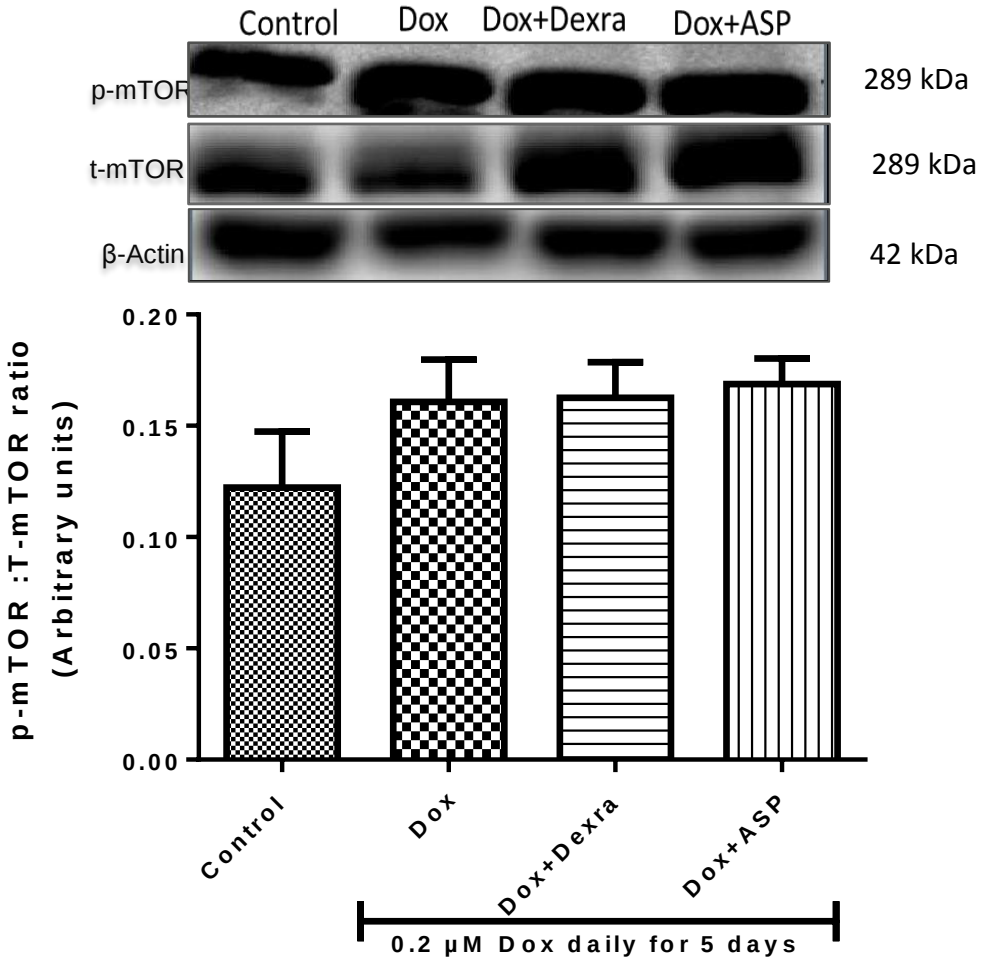

Figure 4.13: The expression of mTOR in Dox-induced cardiotoxicity. H9c2 cells were either treated with 0.2 µM Dox or either co-treatment with 40 µM dexrazoxane (Dexra) or 0.2 µM ASP daily for 5 days. All blots were normalized to beta actin as loading control. Data is represented as three independent biological experiments, each with three technical replicates (n=9). Results are expressed as the mean ± SEM.

4.7 Transcriptional regulation of autophagy genes

4.7.1 The effect of ASP to activate autophagy genes

To further investigate the role of autophagy in Dox-induced cardiotoxicity, mRNA expression of 6 genes, essential activators of Autophagy (*Atg5*, *Atg7*, *Becln1 (Atg6),* *BNIP3*, *Fox01* and *AMPK*) and the inhibitor (mTOR) of autophagy was assessed. The mRNA expression of autophagy-related genes, *Atg 5*, *7* and *6* was decreased upon Dox treatment (0.55 ± 0.19, $p < 0.01$; 0.64 ± 0.2, $p < 0.01$ and 0.62 ± 0.21, $p < 0.01$, respectively) when compared to the untreated control (Figure 4.14 and Table 4.1). Interestingly, an increase in mRNA expression of autophagy genes was observed after H9c2 cells were treated with Dox and ASP (0.85 ± 0.24, 1.06 ± 0.3, 0.97 ± 0.26, respectively), or Dox and Dexra (0.80 ± 0.24, 1.02 ± 0.28, 0.88 ± 0.24, respectively), though not significantly. Similarly, the expression of *AMPK*, *BNIP3* and *Fox01* was decreased upon treatment with Dox (0.94 ± 0.28, 0.72 ± 0.23, 0.71 ± 0.24, respectively) whereas mRNA expression of *mTOR* (1.30 ± 0.21) was increased when compared to the normal control. Co-treatment with ASP increased mRNA expressions of the latter (1.21 ± 0.33, 1.17 ± 0.39, 1.18 ± 0.32, respectively) and results obtained were comparable to our reference control, Dexra (1.38 ± 0.41, 1.04 ± 0.33, 1.14 ± 0.31, respectively).

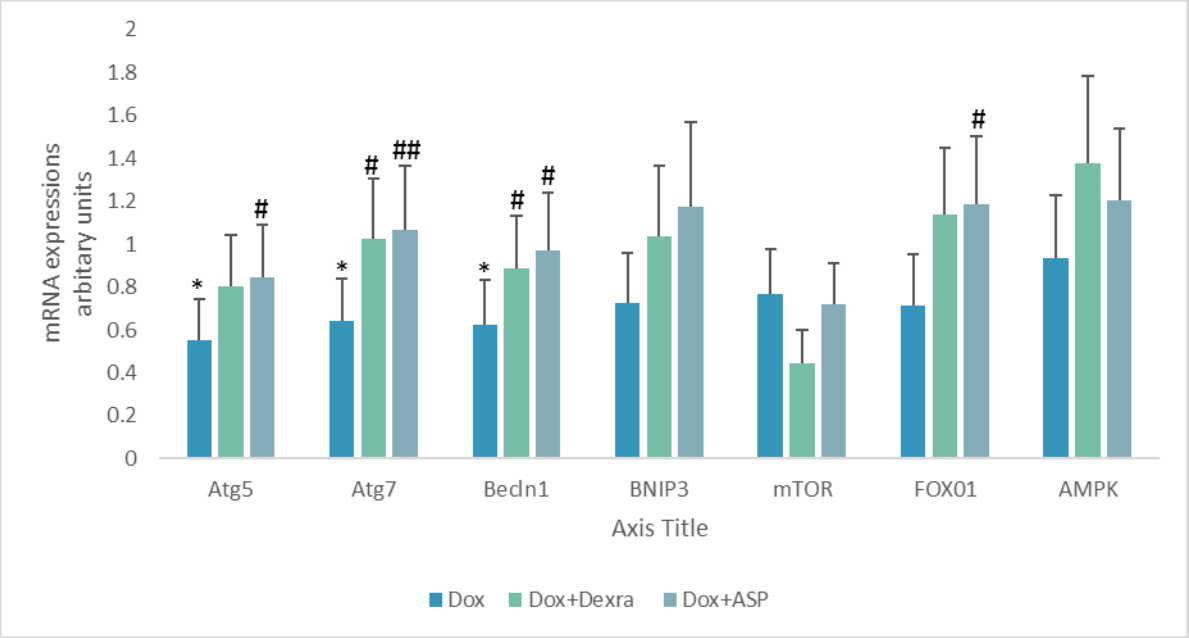

Figure 4.14: The effect of ASP on the mRNA expression of autophagy genes. H9c2 cells were either treated with 0.2 µM Dox or either co-treatment with 40 µM dexrazoxane (Dexra) or 0.2 µM ASP daily for 5 days. The results were normalized to *ActB* and *Hprt1* as housekeeping genes. Data is represented as three independent biological experiments, each with three technical replicates (n=9). Results are expressed as the mean ± SEM. *p < 0.05 versus control and #p < 0.05 and ##p < 0.01 versus Dox.

Table 4.1: Summary of mRNA gene expression results

Genes	***Dox***	***Dox+Dexra***	***Dox+ASP***
Atg5	↓1.81 ± 0.19 *	↑1.24 ± 0.24	↑1.18 ± 0.25 #
Atg7	↓1.56 ± 0.2 *	↑1.02 ± 0.28 #	↑1.06± 0.30 ##
Beclin1	↓1.61 ± 0.21 *	↑1.13 ± 0.25 #	↑1.03± 0.27 #
BNIP3	↓1.38 ± 0.23	↑1.04 ± 0.33	↑1.17± 0.4
Fox01	↓1.40 ± 0.24	↑1.14 ± 0.31	↑1.18± 0.32 #
AMPK	↓1.72 ± 0.29	↑1.38 ± 0.41	↑1.2± 0.34
mTOR	↑1.30 ± 0.21	↓2.24 ± 0.16	↓1.39± 0.19

Legend to Figure*:* Arrows indicate fold difference relative to the control set as 1. ↓: Down regulated; ↑: Up regulated. Results are expressed as the mean ± SEM. *p < 0.05 versus control and #p < 0.05 and ##p < 0.01 versus Dox.

4.8 The effect of ASP on Dox efficacy to apoptosis in Caov-3

4.8.1 Metabolic activity

To determine if ASP treatment inhibits the cancer efficacy of Dox, Caov-3 ovarian carcinoma cells were either treated with Dox, ASP or a combination of Dox and ASP for 5 days. Results obtained showed that ATP activity was significantly decreased after 5 days of Dox exposure when compared to the normal control group (14.15 ± 1.5, $p < 0.01$ compared to 100.0 ± 19.16). Interestingly, when compared to the Dox control, ASP did not decrease the efficacy of Dox after Caov-3 cells were co-treated with Dox and ASP for 5 days (14.84 ± 1.9, $p < 0.01$). Conversely, Caov-3 cells treated with ASP only did not have any effect in metabolic activity (94.75 ± 14.51) when compared to the normal control.

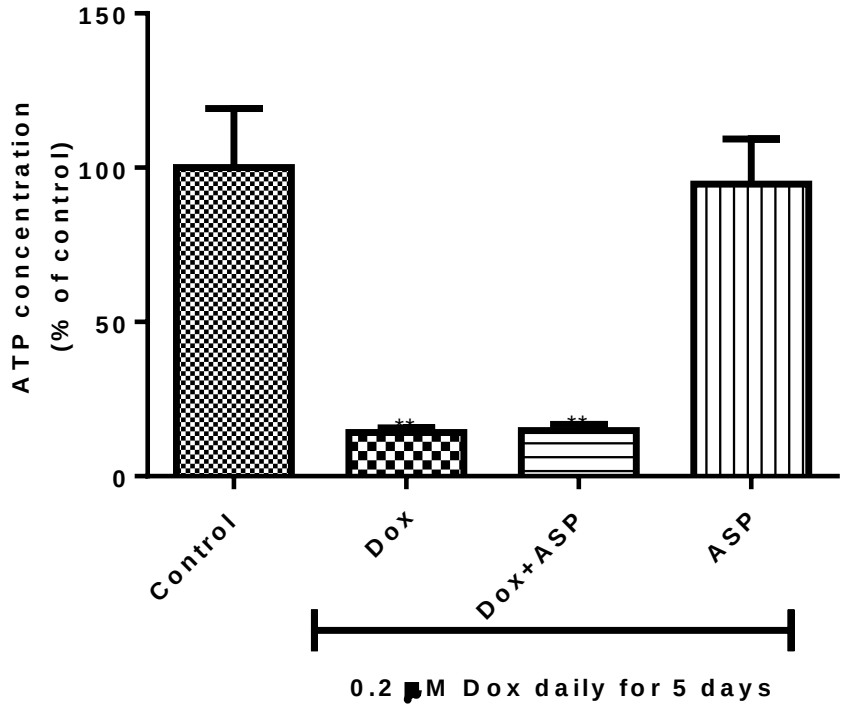

Figure 4.15: ASP co-treatment decrease ATP activity in Caov-3 cells. ATP assay was used to determine the metabolic activity. Caov-3 cells were either treated with 0.2 µM Dox or co-treated with ASP daily for 5 days. Data is represented as three independent biological experiments, each with three technical replicates (n=9). Results are expressed as the mean ± SEM. **p < 0.01 versus control.

4.8.2 Caspase 3/7 activity

To further investigate the effect of ASP on Dox anti-cancer efficacy, Caspase 3/7 activity was evaluated in Caov-3 cells. Caspase 3/7 activity was slightly increased upon Dox treatment (127.9 ± 2.8) when compared to the normal control (116.3 ± 5.4) (Figure 4.15).A similar effect was observed upon co-treatment with ASP (133.5 ± 15.2). Surprisingly, ASP treatment alone significantly increased caspase 3/7 activity (155.2 ± 0.3, $p < 0.05$) when compared to the untreated control group.

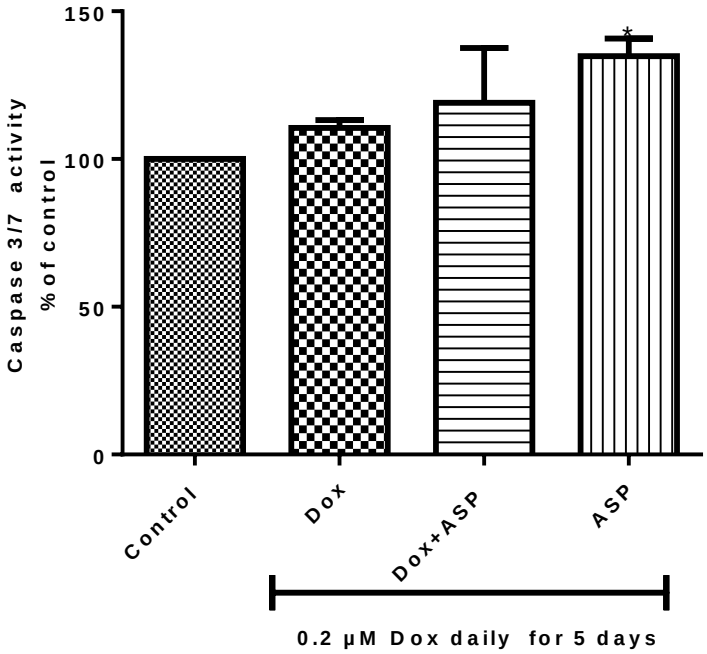

Figure 4.16: The effect of ASP on Caspase 3/7 activity in Caov-3 cells treated with 0.2 µM of Dox for 5 days. Caov-3 cells were either treated with 0.2 µM Dox or co-treated with ASP daily for 5 days. Data is represented as three independent biological experiments, each with three technical replicates (n=9). Results are expressed as the mean ± SEM. *$p < 0.05$ versus control**.**

4.8.3 The effect of ASP co-treatment on expression of some pro-apoptotic proteins

To determine if ASP co-treatment decreases the anti-cancer efficacy of Dox, various pro-apoptotic and tumor suppressor proteins were evaluated (Table 2). Results obtained showed that Dox treatment was unable to increase the expression of pro apoptotic proteins; Bad, Clap-1, Trial-2, Omi and Smac when compared to the untreated control group. However, co-treatment of Dox with ASP was able to induce apoptosis and significantly increase the expression of the latter genes, as can be seen in Table 2. Furthermore, the expression of p27, p21, p53, tumor suppressers that are known to inhibit the proliferation of cancer cells was determined. Interestingly, the latter proteins were significantly upregulated after Dox treatment and combination of Dox and ASP was able to enhance this effect.

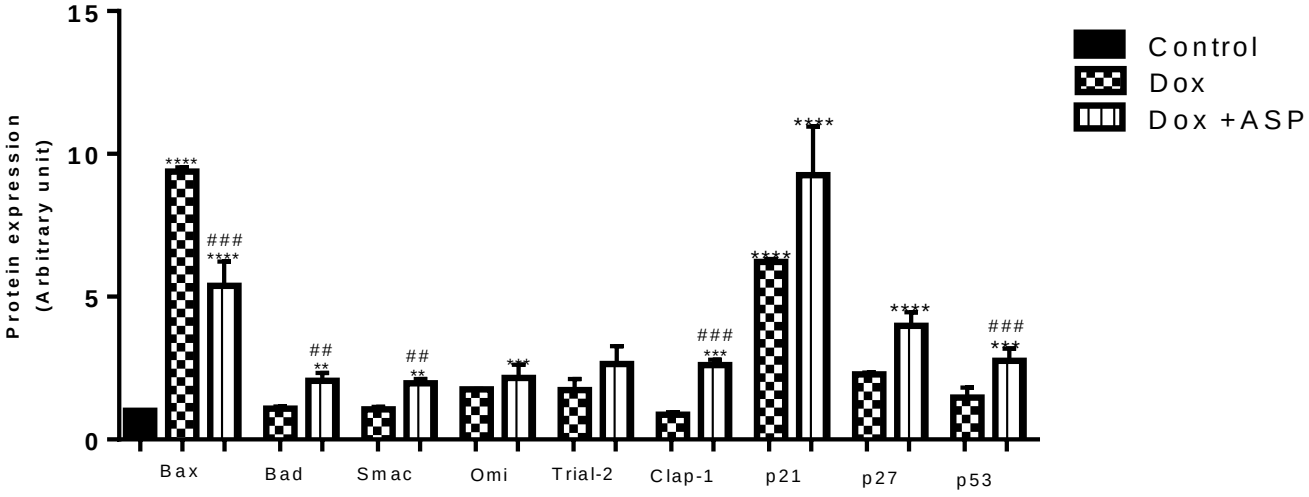

Figure 4.17: The effect of ASP on pro-apoptotic protein expression in Caov-3 cells. Caov-3 cells were either treated with 0.2 µM Dox or co-treated with ASP daily for 5 days. Data is represented as three independent biological experiments, each with three technical replicates (n=9). Results are expressed as the mean ± SEM. **p < 0.01, ***p < 0.001 and ****p < 0.0001 vs control and $^{\#\#}$p < 0.01 and $^{\#\#\#}$p < 0.001 vs Dox**.**

Table 4: Summary of apoptotic proteins results

Proteins	***Dox***	***Dox+ ASP***
Bax	↑ 9.4 ± 0.13****	↑ 5.4 ± 0.74**** ###
Bad	↔ 1.08 ± 0.07	↑ *2.05 ± 0.24*** ##
Clap-1	↔ 0.87 ± 0.07	↑*2.6 ± 0.16**** ###
Trial-2	↑1.7 ± 0.34	↑*2.64 ± 0.5*
Omi	↑1.76 ± 0.02	↑*2.16 ± 0.4*
Smac	↔1.06 ± 0.24	↑ *1.97 ± 0.13*** ##
p21	↑ 6.2 ± 0.08****	↑ *9.26 ± 0.85****
p27	↑ 2.2 ± 0.03	↑ *3.99 ± 0.23****
p53	↑1.47 ± 0.17	↑*2.7 ± 0.21**** ###
Tnf	↑ 2.06 ± 0.015	↑ *2.6 ± 0.15*

Legend to table: *A*rrows represent fold difference relative to the control set as 1. ↓: Down regulated; ↑: Up regulated; ↔: Not regulated. Results are expressed as the mean ± SEM. $^{**}p < 0.01$, $^{***}p < 0.001$ and $^{****}p < 0.0001$ vs control and $^{\#\#}p < 0.001$ and $^{\#\#\#}p < 0.0001$ vs Dox.

CHAPTER 5

DISCUSSION

Dox is a commonly prescribed first line anti-cancer drug that is used in the treatment of various cancers (Takemura and Fujiwara, 2007). Despite its sustained anti-tumor effects, Dox remains one of the most deleterious chemotherapeutic agents due to its cumulative and dose-dependent cardio-toxic side effect (Swamy *et al*., 2012, Von Hoff *et al*., 1979). Years after cessation of Dox treatment, cancer patients can develop cardiac dysfunction that may progress to heart failure (Kumar *et al*., 2012). This is a particular problem in pediatric cancer survivors that are young adults at the onset of the disease (Lipshultz and Adams, 2010).

Although the pathophysiological mechanism of Dox-induced cardiotoxicity remains to be fully elucidated, increased ROS production is implicated as the primary cause of cardiotoxicity (Chatterjee *et al*., 2010), Wallace, 2003, Octavia *et al*., 2012). During this process, superoxide anions are generated that interact with SOD, leading to increased production of H_2O_2 and subsequent activation of detoxifying agents such as CAT and GPx in the presence of GSH (Bhattacharyya *et al*., 2014). Conversely, Dox is known to react with Fe^{2+} to form a Dox-Fe^{2+} complex that reduces H_2O_2 to hydroxyl radical, a process that accelerates lipid peroxidation and contributes to the development of cardiotoxicity. Dexra, an iron chelator, is the only FDA approved drug used in combination with Dox to decrease such disturbances (Chatterjee *et al*., 2010). Though effective, Dexra is known to diminish the efficacy of Dox in a number of experimental settings (Hahn *et al*., 2014). Therefore, the need to develop a new treatment regimen that can prevent Dox-induced cardiotoxicity without decreasing the chemotherapeutic value of Dox.

In recent years, researchers have investigated the use of plant-derived polyphenols as nutraceuticals to lower the risk of chronic diseases (Lecour and Lamont, 2011, Pandey and Rizvi, 2009). Of particular interest is ASP, a dihydrochalcone *C*-glucoside, unique to *Aspalathus linearis* with known antioxidant properties (Snijman *et al*., 2009). High Performance Liquid Chromatography (HPLC) and Mass Spectrometry (MS) analysis done by Snijman and colleagues (2009) showed that of all rooibos flavonoids tested, ASP was the most effective free radical scavenger and inhibitor of lipid peroxidation (Snijman *et al*., 2009). This result was confirmed in a study done by Chen *et al*. (2013) showing that an ASP- enriched rooibos extract was able to attenuate high glucose-induced oxidative stress when tested using *Caenorhabditis elegans* (Chen *et al*., 2013). Similarly, in a study done by Johnson *et al*. (2016), it was shown that ASP

was able to decrease high glucose-induced oxidative stress in H9c2 cardiomyocytes by enhancing intracellular antioxidants such as GSH and SOD (Johnson *et al*., 2016). Findings from this study prompted investigation into whether ASP can ameliorate Dox-induced cardiotoxicity in H9c2 cardio myoblasts without reducing the anti-cancer efficacy of Dox.

The effect of ASP on H9c2 cardio myoblast metabolic activity. This study confirmed that ASP treatment of H9c2 cardio myoblasts was not toxic at any of the concentrations tested (0.01-1000 µM), and that concentrations of 0.1 as well 1 µM ASP enhanced the metabolic activity of H9c2 cells. However, a time-dependent decrease in metabolic activity was observed, a result that matched with ASP's half-life of 8 hrs (Viljoen *et al*., 2008). Thus if used as a nutraceutical in combination with a current treatment regime, it is suggested that ASP could be administered daily for the duration of Dox treatment.

***Cytotoxic effect of Dox*.** A previous cytotoxic study conducted by Goldswain *et al*. (2014) showed that a cumulative dose of 0.2 µM Dox over a period of 5 days induced cardiotoxicity. Our results support these findings, as observed by a 60% Dox-induced decrease in cardiac metabolic activity of H9c2 cells. To investigate if ASP can alleviate this effect, the compound was administered in combination with Dox for 5 days. Results from this study showed for the first time that ASP co-treatment was able to ablate Dox-induced cardiotoxicity. The observed effect was comparable to the untreated control and better than the current FDA approved drug, Dexra. It was evident from our data that pre-treatment with ASP was able to increase metabolic activity. However, ASP pre-treatment was not as effective as co-treatment but the effect was comparable to the Dexra treated group. We therefore propose that a low dose of ASP may have a cytoprotective effect which could attributed to ASP antioxidant properties. To test this hypothesis, the antioxidant activity was tested after H9c2 cells were exposed to Dox as well as a combination of Dox and ASP.

Oxidative stress and lipid peroxidation. It is well known that Dox, as a chemotherapeutic agent, is dependent on the production of ROS to destroy malignant cells by inducing apoptosis (Bhattacharyya *et al*., 2014). This increased generation of ROS is important in the disease pathophysiology of cancer cells. However, in the heart, the disparate generation of ROS leads to increased oxidative stress and

subsequent lipid peroxidation, which is detrimental to the heart. Some of the major antioxidants required to balance increased ROS production include SOD, CAT, GPx and GSH (Sharma *et al*., 2012). The present study showed that ASP was able to ablate abnormal redox cycling induced by Dox as observed with decreased MDA activity. Concomitantly, ASP as a known antioxidant increased the endogenous antioxidant activity of H9c2 cells. Interestingly, this study showed that ASP co-treatment was more effective to increase endogenous SOD and CAT activity compared to Dexra, whereas Dexra was more effective in increasing GSH activity. These results are of interest, as CAT detoxifies increased H_2O_2 to O_2 and water. However, it has been reported that in the presence of low levels of CAT, GPx together with GSH forms a glutathione complex that reduces increased H_2O_2 *(*Bhattacharyya *et al*., 2014). Thus we propose that ASP reduces H_2O_2 by increasing CAT activity whereas Dexra works via GSH. This study therefore confirms that ASP has potent antioxidant effects against aberrant Dox-induced redox cycling. This is an important finding as the heart has a low antioxidant capacity and co-treatment with ASP may be able to boost the endogenous antioxidants activity. Thus, reversing anomalous redox cycling induced by Dox can augment cardiotoxicity which may lead to the development of myocardial apoptosis (Narula *et al*., 1996)

Apoptosis. This study investigated the capability of ASP to inhibit Dox-induced apoptosis. Apoptosis, a form of programmed cell death, is activated by two distinct pathways; the intrinsic and extrinsic apoptotic pathway. The intrinsic pathway is mitochondrial mediated and involves the activation of caspases through the interaction of the Bcl-2 family of proteins; Bcl-2 (inhibits cell death) and Bax (promotes cell death) (Saelens *et al*., 2004). Bcl-2 and Bax forms a heterodimer whose expression ratio is important in the activation or inhibition of apoptosis. Dox is known to activate apoptosis through enhanced production of ROS (Li *et al*., 2000, Minotti *et al*., 2004) as well as decreasing the Bcl-2/Bax ratio, which results in mitochondria depolarization and a release of Cyt c (Crompton, 2000).

Apart from increased oxidative stress, the Bcl-2 family of proteins can be directly activated by the tumor suppressor protein, p53 (Yee and Vousden, 2005). This tumor suppressor protein induces apoptosis in response to DNA damage, activating Bax while repressing Bcl-2, which leads to mitochondrial depolarization and the induction of apoptosis. Likewise, Dox can activate the intrinsic pathway via a p53-dependent

(L'Ecuyer *et al*., 2006) and p53 independent pathway (Tsang *et al*., 2003). Dox is known to intercalate with DNA Topoisomerase II-β to induce DNA damage (Hurley, 2002) which results in the activation of p53 and induction apoptosis.

Our study supports the notion that Dox activated the intrinsic pathway and induced DNA damage in cardiac cells in a p53-dependent manner. The present study showed that Dox increased the expression of p53 which lead to the suppression of Bcl-2, increased caspase3/7 activity, DNA fragmentation and subsequent myocardial apoptosis. ASP was able to reduce Dox-mediated apoptosis by decreasing the p53-induced Bcl-2 inhibition, leading to decreased caspase 3/7 activity. Interestingly, ASP was as effective as Dexra to prevent apoptosis. However, Dexra had no effect on p53 suggesting that it may inhibit apoptosis in a p53-independent manner. Following on this we next investigated if ASP could activate autophagy.

Autophagy: Autophagy can be defined as a process the cell uses to clear itself of damaged proteins, organelles or aggregates (Hale *et al*., 2013). Though active in all cells, this process is only triggered in response to various types of cellular stresses (Fulda *et al*., 2010). Therefore, pursuing genes that are activated upon autophagy would be an effective therapeutic target to modulate Dox-induced cardiotoxicity. The paradoxes stemming from the therapeutic potential of autophagy to impede Dox-induced cardiotoxicity remains the subject of extensive controversy with autophagy having a dual function, pro-death or survival. This adaptive response depends on the type of stimuli and duration of damage (Fulda *et al*., 2010). In a study done by Sishi and colleagues (2013), a pro-survival response was induced when autophagy was activated with rapamycin in the presence of Dox. The authors showed how a stress stimuli induced by Dox was hindered after autophagy was triggered with rapamycin (Sishi *et al*., 2013). Conversely, various investigators have reported on the pro-death response of Dox, in which they showed that enhanced Dox-induced autophagy can lead to increased cardiotoxicity and subsequent apoptosis (Kobayashi *et al*. 2010, Lu *et al*., 2009). In recent years researchers revealed that a complex interaction exists between apoptosis and autophagy, where autophagy and apoptosis may be triggered by a common upstream signal resulting in either a synergistic or antagonistic effect (Jain *et al*., 2013). In our study we showed that a cumulative dose of Dox was able to

enhance the expression of apoptotic proteins, but inhibited the expression of the autophagy-related genes. However, our compound of interest was able to reverse this effect without decreasing apoptosis in an ovarian carcinoma cell line. This result infers that this antagonistic effect between apoptosis and autophagy may be a biological mechanism that accounts for the pro-survival effect of ASP.

To unravel the mechanism whereby ASP increases autophagy, various genes within the autophagy process were investigated. Autophagy entails five important steps, initiation, nucleation, elongation, maturation and degradation (Kang *et al* 2011). First we investigated the expression of two kinases, mTOR and its upstream regulator, AMPK. Whereas, mTOR is known to inhibit autophagy, AMPK is known to activate the process (Figure 2.5) (Gwinn *et al*., 2008). Though decreased expression of mTOR is required to activate autophagy, AMPK can activate autophagy in an mTOR-independent manner by directly activating *Atg1* (*ULK1*) (Lee *et al*., 2010, Kim *et al*., 2011). This study showed that Dox treatment inhibits autophagy as could be observed with increased mTOR and decreased AMPK expression. However, ASP treatment increased the expression of AMPK without modulating mTOR, suggesting that AMPK might initiate autophagy in an mTOR-independent manner by directly activating *Atg1*. However, *Atg1* was not investigated in this study, and thus requires further investigation.

Beclin1, also known as *Atg6*, is a major regulator of autophagy. Activation of *Beclin1* results in the localization of autophagic proteins to form a pre-autophagosomal structure that will coordinate and regulate the nucleation process. However, this process is inhibited through the co-localization of *Bcl-2* with *Beclin1* in the ER (Kang *et al*., 2011). But, in mitochondria the nucleation process is activated when Bnip3 displace *Bcl-2* from *Beclin 1*. This was confirmed by various studies which showed that increased expression of *BNIP3* triggers upregulation of autophagy in cardiomyocytes inhibiting the *Beclin-Bcl-2* interaction (Quinsay *et al*., 2010). Our study confirmed this effect as could be observed with a decrease in mRNA expression of *BNIP3* and *Beclin1* after Dox treatment. However, ASP was able to increase the expression of the latter autophagy initiation genes. This result confirms previous findings by Dludla *et al.* (2016) where it was shown that ASP is able to activate *BNIP3* and *Beclin1*.

The final step in the activation of autophagy is maturation, elongation and degradation. It has been well demonstrated that the final execution of autophagy depends on the association between *Atg5/Atg7* and the LC3-II protein (He and Klionsky, 2009). Once activated, *Atg5/Atg7* associated with the LC3-II protein to promote the maturation of the autolysosome and subsequent activation of autophagy. Interestingly, the transcriptional factor Fox01 is a known inducer of autophagy, through the activation of various Atg genes, including *Atg5* and *Atg7*. It has been reported that *Fox01* requires phosphorylation by Akt to inhibit autophagy (Zhang *et al.,* 2015). However, *Fox01* can activate autophagy in an Akt independent manner, by direct activating *Atg7*.

Our study was able to support such a finding, in which we observed that ASP potentiate *Fox01*-induced autophagy by increasing the association of *Atg5/Atg7* with LC3-II, a process indicative of decreased apoptosis. We also showed that while Dox induces cardiotoxicity and subsequent apoptosis, ASP co-treatment was able to inhibit p53, leading to a decrease in apoptosis and an increase in autophagy. The increase in autophagy was associated with the activation of AMPK, an ideal strategy to prevent Dox-induced cardiotoxicity.

The effect of ASP on Dox efficacy

Lastly, in the present study we also evaluated the effect of ASP on the anti-tumor activity of Dox. A Caov-3 ovarian carcinoma cell line was used to investigate if ASP co-treatment will decrease the anti-cancer efficacy of Dox. Our results showed that the combination of ASP and Dox decreased ATP content to a similar extent when compared to Dox treatment alone. These results strongly suggest that ASP does not reduce the anti-cancer effect of Dox. We further explored the effect of ASP co-treatment on the protein expression of pro-apoptotic proteins and observed that ASP co-treatment was more effective in increasing the expression of the pro-apoptotic proteins compared to Dox treatment alone. This result proposes that ASP alleviates Dox-induced cardiotoxicity without decreasing the enhanced cancer efficacy of Dox.

CHAPTER 6

CONCLUSION

There is a global pursuit to increase the cancer survival rate, and thus more effective chemotherapeutic agents with minimal side-effects are continuously being investigated. However, apart from all these efforts Dox remains the most effective but cardio toxic first line chemotherapeutic agent. In an effort to reduce Dox-mediated cardiotoxicity, the iron chelator Dexra was introduced. However, Dexra as a cardioprotective agent is able to reduce the development of myocardial damage, but attenuate the efficacy of Dox. Thus, the search for an alternative and improved chemotherapeutic agent with minimal side effects continues (Swain *et al.*, 1997, Trachtenberg *et al*., 2011). In this study, we aimed to investigate the potential use of ASP to alleviate Dox-induced cardiotoxicity in an *in vitro* H9c2 cell culture model.

To the best of our knowledge, this study was the first to investigate if ASP, a dihydrochalcone *C*-glucoside, was able to reduce Dox-mediated cardiotoxicity. Previous studies from our group confirmed that ASP was able to protect the myocardium from high glucose-induced oxidative stress and subsequent myocardial apoptosis (Johnson *et al*., 2016). Similarly, this study confirmed such a protection, however, instead of using high glucose as a stress, Dox was used. Noteworthy, our data demonstrated that ASP was able to attenuate Dox-induced cardiotoxicity in H9c2 cardio myoblasts without decreasing the efficacy of Dox. This was reiterated using both H9c2 cardio myoblasts and a rapidly dividing ovarian cancer cell line, Caov-3. Data from this study furthermore confirmed that co-treatment with ASP was more effective compared to the current FDA approved drug, Dexra. Subsequently, we investigated the proposed mechanism by which ASP protects the myocardium against Dox-induced oxidative stress, cell apoptosis and dysregulation of autophagy (Figure 6.1).

ASP protects against Dox-induced oxidative damage: The present study concluded that ASP was able to directly scavenge superoxide radicals through activation of SOD and CAT. This decrease in oxidative stress ablated the effect of ROS to induce lipid peroxidation, an important finding for the heart at risk of developing Dox-induced cytotoxicity (Figure 6.1).

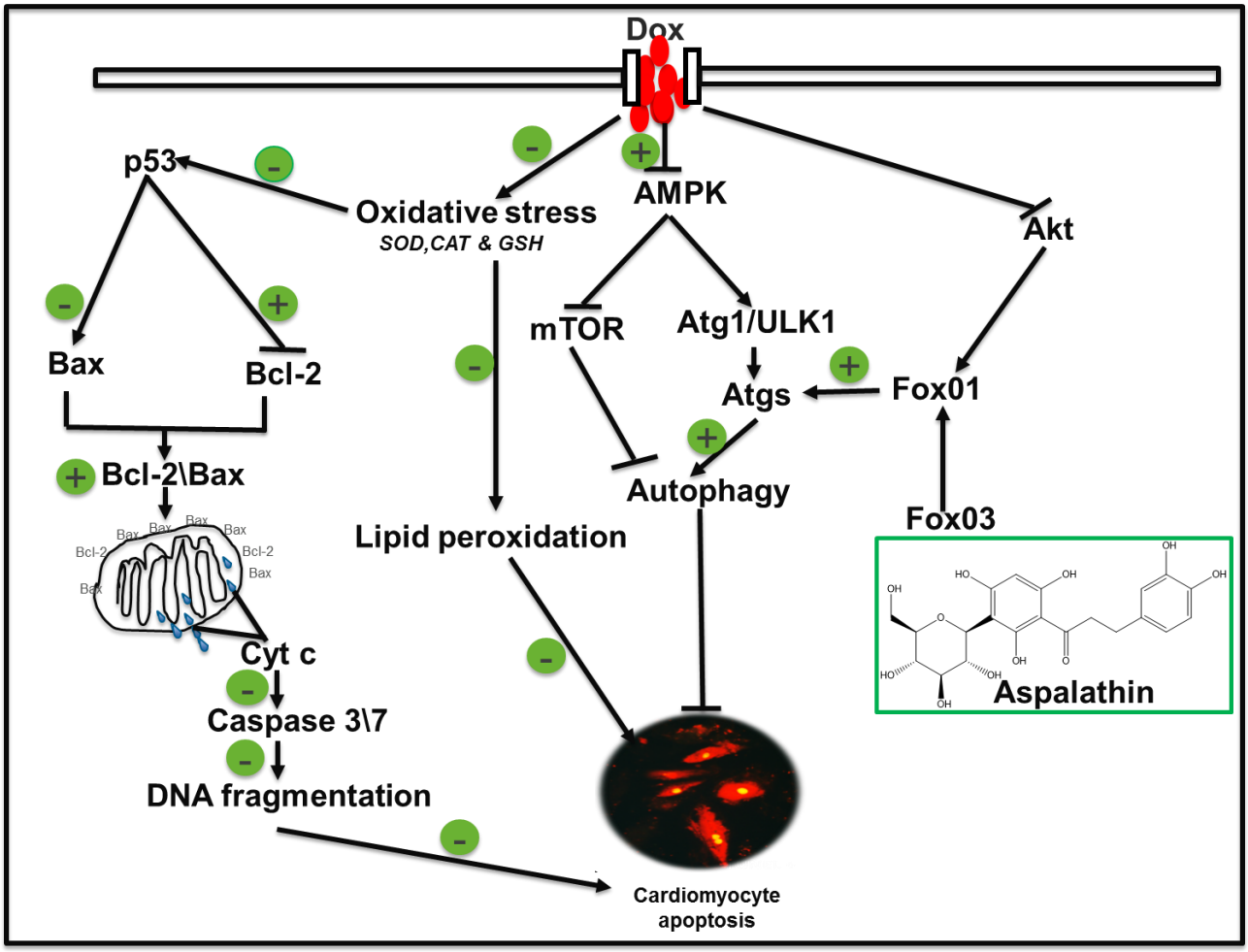

Figure 6.1: Aspalathin protect against Dox-induced cardiotoxicity Doxorubicin-induced oxidative stress, DNA damage, lipid peroxidation and myocardial apoptosis. Aspalathin decreased lipid peroxidation and myocardial apoptosis by increasing endogenous superoxide dismutase and catalase activity, protecting the cell from excessive ROS production. Increased ROS production can lead to membrane depolarization and release of cytochrome C, leading to cardiomyocytes apoptosis. This increase in apoptosis is largely mediated through Bcl-2 family of proteins. Aspalathin co-treatment was able to prevent a decrease in Bcl-2/Bax ratio and subsequently decreasing cell apoptosis. Furthermore, Doxorubicin decreased autophagy in a mTOR-dependent manner, and aspalathin co-treatment was able to attenuate this effect in a AMPK/Fox01-dependent, but mTOR-independent manner. **AMPK**, Adenosine monophosphate-activated protein kinase **Atgs**: Autophagy-related genes, **Bax**: Bcl-2-like protein 4, **Bcl-2:** B-cell lymphoma-2, **CAT**: Catalase, **Cyt c**: Cytochrome c, **GSH**: Glutathione, **LC3-II**: Light chain -3, **mTOR**: Mammalian target of rapamycin, **SOD**: superoxide dismutase.

ASP protects against Dox-induced apoptosis: Increased ROS production can lead to membrane depolarization, release of Cyt c and subsequent cardiomyocytes apoptosis. This study presented compelling evidence, showing that ASP mediates its cytoprotective effect in a p53-dependent pathway by significantly increasing the Bcl-2\Bax ratio which resulted in decreased apoptosis (Figure 6.1).

ASP restores autophagy reduced by Dox treatment: The present study further confirmed that Dox impaired autophagy in an mTOR-dependent manner. This effect was diminished by ASP-induced activation of known autophagy regulators, *Atgs* and LC3-II, via two mechanisms; i) AMPK-induced activation of *Atg1* and ii) direct activation of *Fox01*(Figure 6.1). This infers that ASP-mediated autophagy might play a significant role in autophagy-induced cardio protection.

In conclusion, this study provides plausible evidence that ASP was able to attenuate Dox-induced oxidative stress, DNA damage, lipid peroxidation and subsequent myocardial apoptosis in H9c2 cardiomyocytes. Furthermore, we showed that ASP was able to potentiate this effect without decreasing the anti-cancer efficacy of Dox, as could be observed in Caov-3 ovarian cancer cells. Taken together, the data presented in this study provides a credible mechanism by which ASP co-treatment could protect the myocardium from Dox-induced cardiotoxicity.

Shortcomings of this study:

- Due to time and budget constraints, we were unable to evaluate *Ferritin* and *Atg1* gene expression as well as ROS. However, free radical generation result in increased lipid peroxidation which was measured in this study.
- JC-1, as a marker for membrane depolarization could not be performed as Dox autofluoresces in the red channel.

Future studies will include

- Evaluation of *Atg1* expression to confirm the mechanism of ASP on autophagy
- Investigating the protective effect of ASP on Dox-induced cardiotoxicity in an *in vivo* model.

CHAPTER 7

REFERENCES

ALEMAN, B. M. P., MOSER, E. C., NUVER, J., SUTER, T. M., MARALDO, M. V., SPECHT, L., VRIELING, C. & DARBY, S. C. 2014. Cardiovascular disease after cancer therapy. *EJC Supplements*, 12, 18-28.

ARTS, I. C. & HOLLMAN, P. C. 2005. Polyphenols and disease risk in epidemiologic studies. *Am J Clin Nutr*, 81, 317s-325s.

ARYAL, B., JEONG, J. & RAO, V. A. 2014. Doxorubicin-induced carbonylation and degradation of cardiac myosin binding protein C promote cardiotoxicity. *Proceedings of the National Academy of Sciences of the United States of America,* 111, 2011-2016.

BARRERA, G. 2012. Oxidative Stress and Lipid Peroxidation Products in Cancer Progression and Therapy. *ISRN Oncology*, 2012, 137289.

BERTHIAUME, J. M., OLIVEIRA, P. J., FARISS, M. W. & WALLACE, K. B. 2005. Dietary vitamin E decreases doxorubicin-induced oxidative stress without preventing mitochondrial dysfunction. *Cardiovasc Toxicol*, 5, 257-67.

BHATTACHARYYA, A., CHATTOPADHYAY, R., MITRA, S. & CROWE, S. E. 2014. Oxidative Stress: An Essential Factor in the Pathogenesis of Gastrointestinal Mucosal Diseases. *Physiological Reviews*, 94, 329-354.

BILLINGHAM, M. E., MASON, J. W., BRISTOW, M. R. & DANIELS, J. R. 1978. Anthracycline cardiomyopathy monitored by morphologic changes. *Cancer Treat Rep,* 62**,** 865-72.

BLOOM, D.E., CAFIERO, E.T., JANÉ-LLOPIS, E., ABRAHAMS-GESSEL, S., BLOOM, L.R., FATHIMA, S., FEIGL, A.B., GAZIANO, T., MOWAFI, M., PANDYA, A., PRETTNER, K., ROSENBERG, L., SELIGMAN, B., STEIN, A.Z., & WEINSTEIN, C. (2011). The Global Economic Burden of Non-communicable Diseases. Geneva: World Economic Forum.

BRAVO, L. 1998. Polyphenols: chemistry, dietary sources, metabolism, and nutritional significance. *Nutr Rev*, 56, 317-33.

CANCER RESEARCH UK 2013. Cancer survival in England: Adults diagnosed in 2009 to 2013, *Cancer Research UK. https://www.cancerresearchuk.org/*

CARLSON, L. J., COTE, B., ALANI, A. W. G. & RAO, D. A. Polymeric Micellar Co-delivery of Resveratrol and Curcumin to Mitigate Doxorubicin-Induced Cardiotoxicity. *Journal of Pharmaceutical Sciences*, 103, 2315-2322.

CHATTERJEE, K., ZHANG, J., HONBO, N. & KARLINER, J. S. 2010. Doxorubicin Cardiomyopathy. *Cardiology*, 115, 155-162.

CHEN, W., SUDJI, I. R., WANG, E., JOUBERT, E., VAN WYK, B. E. & WINK, M. 2013. Ameliorative effect of aspalathin from rooibos (Aspalathus linearis) on acute oxidative stress in Caenorhabditis elegans*. Phytomedicine*, 20, 380-6.

CHLOPCIKOVA, S., PSOTOVA, J., MIKETOVA, P., SOUSEK, J., LICHNOVSKY, V. & SIMANEK, V. 2004. Chemoprotective effect of plant phenolics against anthracycline-induced toxicity on rat cardiomyocytes. Part II. caffeic, chlorogenic and rosmarinic acids*. Phytother Res*, 18, 408-13.

CHUNG, S., YAO, H., CAITO, S., HWANG, J.-W., ARUNACHALAM, G. & RAHMAN, I. 2010. Regulation of SIRT1 in cellular functions: role of polyphenols. *Archives of biochemistry and biophysics*, 501, 79-90.

CROMPTON, M. 2000. Bax, Bid and the permeabilization of the mitochondrial outer membrane in apoptosis. *Curr Opin Cell Biol*, 12, 414-9.

CUMMINGS, J., ANDERSON, L., WILLMOTT, N. & SMYTH, J. F. 1991. The molecular pharmacology of doxorubicin in vivo. *Eur J Cancer*, 27, 532-5.

DAHLGREN R. 1968. Revision of the genus Aspalathus II: the species with ericoid and pinoid leaves. 7 subgenus Nortieria. With remarks on rooibos cultivation. *Bot. Notiser*.;121:165–208.

DENG, S., YAN, T., JENDRNY, C., NEMECEK, A., VINCETIC, M., GÖDTEL-ARMBRUST, U. & WOJNOWSKI, L. 2014. Dexrazoxane may prevent doxorubicin-induced DNA damage via depleting both Topoisomerase II isoforms. *BMC Cancer*, 14, 842.

DI MARCO, A., CASSINELLI, G. & ARCAMONE, F. 1981. The discovery of daunorubicin*. Cancer Treat Rep*, 65 Suppl 4, 3-8.

DIMITRAKIS, P., ROMAY-OGANDO, M. I., TIMOLATI, F., SUTER, T. M. & ZUPPINGER, C. 2012. Effects of doxorubicin cancer therapy on autophagy and the ubiquitin-proteasome system in long-term cultured adult rat cardiomyocytes. *Cell Tissue Res*, 350, 361-72.

DIOTTE, N. M., XIONG, Y., GAO, J., CHUA, B. H. L. & HO, Y.-S. 2009. Attenuation of doxorubicin-induced cardiac injury by mitochondrial glutaredoxin 2. Biochimica et Biophysica Acta (BBA) - *Molecular Cell Research*, 1793, 427-438.

DIRKS-NAYLOR, A.J. 2013. The role of autophagy in doxorubicin-induced cardiotoxicity. Life sciences. 93(13): 913–916

STALMACH, A., MULLEN, W., PECORARI, M., SERAFINI, M. & CROZIER, A. 2009. Bioavailability of C -Linked Dihydrochalcone and Flavanone Glucosides in Humans Following Ingestion of Unfermented and Fermented Rooibos Teas. J.Agric.Food Chem., 57 :7104-7111

DLUDLA, P. V., MULLER, C. J., LOUW, J., JOUBERT, E., SALIE, R., OPOKU, A. R. & JOHNSON, R. 2014. The cardioprotective effect of an aqueous extract of fermented rooibos (Aspalathus linearis) on cultured cardiomyocytes derived from diabetic rats. Phytomedicine, 21, 595-601.

DLUDLA, PV.2016, PhD Thesis, Compounds specific to Aspalathus linearis protects the diabetic heart against oxidative stress: a mechanistic study. Stellenbosch University

DOROSHOW, J. H. 1983. Effect of anthracycline antibiotics on oxygen radical formation in rat heart. Cancer Res, 43, 460-72.

DUTTA, D., XU, J., DIRAIN, M. L. & LEEUWENBURGH, C. 2014. Calorie restriction combined with resveratrol induces autophagy and protects 26-month-old rat hearts from doxorubicin-induced toxicity. Free Radic Biol Med, 74, 252-62.

EL-MISSIRY, M. A., OTHMAN, A. I., AMER, M. A. & ABD EL-AZIZ, M. A. 2001. Attenuation of the acute adriamycin-induced cardiac and hepatic oxidative toxicity by N-(2-mercaptopropionyl) glycine in rats. Free Radic Res, 35, 575-81.

ELMORE, S. 2007. Apoptosis: A Review of Programmed Cell Death. Toxicologic pathology, 35, 495-516.

ESKELINEN, E.-L. & SAFTIG, P. 2009. Autophagy: A lysosomal degradation pathway with a central role in health and disease. Biochimica et Biophysica Acta (BBA) - Molecular Cell Research, 1793, 664-673.

EWER, M. S. & EWER, S. M. 2015. Cardiotoxicity of anticancer treatments. Nat Rev Cardiol, 12, 547-558.

FAN, J., ZHANG, Z., CHAO, X., GU, J., CAI, W., ZHOU, W., YIN, G. & LI, Q. 2014. Ischemic preconditioning enhances autophagy but suppresses autophagic cell death in rat spinal neurons following ischemia-reperfusion. Brain Res, 1562, 76-86.

FERRARESI, R., TROIANO, L., ROAT, E., LUGLI, E., NEMES, E., NASI, M., PINTI, M., FERNANDEZ, M. I., COOPER, E. L. & COSSARIZZA, A. 2005. Essential requirement of reduced glutathione (GSH) for the anti-oxidant effect of the flavonoid quercetin. Free Radic Res, 39, 1249-58.

FUKAI, T. & USHIO-FUKAI, M. 2011. Superoxide Dismutases: Role in Redox Signaling, Vascular Function, and Diseases. Antioxidants & Redox Signaling, 15, 1583-1606.

FULDA, S., GORMAN, A. M., HORI, O. & SAMALI, A. 2010. Cellular Stress Responses: Cell Survival and Cell Death. International Journal of Cell Biology, 2010, 23.

GAMEN, S., ANEL, A., PEREZ-GALAN, P., LASIERRA, P., JOHNSON, D., PINEIRO, A. & NAVAL, J. 2000. Doxorubicin treatment activates a Z-VAD-sensitive caspase, which causes deltapsim loss, caspase-9 activity, and apoptosis in Jurkat cells. Exp Cell Res, 258, 223-35.

GEWIRTZ, D. A. 1999. A critical evaluation of the mechanisms of action proposed for the antitumor effects of the anthracycline antibiotics Adriamycin and daunorubicin. Biochem Pharmacol, 57, 727-41.

GOLDSWAIN, TL. 2014, MSc thesis, The (un)SAFE and RISK(y) sides of Doxorubicin-induced cardiotoxicity, Stellenbosch University

GREEN, P. S. & LEEUWENBURGH, C. 2002. Mitochondrial dysfunction is an early indicator of doxorubicin-induced apoptosis. Biochim Biophys Acta, 1588, 94-101.

GROARKE, J. D. & NOHRIA, A. 2015. Anthracycline Cardiotoxicity. A New Paradigm for an Old Classic, 131, 1946-1949.

GU, J., HU, W. & ZHANG, D.-D. 2015. Resveratrol, a polyphenol phytoalexin, protects against doxorubicin-induced cardiotoxicity. Journal of Cellular and Molecular Medicine, 19, 2324-2328.

GWINN, D. M., SHACKELFORD, D. B., EGAN, D. F., MIHAYLOVA, M. M., MERY, A., VASQUEZ, D. S., TURK, B. E. & SHAW, R. J. 2008. AMPK phosphorylation of raptor mediates a metabolic checkpoint. Mol Cell, 30, 214-26.

HABAUZIT, V. & MORAND, C. 2012. Evidence for a protective effect of polyphenols-containing foods on cardiovascular health: an update for clinicians. Therapeutic Advances in Chronic Disease, 3, 87-106.

HALE, A. N., LEDBETTER, D. J., GAWRILUK, T. R. & RUCKER, I. I. I. E. B. 2013. Autophagy: Regulation and role in development. Autophagy, 9, 951-972.

HAHN, V. S., LENIHAN, D. J. & KY, B. 2014. Cancer therapy-induced cardiotoxicity: basic mechanisms and potential cardioprotective therapies. *J Am Heart Assoc,* 3**,** e000665.

HE, C. & KLIONSKY, D. J. 2009. Regulation mechanisms and signaling pathways of autophagy. Annu Rev Genet, 43, 67-93.

HERBAL TEAS ONLINE. 2015. Benefits of herbal teas: how are they good for you? *Published on March 20th 2015. http://www.herbalteasonline.com/*

HRELIA, S., BORDONI, A., ANGELONI, C., LEONCINI, E., TOSCHI, T. G., LERCKER, G. & BIAGI, P. L. 2002. Green tea extracts can counteract the modification of fatty acid composition induced by doxorubicin in cultured cardiomyocytes. Prostaglandins, Leukotrienes and Essential Fatty Acids, 66, 519-524.

HUANG, S. 2013. Inhibition of PI3K/Akt/mTOR signaling by natural products. Anticancer Agents Med Chem, 13, 967-70.

HUDSON, S. V., MILLER, S. M., HEMLER, J., FERRANTE, J. M., LYLE, J., OEFFINGER, K. C. & DIPAOLA, R. S. 2012. Adult cancer survivors discuss follow-up in primary care: 'not what i want, but maybe what i need'. Ann Fam Med, 10, 418-27.

HURLEY, L. H. 2002. DNA and its associated processes as targets for cancer therapy. Nat Rev Cancer, 2, 188-200.

HYDOCK, D. S., WONDERS, K. Y., SCHNEIDER, C. M. & HAYWARD, R. 2009. Voluntary wheel running in rats receiving doxorubicin: effects on running activity and cardiac myosin heavy chain. Anticancer Res, 29, 4401-7.

ICHIKAWA, Y., GHANEFAR, M., BAYEVA, M., WU, R., KHECHADURI, A., PRASAD, S. V. N., MUTHARASAN, R. K., NAIK, T. J. & ARDEHALI, H. 2014. Cardiotoxicity of doxorubicin is mediated through mitochondrial iron accumulation. The Journal of Clinical Investigation, 124, 617-630.

IMBABY, S., EWAIS, M., ESSAWY, S. & FARAG, N. 2014. Cardioprotective effects of curcumin and nebivolol against doxorubicin-induced cardiac toxicity in rats. Hum Exp Toxicol, 33, 800-13.

INGUSCIO, V., PANZARINI, E. & DINI, L. 2012. Autophagy Contributes to the Death/Survival Balance in Cancer PhotoDynamic Therapy. Cells, 1, 464-491.

INOKI, K., ZHU, T. & GUAN, K. L. 2003. TSC2 mediates cellular energy response to control cell growth and survival. Cell, 115, 577-90.

JAIN, M. V., PACZULLA, A. M., KLONISCH, T., DIMGBA, F. N., RAO, S. B., ROBERG, K., SCHWEIZER, F., LENGERKE, C., DAVOODPOUR, P., PALICHARLA, V. R., MADDIKA, S. & ŁOS, M. 2013. Interconnections between apoptotic, autophagic and necrotic pathways: implications for cancer therapy development. Journal of Cellular and Molecular Medicine, 17, 12-29.

JOHNSON, R., DLUDLA, P., JOUBERT, E., FEBRUARY, F., MAZIBUKO, S., GHOOR, S., MULLER, C. & LOUW, J. 2016. Aspalathin, a dihydrochalcone C-glucoside, protects H9c2 cardiomyocytes against high glucose induced shifts in substrate preference and apoptosis. Mol Nutr Food Res, 60, 922-34.

JOUBERT, E., & DE BEER, D. 2011. Rooibos (Aspalathus linearis) beyond the farm gate: From herbal tea to potential phytopharmaceutical. South African Journal of Botany, 77, (4) 869-886.

JOUBERT, E., GELDERBLOM, W. C., LOUW, A. & DE BEER, D. 2008. South African herbal teas: Aspalathus linearis, Cyclopia spp. and Athrixia phylicoides--a review. *J Ethnopharmacol*, 119, 376-412.

KABEYA, Y., MIZUSHIMA, N., UENO, T., YAMAMOTO, A., KIRISAKO, T., NODA, T., KOMINAMI, E., OHSUMI, Y. & YOSHIMORI, T. 2000. LC3, a mammalian homologue of yeast Apg8p, is localized in autophagosome membranes after processing. The *EMBO Journal*, 19, 5720-5728.

KALIMUTHU, S. & SE-KWON, K. 2013. Cell Survival and Apoptosis Signaling as Therapeutic Target for Cancer: Marine Bioactive Compounds. *International Journal of Molecular Sciences,* 14**,** 2334-2354.

KATAMURA M, IWAI-KANAI E, NAKAOKA M, OKAWA Y, ARIYOSHI M. (2014) Curcumin Attenuates Doxorubicin-Induced Cardiotoxicity by inducing Autophagy via the Regulation of JNK Phosphorylation. *J Clin Exp Cardiolog* 5: 337. doi:10.4172/2155-9880.1000337

KAWAGUCHI, T., TAKEMURA, G., KANAMORI, H., TAKEYAMA, T., WATANABE, T., MORISHITA, K., OGINO, A., TSUJIMOTO, A., GOTO, K., MARUYAMA, R., KAWASAKI, M., MIKAMI, A., FUJIWARA, T., FUJIWARA, H. & MINATOGUCHI, S. 2012. Prior starvation mitigates acute doxorubicin cardiotoxicity through restoration of autophagy in affected cardiomyocytes. Cardiovasc Res, 96, 456-65.

KANG, R., ZEH, H. J., LOTZE, M. T. & TANG, D. 2011. The Beclin 1 network regulates autophagy and apoptosis. *Cell Death and Differentiation,* 18**,** 571-580.

KIHARA, A., KABEYA, Y., OHSUMI, Y. & YOSHIMORI, T. 2001. Beclin-phosphatidylinositol 3-kinase complex functions at the trans-Golgi network.

KIM, H. C. & OH, S. M. 2013. Noncommunicable diseases: current status of major modifiable risk factors in Korea. J Prev Med Public Health, 46, 165-72.

KIM, J., KUNDU, M., VIOLLET, B. & GUAN, K. L. 2011. AMPK and mTOR regulate autophagy through direct phosphorylation of Ulk1. Nat Cell Biol, 13, 132-41.

KOBAYASHI, S., VOLDEN, P., TIMM, D., MAO, K., XU, X. & LIANG, Q. 2010. Transcription factor GATA4 inhibits doxorubicin-induced autophagy and cardiomyocyte death. *J Biol Chem*, 285, 793-804.

KOTAMRAJU, S., KONOREV, E. A., JOSEPH, J. & KALYANARAMAN, B. 2000. Doxorubicin-induced apoptosis in endothelial cells and cardiomyocytes is ameliorated by nitrone spin traps and epsilon. Role of reactive oxygen and nitrogen species. *J Biol Chem*, 275, 33585-92.

KOZLUCA, O., OLCAY, E., SURUCU, S., GURAN, Z., KULAKSIZ, T. & USKENT, N. 1996. Prevention of doxorubicin induced cardiotoxicity by catechin. *Cancer Lett*, 99, 1-6.

KUMAR, S., MARFATIA, R., TANNENBAUM, S., YANG, C. & AVELAR, E. 2012. Doxorubicin-Induced Cardiomyopathy 17 Years after Chemotherapy. *Texas Heart Institute Journal*, 39, 424-427.

LAPLANTE, M. & SABATINI, D. M. 2009. mTOR signaling at a glance. *Journal of Cell Science*, 122, 3589.

LAURENT, G. & JAFFREZOU, J. P. 2001. Signaling pathways activated by daunorubicin. *Blood*, 98, 913-24.

LECOUR, S. & LAMONT, K. T. 2011. Natural polyphenols and cardioprotection. *Mini Rev Med Chem*, 11, 1191-9.

L'ECUYER, T., SANJEEV, S., THOMAS, R., NOVAK, R., DAS, L., CAMPBELL, W. & HEIDE, R. V. 2006. DNA damage is an early event in doxorubicin-induced cardiac myocyte death. *Am J Physiol Heart Circ Physiol*, 291, H1273-80.

LEE, J. W., PARK, S., TAKAHASHI, Y. & WANG, H. G. 2010. The association of AMPK with ULK1 regulates autophagy. *PLoS One*, 5, e15394.

LI, J., HUANG, C. Y., ZHENG, R. L., CUI, K. R. & LI, J. F. 2000. Hydrogen peroxide induces apoptosis in human hepatoma cells and alters cell redox status. *Cell Biol Int,* 24**,** 9-23.

LILIENBAUM, A. 2013. Relationship between the proteasomal system and autophagy. *International Journal of Biochemistry and Molecular Biology*, 4, 1-26.

LIPSHULTZ, S. E. & ADAMS, M. J. 2010. Cardiotoxicity after childhood cancer: beginning with the end in mind. *J Clin Oncol*, 28, 1276-81.

LIPSHULTZ, S. E., COCHRAN, T. R., FRANCO, V. I. & MILLER, T. L. 2013. Treatment-related cardiotoxicity in survivors of childhood cancer. *Nat Rev Clin Oncol*, 10, 697-710.

LIU, M. H., LIN, X. L., YUAN, C., HE, J., TAN, T. P., WU, S. J., YU, S., CHEN, L., LIU, J., TIAN, W., CHEN, Y. D., FU, H. Y., LI, J. & ZHANG, Y. 2016. Hydrogen sulfide attenuates doxorubicin-induced cardiotoxicity by inhibiting the expression of peroxiredoxin III in H9c2 cells. *Mol Med Rep*, 13, 367-72.

LIU, M. H., LIN, X. L., ZHANG, Y., HE, J., TAN, T. P., WU, S. J., LIU, J., TIAN, W., CHEN, L., YU, S., LI, J. & YUAN, C. 2015. Hydrogen sulfide attenuates doxorubicin-induced cardiotoxicity by inhibiting reactive oxygen species-activated extracellular signal-regulated kinase 1/2 in H9c2 cardiac myocytes. *Mol Med Rep*, 12, 6841-8.

LIU, X., CHUA, C. C., GAO, J., CHEN, Z., LANDY, C. L., HAMDY, R. & CHUA, B. H. 2004. Pifithrin-alpha protects against doxorubicin-induced apoptosis and acute cardiotoxicityin mice. *Am J Physiol Heart Circ Physiol*, 286, H933-9.

LU, L., WU, W., YAN, J., LI, X., YU, H. & YU, X. 2009. Adriamycin-induced autophagic cardiomyocyte death plays a pathogenic role in a rat model of heart failure. Int *J Cardiol*, 134, 82-90.

MATOUK, A. I., TAYE, A., HEEBA, G. H. & EL-MOSELHY, M. A. 2013. Quercetin augments the protective effect of losartan against chronic doxorubicin cardiotoxicity in rats. *Environmental Toxicology and Pharmacology*, 36, 443-450.

MAZIBUKO, S. E., JOUBERT, E., JOHNSON, R., LOUW, J., OPOKU, A. R. & MULLER, C. J. 2015. Aspalathin improves glucose and lipid metabolism in 3T3-L1 adipocytes exposed to palmitate. *Mol Nutr Food Res*, 59, 2199-208.

MEI, Y., THOMPSON, M. D., COHEN, R. A. & TONG, X. 2015. Autophagy and oxidative stress in cardiovascular diseases. *Biochimica et biophysica acta*, 1852, 243-251.

MILLER, K. D., SIEGEL, R. L., LIN, C. C., MARIOTTO, A. B., KRAMER, J. L., ROWLAND, J. H., STEIN, K. D., ALTERI, R. & JEMAL, A. 2016. Cancer treatment and survivorship statistics, 2016. CA: A Cancer Journal for Clinicians, 66, 271-289.

MINOTTI, G., MENNA, P., SALVATORELLI, E., CAIRO, G. & GIANNI, L. 2004. Anthracyclines: molecular advances and pharmacologic developments in antitumor activity and cardiotoxicity. *Pharmacol Rev*, 56, 185-229.

MIZUSHIMA, N. 2007. Autophagy: process and function. Genes Dev, 21, 2861-73.

MOHAMAD, R. H., EL-BASTAWESY, A. M., ZEKRY, Z. K., AL-MEHDAR, H. A., AL-SAID, M. G., ALY, S. S., SHARAWY, S. M. & EL-MERZABANI, M. M. 2009. The role of Curcuma longa against doxorubicin (adriamycin)-induced toxicity in rats. *J Med Food*, 12, 394-402.

MUKHERJEE, S., DUDLEY, J. I. & DAS, D. K. 2010. Dose-Dependency of Resveratrol in Providing Health Benefits. Dose-Response, 8, 478-500.

MULLER, C.J., JOUBERT, E., DE BEER, D., SANDERSON, M., MALHERBE, C.J., FEY, S.J., & LOUW, J. 2012. Acute assessment of an aspalathin-enriched green rooibos (*Aspalathus linearis*) extract with hypoglycemic potential. *Phytomedicine*, 20, (1) 32-39.

NAIR, R., RAMAKRISHNAN, G., NAIR, N. N., SAIKIA, T. K., PARIKH, P. M., JOSHI, S. R., SOMAN, C. S., MUKHADAN, M., DINSHAW, K. T. & ADVANI, S. H. 1998. A randomized comparison of the efficacy and toxicity of epirubicin and doxorubicin in the treatment of patients with non-Hodgkin's lymphoma. *Cancer*, 82, 2282-8.

NAKATOGAWA, H., SUZUKI, K., KAMADA, Y. & OHSUMI, Y. 2009. Dynamics and diversity in autophagy mechanisms: lessons from yeast. *Nat Rev Mol Cell Biol*, 10, 458-67.

NARULA, J., HAIDER, N., VIRMANI, R., DISALVO, T. G., KOLODGIE, F. D., HAJJAR, R. J., SCHMIDT, U., SEMIGRAN, M. J., DEC, G. W. & KHAW, B. A. 1996. Apoptosis in myocytes in end-stage heart failure. *N Engl J Med*, 335, 1182-9.

NITA, M. & GRZYBOWSKI, A. 2016. The Role of the Reactive Oxygen Species and Oxidative Stress in the Pathomechanism of the Age-Related Ocular Diseases and Other Pathologies of the Anterior and Posterior Eye Segments in Adults. *Oxidative Medicine and Cellular Longevity,* 2016**,** 3164734.

NISHIDA, K., KYOI, S., YAMAGUCHI, O., SADOSHIMA, J. & OTSU, K. 2008. The role of autophagy in the heart. *Cell Death Differ*, 16, 31-38.

OCTAVIA, Y., TOCCHETTI, C. G., GABRIELSON, K. L., JANSSENS, S., CRIJNS, H. J. & MOENS, A. L. 2012. Doxorubicin-induced cardiomyopathy: From molecular mechanisms to therapeutic strategies. *Journal of Molecular and Cellular Cardiology*, 52, 1213-1225.

OJHA, S., AL TAEE, H., GOYAL, S., MAHAJAN, U. B., PATIL, C. R., ARYA, D. S. & RAJESH, M. 2016. Cardioprotective Potentials of Plant-Derived Small Molecules against Doxorubicin Associated Cardiotoxicity. *Oxidative Medicine and Cellular Longevity*, 2016, 5724973.

OU, X., LEE, M. R., HUANG, X., MESSINA-GRAHAM, S. & BROXMEYER, H. E. 2014. SIRT1 positively regulates autophagy and mitochondria function in embryonic stem cells under oxidative stress. *Stem Cells*, 32, 1183-94.

PANDEY, K. B. & RIZVI, S. I. 2009. Plant polyphenols as dietary antioxidants in human health and disease. *Oxidative Medicine and Cellular Longevity*, 2, 270-278.

PARK, H. K., CHU, K., JUNG, K. H., LEE, S. T., BAHN, J. J., KIM, M., LEE, S. K. & ROH, J. K. 2009. Autophagy is involved in the ischemic preconditioning. *Neurosci Lett*, 451, 16-9.

PARRISH, A. B., FREEL, C. D. & KORNBLUTH, S. 2013. Cellular mechanisms controlling caspase activation and function. *Cold Spring Harb Perspect Biol*, 5.

PATIL, L. & BALARAMAN, R. 2011. Effect of Green Tea Extract on Doxorubicin Induced Cardiovascular Abnormalities: Antioxidant Action. *Iranian Journal of Pharmaceutical Research* : IJPR, 10, 89-96.

PATTINGRE, S., TASSA, A., QU, X., GARUTI, R., LIANG, X. H., MIZUSHIMA, N., PACKER, M., SCHNEIDER, M. D. & LEVINE, B. 2005. Bcl-2 Antiapoptotic Proteins Inhibit Beclin 1-Dependent Autophagy. *Cell*, 122, 927-939.

QUINSAY, M. N., THOMAS, R. L., LEE, Y. & GUSTAFSSON, Å. B. 2010. Bnip3-mediated mitochondrial autophagy is independent of the mitochondrial permeability transition pore. *Autophagy*, 6, 855-862.

RAHMAN, A. M., YUSUF, S. W. & EWER, M. S. 2007. Anthracycline-induced cardiotoxicity and the cardiac-sparing effect of liposomal formulation. *International Journal of Nanomedicine*, 2, 567-583.

RAVIZZA, R., GARIBOLDI, M. B., PASSARELLI, L. & MONTI, E. 2004. Role of the p53/p21 system in the response of human colon carcinoma cells to Doxorubicin. BMC *Cancer*, 4, 92.

RIDDICK, D. S., LEE, C., RAMJI, S., CHINJE, E. C., COWEN, R. L., WILLIAMS, K. J., PATTERSON, A. V., STRATFORD, I. J., MORROW, C. S., TOWNSEND, A. J., JOUNAIDI, Y., CHEN, C.-S., SU, T., LU, H., SCHWARTZ, P. S. & WAXMAN, D. J. 2005. CANCER CHEMOTHERAPY AND DRUG METABOLISM. *Drug Metabolism and Disposition*, 33, 1083-1096.

SAELENS, X., FESTJENS, N., VANDE WALLE, L., VAN GURP, M., VAN LOO, G. & VANDENABEELE, P. 2004. Toxic proteins released from mitochondria in cell death. *Oncogene*, 23, 2861-74.

SARVAZYAN, N. 1996. Visualization of doxorubicin-induced oxidative stress in isolated cardiac myocytes. *Am J Physiol*, 271, H2079-85.

SCALBERT, A., MANACH, C., MORAND, C., REMESY, C. & JIMENEZ, L. 2005. Dietary polyphenols and the prevention of diseases. *Crit Rev Food Sci Nutr*, 45, 287-306.

SENGUPTA, S., PETERSON, T. R. & SABATINI, D. M. 2010. Regulation of the mTOR complex 1 pathway by nutrients, growth factors, and stress. *Molecular cell*, 40, 310-322.

SHAKIR, D. K. & RASUL, K. I. 2009. Chemotherapy Induced Cardiomyopathy: Pathogenesis, Monitoring and Management. *Journal of Clinical Medicine Research*, 1, 8-12.

SHARMA, P., JHA, A. B., DUBEY, R. S. & PESSARAKLI, M. 2012. Reactive Oxygen Species, Oxidative Damage, and Antioxidative Defense Mechanism in Plants under Stressful Conditions. *Journal of Botany*, 2012, 26.

SHEVCHUK, O. O., POSOKHOVA, E. A., SAKHNO, L. A. & NIKOLAEV, V. G. 2012. Theoretical ground for adsorptive therapy of anthracyclines cardiotoxicity. *Exp Oncol,* 34**,** 314-22.

SIN, T. K., TAM, B. T., YUNG, B. Y., YIP, S. P., CHAN, L. W., WONG, C. S., YING, M., RUDD, J. A. & SIU, P. M. 2015. Resveratrol protects against doxorubicin-induced

cardiotoxicityin aged hearts through the SIRT1-USP7 axis. *The Journal of Physiology*, 593, 1887-1899.

SINGAL, P. K., DEALLY, C. M. & WEINBERG, L. E. 1987. Subcellular effects of Adriamycin in the heart: a concise review. *J Mol Cell Cardiol*, 19, 817-28.

SISHI, B. J., LOOS, B., VAN ROOYEN, J. & ENGELBRECHT, A. M. 2013. Autophagy upregulation promotes survival and attenuates doxorubicin-induced cardiotoxicity. *Biochem Pharmacol*, 85, 124-34.

SMITH, L. A., CORNELIUS, V. R., PLUMMER, C. J., LEVITT, G., VERRILL, M., CANNEY, P. & JONES, A. 2010. Cardiotoxicityof anthracycline agents for the treatment of cancer: Systematic review and meta-analysis of randomised controlled trials. *BMC Cancer*, 10, 337.

SNIJMAN, P. W., JOUBERT, E., FERREIRA, D., LI, X. C., DING, Y., GREEN, I. R. & GELDERBLOM, W. C. 2009. Antioxidant activity of the dihydrochalcones Aspalathin and Nothofagin and their corresponding flavones in relation to other Rooibos (Aspalathus linearis) Flavonoids, Epigallocatechin Gallate, and Trolox. *J Agric Food Chem*, 57, 6678-84.

SNIJMAN, P.W., SWANEVELDER, S., JOUBERT, E., GREEN, I.R. & GELDERBLOM, W.C.A. 2007. The Antimutagenic Activity of the Major Flavonoids of Rooibos (Aspalathus Linearis): Some Dose-Response Effects on Mutagen Activation-Flavonoid Interactions. *Mutation Research Genetic Toxicology and Environmental Mutagenesis,* 631(2):111-123.

SÖKMEN, M. & AKRAM KHAN, M. 2016. The antioxidant activity of some curcuminoids and chalcones. *Inflammopharmacology*, 24, 81-86.

SOUTH AFRICAN HEART ASSOCIATION. 2014. Non-communicable disease profiles for South Africa. http://www.stentforlife.com/participating-countries/south-africa/

SPALLAROSSA, P., GARIBALDI, S., ALTIERI, P., FABBI, P., MANCA, V., NASTI, S., ROSSETTIN, P., GHIGLIOTTI, G., BALLESTRERO, A., PATRONE, F., BARSOTTI, A. & BRUNELLI, C. 2004. Carvedilol prevents doxorubicin-induced free radical release and apoptosis in cardiomyocytes in vitro. *J Mol Cell Cardiol*, 37, 837-46.

SWAIN, S. M., WHALEY, F. S. & EWER, M. S. 2003. Congestive heart failure in patients treated with doxorubicin: a retrospective analysis of three trials. *Cancer*, 97, 2869-79.

SWAIN, S. M., WHALEY, F. S., GERBER, M. C., WEISBERG, S., YORK, M., SPICER, D., JONES, S. E., WADLER, S., DESAI, A., VOGEL, C., SPEYER, J., MITTELMAN, A., REDDY, S., PENDERGRASS, K., VELEZ-GARCIA, E., EWER, M. S., BIANCHINE, J. R. & GAMS, R. A. 1997. Cardioprotection with dexrazoxane for doxorubicin-containing therapy in advanced breast cancer. *J Clin Oncol*, 15, 1318-32.

SWAMY, A. V., GULLIAYA, S., THIPPESWAMY, A., KOTI, B. C. & MANJULA, D. V. 2012. Cardioprotective effect of curcumin against doxorubicin-induced myocardial toxicity in albino rats. *Indian J Pharmaco*l, 44, 73-7.

TAKEMURA, G. & FUJIWARA, H. 2007. Doxorubicin-induced cardiomyopathy from the cardiotoxic mechanisms to management. Prog Cardiovasc Dis, 49, 330-52.

TAN, C., TASAKA, H., YU, K. P., MURPHY, M. L. & KARNOFSKY, D. A. 1967. Daunomycin, an antitumor antibiotic, in the treatment of neoplastic disease. Clinical evaluation with special reference to childhood leukemia. *Cancer*, 20, 333-53.

TATLIDEDE, E., SEHIRLI, O., VELIOGLU-OGUNC, A., CETINEL, S., YEGEN, B. C., YARAT, A., SULEYMANOGLU, S. & SENER, G. 2009. Resveratrol treatment protects against doxorubicin-induced cardiotoxicity by alleviating oxidative damage. *Free Radic Res*, 43, 195-205.

TEBBI, C. K., LONDON, W. B., FRIEDMAN, D., VILLALUNA, D., DE ALARCON, P. A., CONSTINE, L. S., MENDENHALL, N. P., SPOSTO, R., CHAUVENET, A. & SCHWARTZ, C. L. 2007. Dexrazoxane-associated risk for acute myeloid leukemia/myelodysplastic syndrome and other secondary malignancies in pediatric Hodgkin's disease. *J Clin Oncol*, 25, 493-500.

THORN, C. F., OSHIRO, C., MARSH, S., HERNANDEZ-BOUSSARD, T., MCLEOD, H., KLEIN, T. E. & ALTMAN, R. B. 2011. Doxorubicin pathways: pharmacodynamics and adverse effects. *Pharmacogenetics and Genomics*, 21, 440-446.

TOCCHETTI, C. G., CARPI, A., COPPOLA, C., QUINTAVALLE, C., REA, D., CAMPESAN, M., ARCARI, A., PISCOPO, G., CIPRESSO, C., MONTI, M. G., DE

LORENZO, C., ARRA, C., CONDORELLI, G., DI LISA, F. & MAUREA, N. 2014. Ranolazine protects from doxorubicin-induced oxidative stress and cardiac dysfunction. *Eur J Heart Fail,* 16**,** 358-66.

TRACHTENBERG, B. H., LANDY, D. C., FRANCO, V. I., HENKEL, J. M., PEARSON, E. J., MILLER, T. L. & LIPSHULTZ, S. E. 2011. Anthracycline-associated cardiotoxicity in survivors of childhood cancer. *Pediatr Cardiol*, 32, 342-53.

TSANG, W. P., CHAU, S. P. Y., KONG, S. K., FUNG, K. P. & KWOK, T. T. 2003. Reactive oxygen species mediate doxorubicin induced p53-independent apoptosis. *Life Sciences*, 73, 2047-2058.

TSUJIMOTO, Y. 1998. Role of Bcl-2 family proteins in apoptosis: apoptosomes or mitochondria? *Genes Cells*, 3, 697-707.

VALKO, M., IZAKOVIC, M., MAZUR, M., RHODES, C. J. & TELSER, J. 2004. Role of oxygen radicals in DNA damage and cancer incidence. *Mol Cell Biochem*, 266, 37-56.

VAN DER MERWE, J.D., JOUBERT E., RICHARDS E.S., MANLEY M., SNIJMAN P.W., MARNEWICK J.L., GELDERBLOM W.C. 2006. A comparative study on the antimutagenic properties of aqueous extracts of Aspalathus linearis (rooibos), different Cyclopia spp. (honeybush) and Camellia sinensis teas. *Mutat Res* 611:42-53.

VILJOEN, M, 2008, MSc thesis. The stability of aspalathin, iso-orientin and orientin in rooibos iced tea. Stellenbosch University.

VOLKOVA, M. & RUSSELL, R. 2011. Anthracycline Cardiotoxicity: Prevalence, Pathogenesis and Treatment. *Current Cardiology Reviews*, 7, 214-220.

VON HOFF, D. D., LAYARD, M. W., BASA, P., DAVIS, H. L., JR., VON HOFF, A. L., ROZENCWEIG, M. & MUGGIA, F. M. 1979. Risk factors for doxorubicin-induced congestive heart failure. *Ann Intern Med*, 91, 710-7.

WALLACE, K. B. 2003. Doxorubicin-induced cardiac mitochondrionopathy. *Pharmacol Toxicol*, 93, 105-15.

WANG, X., WANG, X. L., CHEN, H. L., WU, D., CHEN, J. X., WANG, X. X., LI, R. L., HE, J. H., MO, L., CEN, X., WEI, Y. Q. & JIANG, W. 2014. Ghrelin inhibits doxorubicin cardiotoxicityby inhibiting excessive autophagy through AMPK and p38-MAPK. *Biochem Pharmacol*, 88, 334-50.

WORLD HEALTH ORGANIZATION REPORTS, 2008. Burden: mortality, morbidity and risk factors www.who.int/nmh/publications/ncd_report_chapter1

WORLD HEALTH ORGANIZATION, 2015. Reviewed 2016. Cardiovascular diseases (CVDs)

WORLD HEALTH ORGANIZATION, updated 2016. Non-communicable diseases:

WORLD HEART FEDERATION, 2014. 25x25: At the heart of global heart.

WORLD HEART FEDERATION, 2016. World Heart day. Dahttp://www.heartfoundation.co.za/sites/default/files/articles/World%20Heart%20Day_20thSeptPDF%20(1).

XIE, M., MORALES, C. R., LAVANDERO, S. & HILL, J. A. 2011. Tuning flux: autophagy as a target of heart disease therapy. *Current opinion in cardiology*, 26, 216-222.

XU, X., CHEN, K., KOBAYASHI, S., TIMM, D. & LIANG, Q. 2012. Resveratrol attenuates doxorubicin-induced cardiomyocyte death via inhibition of p70 S6 kinase 1-mediated autophagy. *J Pharmacol Exp Ther*, 341, 183-95.

YAMANAKA, S., TATSUMI, T., SHIRAISHI, J., MANO, A., KEIRA, N., MATOBA, S., ASAYAMA, J., FUSHIKI, S., FLISS, H. & NAKAGAWA, M. 2003. Amlodipine inhibits doxorubicin-induced apoptosis in neonatal rat cardiac myocytes. *Journal of the American College of Cardiology*, 41, 870-878.

YANG, X., YU, D.-D., YAN, F., JING, Y.-Y., HAN, Z.-P., SUN, K., LIANG, L., HOU, J. & WEI, L.-X. 2015. The role of autophagy induced by tumor microenvironment in different cells and stages of cancer. *Cell & Bioscience*, 5, 14.

YANG, Z. & KLIONSKY, D. J. 2009. An Overview of the Molecular Mechanism of Autophagy. *Current topics in microbiology and immunology*, 335, 1-32.

YEE, K. S. & VOUSDEN, K. H. 2005. Complicating the complexity of p53. *Carcinogenesis*, 26, 1317-22.

ZERN, T. L. & FERNANDEZ, M. L. 2005. Cardioprotective effects of dietary polyphenols. *J Nutr*, 135, 2291-4.

ZHANG, J., NG, S., WANG, J., ZHOU, J., TAN, S.-H., YANG, N., LIN, Q., XIA, D. & SHEN, H.-M. 2015. Histone deacetylase inhibitors induce autophagy through FOXO1-dependent pathways. *Autophagy*, 11, 629-642.

ZHANG, Y.-W., SHI, J., LI, Y.-J. & WEI, L. 2009. Cardiomyocyte death in doxorubicin-induced cardiotoxicity. *Archive immunological therapies experimentalism*, 57, 435-445.

APPENDIX A

LIST OF REAGENTS, CONSUMABLES AND EQUIPMENT

Table A1: Reagents and Chemicals

Chemical/Reagent	Catalogue number	Company
Aspalathin	SZI-356-54	High force research, Bowburn, Durham, UK
ATP ViaLight assay kit	LT27-008	Lonza, Walkersville, MD, USA
Cell counting chamber slides	C10228	Life Technologies Corporation, Carlsbad, CA, USA
Cell lysis Buffer	FNN0011	Life Technologies Corporation, Carlsbad, CA, USA
Chloroform	136112-00-0	Sigma-Aldrich , St Louis, MO, USA
Coomassie blue stain	161-0437	Bio-Rad, Hercules, CA, USA
Cryotubes	430659	Corning, MA, USA
DeadEnd colometric TUNEL system	PRG3250	Promega,Madison, Wilsconsin, USA
Dexamethasone	D4902	Sigma-Aldrich , St Louis, MO, USA
Dexrazoxane	D1446	Sigma-Aldrich , St Louis, MO, USA
Dimethyl sulfoxide (DMSO)	276855	Sigma-Aldrich , St Louis, MO, USA
Doxorubicin	D1515	Sigma-Aldrich , St Louis, MO, USA
Dulbecco`s modified Eagle`s medium (DMEM) with phenol red	B12-604F	Lonza, Walkersville, MD, USA
Dulbecco`s modified Eagle`s medium (DMEM) without phenol red	B12-917F	Lonza, Walkersville, MD, USA
Dulbecco`sphosphate buffered saline (DPBS)	B17-513F	Lonza, Walkersville, MD, USA
Ethanol	2875	Sigma-Aldrich , St Louis, MO, USA
Fetal bovine serum	BC/S0615-HI	Lonza, Walkersville, MD, USA
Glycine	G7126	Sigma-Aldrich , St Louis, MO, USA
Hybond-P PVDF Membrane	RNP1416F	Amersham
Iso-propornol	I9516	Sigma-Aldrich , St Louis, MO, USA
Methanol	1070182511	Merck, Whitehouse Station, NJ, USA
Non-fat milk powder	N/A	Clover, Johannesburg, SA

Paraformaldehyde	158127	Sigma-Aldrich , St Louis, MO, USA
Penicilin-streptomycin mixture	DE17-602E	Lonza, Walkersville, MD, USA
Phenylmethanesulfonyl fluoride (PMSF)	11206893001	Roche, Basel, Switzerland
Ponceau S Stain	P23295	Sigma-Aldrich, St Louis, MO, USA
Propidium iodide	P4170	Sigma-Aldrich , St Louis, MO, USA
Protease Inhibitors	11206893001	Roche, Basel, Switzerland
Qiazol	79306	Qiagen, Hilden, Germany
RNase free water	Am9937	Ambion, Austin, TX, USA
Running buffer SDS	161-0772	Bio-Rad, Hercules, CA, USA
SDS-PAGE gels	161-0993	Bio-Rad, Hercules, CA, USA
Sodium bicarbonate (NaHCO3)	M2645	Sigma-Aldrich , St Louis, MO, USA
Sodium hydroxide (NaOH)	109140	Merck, Whitehouse Station, NJ, USA
Stainless steel beads 5mm	69989	Qiagen, Hilden, Germany
Sterile TC water	59900C	Lonza, Walkersville, MD, USA
SYBR Green mix	4385612	Applied Biosystems, Foster City, CA, USA
Tris-base	93352	Sigma-Aldrich , St Louis, MO, USA
Trypan blue	15050-065	Invitrogen, Carlsbad, CA, USA
Trypsin	17-161F	Lonza, Walkersville, MD, USA
Tween 20	58980C	Sigma-Aldrich , St Louis, MO, USA
Restore plus Western blot stripping buffer	46430	Thermo Fisher Scientific, Waltham, MA, USA

Table A2: Consumables

Consumables	**Catalogue number**	**Company**
0. 2 PCR tubes, flat cap	AX/PCR-02-C/S	Axgyen, Corning, NY
0.5 mL Eppendorf safe-lock tubes	0030 123.301	Eppendorf, Hamburg, Germany
1.5 mL Eppendorf safe- lock tubes	0030 123.328	Eppendorf, Hamburg, Germany
2 mL Eppendorf safe- lock tubes	0030 123. 344	Eppendorf, Hamburg, Germany
15 mL centrifuge tubes	602072	NEST Biotechnology, Jiangsu China Wuxi
50 mL centrifuge tubes	601001	NEST Biotechnology, Jiangsu China Wuxi
CELLBIND 24- well plates	3337	Corning, MA, USA

CELLBIND 6- well plates	3335	Corning, MA, USA
CELLBIND 6-well plates	3335	Corning, MA, USA
CELLBIND 96-well clear plates	3300	Corning, MA, USA
Cryotubes	430659	Corning, MA, USA
Filter Pads	23385	Sigma-Aldrich , St Louis, MO, USA
MicroAmp Optical PCR 96-well clear plates	N8010560	Applied Biosystems, Foster City, CA, USA
T75 Flasks	658975	Greiner bio-one, Frickenhausen, Germany

Table A3: Experimental kits

Experimental kits	**Catalogue no**	**Company**
ViaLight ATP assay kit	LT27-008	Lonza, Walkersville, MD, USA
Biorad RC DC protein kit	500-0201	Bio-Rad, Hercules, CA, USA
Caspase-Glo 3/7 Assay	PRG8091	Promega,Madison, Wilsconsin, USA
Catalase kit	707002	Cayman chemical, Ellsworth
DeadEnd Fluorometric TUNEL system	G3250	Promega, Madison, Wilsconsin, USA
GSH/GSSH assay kits	PRV6612	Promega, Madison, Wilsconsin, USA
High Capacity cDNA kit	PN 4375575	Applied biosystem, Foster City, CA, USA
Turbo DNase kit	AM1907	Ambion, Austin, TX, USA
SOD activity kit	K335-100	Biovision, Milpitas, CA, USA
RNeasy mini kit	74106	Qiagen, Hilden, Germany
TBARS assay kit	STA-330	Cell Biolabs, San Diego,US
Clarity™ Western ECL substrate	1705060	Bio-Rad, Hercules, CA, USA

Table A4: Antibodies

Primary Antibodies	**Catalogue number**	**Company**
AMPK	3535	Cell signalling, Danvers, MA, US
Bax	Sc-493	Santa Cruz Biotechnology, Santa Cruz, CA, USA
Bcl-2	2870S	Cell signalling, Danvers, MA, US
LC3A/B	4108S	Cell signalling, Danvers, MA, US
mTOR (7C10)	2983S	Cell signalling, Danvers, MA, US
p53	9282S	Cell signalling, Danvers, MA, US

p-mTOR (Ser2481)	2974S	Cell signalling, Danvers, MA, US
SQSTM1/p62	5114S	Cell signalling, Danvers, MA, US
B-actin	Sc-47778	Santa Cruz Biotechnology, Santa Cruz, CA, USA
Donkey anti-mouse IgG-HRP	Sc-2318	Santa Cruz Biotechnology, Santa Cruz, CA, USA
Donkey anti-rabbit IgG-HRP	Sc-2012	Santa Cruz Biotechnology, Santa Cruz, CA, USA

Table A5: Equipment

Equipment	**Product Number**	**Supplier**
Agilent Bioanalyser	G2946-90004	Agilent Technologies,Santa Clara, California
CountessTM Automated Cell Counter	C10227	Invitrogen, Carlsbad, CA, USA
D1200-230V Heating block	S62927099	Labnet, Adison,NJ,USA
IKA® MS 3 digital shakers	IKA 331900X	Sigma-Aldrich , St Louis, MO, USA
Benchtop Centrifuge	SL16R	Thermo Fisher Scientific, Waltham, MA, USA
Micro-centrifuge	001977	Eppendorf, Hamburg, Germany
Mini Protean casting frame	165-3304	Bio-Rad, Hercules, CA, USA
Mini Protean casting stand	165-3303	Bio-Rad, Hercules, CA, USA
Mini Protein tetra cell	165-8030	Bio-Rad, Hercules, CA, USA
Mini Trans-blot cell	170-4070	Bio-Rad, Hercules, CA, USA
NanoDrop™1000 Spectrophotometer	A984	Thermo Fisher Scientific, Waltham, MA, USA
Orbital shaker ITPSIC 10	20197	Torrey pines Scientific
PowerPac HC	165-8025	Bio-Rad, Hercules, CA, USA
TissueLyser	85300	Qiagen, Hilden, Germany
ABI 7500 Real time PCR system	4351104	Applied Biosystem, Foster City, CA, USA
2720 Thermal cycler	4413750	Applied Biosystem, Foster City, CA, USA
Nikon Eclipse Ti inverted microscope	Ti inverted	Nikon, Tokyo, Japan
Biotek® FLX 800 plate reader	FLX 800	BioTek Instruments Inc., Winooski, VT, USA

BioTek® ELX800 plate reader	ELX800	BioTek Instruments Inc., Winooski, VT, USA
Orbital shacker	20197	Stoval life Sciecne

APPENDIX B

PREPARATION OF REAGENTS

I. Preparation of DMEM

A 500mL of DMEM with phenol red and glutamate was supplemented with;

- 50 mL of FBS (Final FBS concentration of 10%)
- 5.5ml of pen-strep (Final concentration of 1%)

The media was then aliquoted in 50 mL tubes and stored at 4°C until used.

II. Preparation of treatment media

A 500 mL of DMEM without phenol red and glutamate was supplemented with

- 10 mL of FBS (Final FBS concentration of 2%)

The media was then aliquoted in 50 mL tubes and stored at 4°C until used.

III. Preparation of 10x Tris-buffered saline (TBS) wash buffer

The 10x TBS wash buffer was prepared by dissolving:

- 200 mM of Tris (24.22 g)
- 1.37 mM NaCl (80.06 g)
- Topped up with distilled to a total volume of 1L.

IV. 1X TBS and Tween 20 (1X TBST-20)

1X TBST-20 was prepared by added:

- 100 mL of 10 x TBST
- 900 mL of distilled water (v/v)
- 1 mL Tween 20

The buffer was kept at 4°C.

V. Transfer buffer for Western Blot

The buffer was prepared by adding:

- 25 mM of Tris (3.03 g)
- 192 mM glycine (14.4 g)
- 800 mL of distilled water,
- 200mL of methanol to make up a total volume of 1L.
-

VI. RIPA Buffer

- 25mM Tris (10 mM sodium phosphate may be used instead), pH 7–8
- 150 mM NaCl
- 0.1% SDS (optional)
- 0.5% sodium deoxycholate
- 1% Triton X-100 or NP-40

VII. Preparation of Aspalathin

Aspalathin (ASP) (ca. 98%, batch SZI-356-54) was synthesised by High Force Research LTD as previously described by Han *et al*. (2014). ASP (MW 452.41 g·mol−1) at an initial stock of 100 mg/mL (22.2 mM) was prepared by dissolving 10 mg of ASP in 100 µL 100% dimethyl sulfoxide (DMSO) and stored at -80°C. A working solution of 1 mM ASP was prepared by diluting the initial stock in DMEM media to yield a final concentration of 0.2 µM ASP with a DMSO concentration < 0.001%.

VIII. Preparation of Doxorubicin (Dox)

A 10 mg of Dox (Sigma-Aldrich, D1515, MW 543.52 g/mol) was dissolved in 5.4 mL of treatment media to obtain a stock concentration of 3.4 mM, aliquoted and the aliquots were stored in -180° C until required. A working solution of 1mM was prepared by diluting the initial stock in treatment media to yield the concentration of 0.2 µM.

IX. Preparation of Dexrazoxane (Dexra)

Five milligram of Dexra (Sigma-Aldrich, D1446, MW 268.27 g/mol) was dissolve in 1mL of 100 % DMSO to obtain a stock concentration of 18.6 mM and stored in -180° C until required. The working solution of 1mM was prepared by diluting the initial stock in treatment media to yield the final concentration of 20 µM with a DMSO concentration of 0.01%.

X. Freezing media for cryopreservation of Cells

To cryopreserve cells for future use, both H9c2 and Caov-3 cells were trypsinized (section 3.3.2). Thereafter cell pellets were re-suspended in cold freezing media (made up of 80%, 10% (v/v) FBS and 10% (v/v) DMSO). Subsequently cells were kept on ice for 5 min before stored in LN2 for long term storage.